UNIVERSITÀ DEGLI STUDI DI SALERNO

DIPARTIMENTO DI SCIENZE FARMACEUTICHE

Dottorato di Ricerca in Scienze Farmaceutiche
IX-Ciclo NS
2007-2010

Design and synthesis of "small molecules" as antiviral and radiotracer agents

Tutor
Prof. Paolo de Caprariis

PhD Student
Grazia Sellitto

Coordinator
Prof.ssa Nunziatina De Tommasi

Ai miei genitori Raffaele e Anna

...e a Rocco

Table of Content

ABSTRACT

The present Ph.D. project was divided into different work parts, in a way that helps to understand and define the goals of this project. In particular:

I) Design, synthesis and evaluation of antiviral activity of Arbidol analogs.

II) Evaluation of mechanism of Arbidol anti-influenza action.

III) Synthesis and characterization of a P.E.T. radiotracer for tumor hypoxia: *1- (5- [18F] Fluoro-5-deoxy-α-D-arabinofuranosyl) -2-nitroimidazole* or ^{18}F-FAZA.

The initial research activity concerned the design and synthesis of indole derivatives using as a lead compound Arbidol (ARB), a compound that exerts immunomodulatory, antioxidant, antiviral and antimetastatic effects[1]. ARB is a Russian-made potent broad-spectrum antiviral with demonstrated activity against a number of enveloped and non-enveloped viruses, and pH-dependent and pH-independent viruses. It exhibits antiviral activity against a number of viruses including *influenza A (H1N1, H2N2 and H3N2), B* and *C viruses*, *respiratory syncytial virus (RSV)*, *adenovirus type 7*, *coxsackie B3 virus*, *parainfluenza type 5* and *rhinovirus type 14*, *avian coronavirus*, *infectious bronchitis virus* and *Marek disease virus*, *hepatitis B virus* and *hepatitis C virus*. The wide spectrum of ARB's activity suggests that ARB targets common critical step(s) in virus – cell interaction. Several studies have shown that the affinity of ARB for lipid membranes could account for its antiviral actions, together with a differential level of interaction with key motifs in glycoproteins of different viruses. Its antiviral activity toward viruses is due probably to a direct effect of ARB on virus-cell membrane interactions where ARB intercalates into membranes and induces membrane alterations. This leads to excessive stabilization of cell membranes, which become resistant to virus fusion and in some cases (HCV) to virus replication[2-4]. The known biological properties of Arbidol led us to focus on its derivatives as potential antiviral agents. In order to maintain antiviral activity we preserved the groups

responsible of Arbidol interaction with membranes (indole ring, S-phenyl group, ester group and amino group) eliminating those that were not considered pharmacophores (*hydroxy* and *bromo* groups at the 5- and 6-positions of the indole ring). Moreover we introduced different substituents at the 2- and 5-position of the indole ring to investigate the influence of these variations on antiviral activity. The synthesis of Arbidol derivatives has been established through the validation of two synthetic schemes. Then, to evaluate anti-HCV and anti-HSV activity of synthesized compounds, biological assays were made. ARB derivatives showed antiviral activity comparable and, in some cases, even better than those of lead Arbidol, on both systems. In particular, it was shown that synthesized compounds are fusion inhibitors on both viruses and also non-selective inhibitors of HCV replication.

The second part of the present research project concerned the study of mechanism of Arbidol anti-influenza action. There are experimental evidences that ARB does not affect viral neuraminidase (NA, a surface protein of influenza virus) activity. It affects early post-adsorption stages of virus replication with possible involvement of the second surface viral protein, the haemagglutinin (HA). Arbidol could act increasing influenza virus HA stability and preventing low pH induced HA transition to its fusogenic state, thus blocking infection at the viral fusion stage[5]. To support this hypothesis, the interaction of Arbidol with the N-terminal hydrophobic fusion domain of haemagglutinin (HA) was evaluated. Therefore, the peptide host-guest (P20H6) was synthesized using techniques of Solid Phase Peptide Synthesis (SPPS) and *Circular dichroism* studies were made[6]. From these studies we demonstrated that Arbidol interacts with the haemagglutinin fusion domain at pH 5 and 7, through changes in the secondary structure of peptide.

At the end of present Ph.D. project, I spent six months at the University of Aberdeen where I worked to the synthesis of a PET (Positron Emission

Tomography) radiotracer for tumour hypoxia: the *[^{18}F]1-α-D-(5-Fluoro-5-deoxyarabinofuranosyl)-2-nitroimidazole*, known as ^{18}F-FAZA.

^{18}F-FAZA is currently the gold standard for PET Imaging of diseases characterized by hypoxia (solid tumours, ischemia, stroke)[7], but it is not routinely used and synthesized in Scotland. The work done is an important starting point for the introduction of ^{18}F-FAZA in Scotland with the aim of using it in clinical imaging and research. In particular, following a detailed bibliography research on this compound and its synthesis, that is not fully reported, and a subsequent optimization of the synthetic scheme used, the ^{18}F-FAZA precursor was obtained: *1-α-D-[5'-O-Toluenesulfonyl-2',3'-Di-Oacetylarabinofuranosyl]-2-nitroimidazole* (DAcTs-AZA).

[1] Surinova B. N., Karpova N. A., Kumin Yu. C. (1995). Khim. Farm. Zh.;Chem.-Pharm. J., 3, 14-15.

[2] Eve-Isabelle Pe´cheur, Dimitri Lavillette, Fanny Alcaras, Jennifer Molle, Yury S. Boriskin, Michael Roberts, Francüois-Loı¨c Cosset, and Stephen J. Polyak; *Biochemistry* **2007,** *46,* 6050-6059.

[3] Yury S Boriskin1, Eve-Isabelle Pécheur and Stephen J Polyak; *Virology Journal* **2006**, 3:56:1-9.

[4] Irina A. Leneva, Rupert J. Russell, Yury S. Boriskin, Alan J. Hay; *Antiviral Research* **2009**; 81:132–140.

[5] Irina A. Leneva, Rupert J. Russell, Yury S. Boriskin, Alan J. Hay; Antiviral Research; 81 (2009) 132–140.

[6] Xing Han, John H. Bushweller, David S. Cafiso and Lukas K. Tamm; *Nature Structural Biology*; **2001**, Volume 8 N.8.

[7] Ernst J. Postema, Alexander J. B. McEwan, Terence A. Riauka, Piyush Kumar, Dacia A. Richmond, Douglas N. Abrams, Leonard I. Wiebe; *Eur J Nucl Med Mol Imaging* (**2009**) 36:1565–1573.

CHAPTER 1

INTRODUCTION

1.1 Viruses

The word virus is from the Latin *virus* referring to *poison* and other noxious substances, first used in English in 1392[1]. A virus (**Fig.1.1**) is a small infectious agent that can replicate only inside the living cells of organisms. Most viruses are too small to be seen directly with a light microscope. Viruses infect all types of organisms, from animals and plants to bacteria and archaea[2]. They are found in almost every ecosystem on Earth and are the most abundant type of biological entity[3,4].

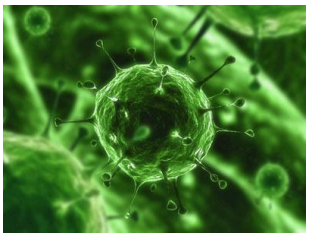

Figure 1.1: *Virus.*

Despite continuing advances, established and emerging viruses remain major causes of human disease, with dramatic costs in mortality, morbidity and economic terms. In addition to acute diseases, viruses cause at least 15–20% of human cancers and are implicated in neurological and other chronic disorders. One of many challenges in controlling viruses and virus-mediated diseases is that viruses show an amazing diversity in basic characteristics and life cycles, including differences in virion structure, replication strategies, genetic organization, gene expression and many other fundamental processes. Therefore, even the very processes against which antivirals are targeted often differ radically among virus classes[5].

1.1.1 Discovery

Viral diseases such as rabies have affected humans for many centuries. There is hieroglyphical evidence of Polio in the ancient Egyptian empire. However, the cause of these diseases was discovered relatively recently.

In 1717, Mary Montagu, the wife of an English ambassador to the Ottoman Empire, observed local women inoculating their children against Smallpox.

In the late 18th century, Edward Jenner observed and studied Miss Sarah Nelmes, a milkmaid who had previously caught Cowpox and was subsequently found to be immune to Smallpox, a similar, but devastating virus. Jenner developed the first vaccine, based on these findings, and smallpox is currently all but wiped out.

In the late 19th century Charles Chamberland (known today as the Chamberland filter or Chamberland-Pasteur filter) developed a porcelain filterwith pores smaller than bacteria. Thus, he could pass a solution containing bacteria through the filter and completely remove them from the solution (**Fig. 1.2**)[6]. This filter was used to study the first documented virus, *tobacco mosaic virus*. Shortly afterwards, Dimitri Ivanovski published experiments showing that crushed leaf extracts of infected tobacco plants were still infectious even after filtering the bacteria from the solution[7].

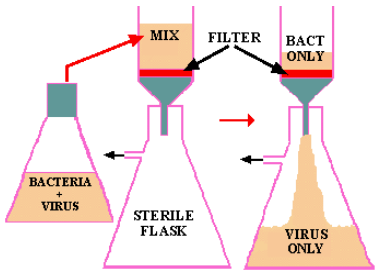

Figure 1.2: *Filtration of a mixture of bacteria and viruses.*

At about the same time, several others documented filterable disease-causing agents, with several independent experiments showing that viruses were

different from bacteria, yet they could also cause disease in living organisms. These experiments showed that viruses are orders of magnitudes smaller than bacteria. The term virus was coined by the Dutch microbiologist Martinus Beijerinck. He observed that the agent multiplied only in cells that were dividing, but as his experiments did not show that it was made of particles, he called it a *contagium vivum fluidum* (soluble living germ) and re-introduced the word *virus*[8-10]. Beijerinck maintained that viruses were liquid in nature, a theory later discredited by Wendell Stanley.

Since the initial discovery of *tobacco mosaic virus* by Martinus Beijerinck in 1898,[2] about 5,000 viruses have been described in detail[11], although there are millions of different types[12].

In 1957, *equine arterivirus* and the cause of *bovine virus* diarrhea (a *pestivirus*) were discovered. In 1963, the *hepatitis B virus* was discovered by Baruch Blumberg[13], and in 1965, Howard Temin described the first *retrovirus*. Reverse transcriptase, the key enzyme that *retroviruses* use to translate their RNA into DNA, was first described in 1970, independently by Howard Martin Temin and David Baltimore[14]. In 1983 Luc Montagnier's team at the Pasteur Institute in France, first isolated the retrovirus now called *HIV*[15].

1.1.2 Origins

The origins of modern viruses are not entirely clear, and there may not be a single mechanism of origin that can account for all viruses. As viruses do not form fossils, molecular techniques have been the most useful means of hypothesising how they arose[16]. These techniques rely on the availability of ancient viral DNA or RNA, but, unfortunately, most of the viruses that have been preserved and stored in laboratories are less than 90 years old. There are three main hypotheses that try to explain the origins of viruses[17,18]:

- **Regressive hypothesis:** Viruses may have once been small cells that parasitised larger cells. Over time, genes not required by their parasitism

were lost. The bacteria *rickettsia* and *chlamydia* are living cells that, like viruses, can reproduce only inside host cells. They lend support to this hypothesis, as their dependence on parasitism is likely to have caused the loss of genes that enabled them to survive outside a cell. This is also called the *degeneracy hypothesis.*

- **Cellular origin hypothesis:** Some viruses may have evolved from bits of DNA or RNA that "escaped" from the genes of a larger organism. The escaped DNA could have come from plasmids (pieces of naked DNA that can move between cells) or transposons (molecules of DNA that replicate and move around to different positions within the genes of the cell)[19]. Once called "jumping genes", transposons are examples of mobile genetic elements and could be the origin of some viruses. They were discovered in maize by Barbara McClintock in 1950. This is sometimes called the *vagrancy hypothesis*[20].
- **Coevolution hypothesis:** Viruses may have evolved from complex molecules of protein and nucleic acid at the same time as cells first appeared on earth and would have been dependent on cellular life for billions of years. Viroids are molecules of RNA that are not classified as viruses because they lack a protein coat. However, they have characteristics that are common to several viruses and are often called subviral agents[21]. Viroids are important pathogens of plants[22]. They do not code for proteins but interact with the host cell and use the host machinery for their replication[23]. The *hepatitis delta virus* of humans has an RNA genome similar to viroids but has protein coat derived from *hepatitis B virus (HBV)* and cannot produce one of its own. It is therefore a defective virus and cannot replicate without the help of *HBV*[24]. Similarly, the virophage '*sputnik*' is dependent on mimivirus, which infects the protozoan *Acanthamoeba castellanii*[25]. These viruses that are dependent on the

presence of other virus species in the host cell are called *satellites* and may represent evolutionary intermediates of viroids and viruses.

Computer analysis of viral and host DNA sequences is giving a better understanding of the evolutionary relationships between different viruses and may help identify the ancestors of modern viruses. To date, such analyses have not helped to decide on which of these hypotheses are correct. However, it seems unlikely that all currently known viruses have a common ancestor and viruses have probably arisen numerous times in the past by one or more mechanisms[20].

1.1.3 Structure

Viruses display a wide diversity of shapes and sizes, called *morphologies*. Generally viruses are much smaller than bacteria. Most viruses that have been studied have a diameter between 10 and 300 nanometres. Some *filoviruses* have a total length of up to 1400 nm; their diameters are only about 80 nm[26]. Most viruses cannot be seen with a *light microscope* so scanning and transmission *electron microscopes* are used to visualise virions.[59] To increase the contrast between viruses and the background, electron-dense "stains" are used.

A complete virus particle, known as a virion, consists of nucleic acid surrounded by a protective coat of protein called a *capsid*. These are formed from identical protein subunits called *capsomers*. Viruses can have a lipid "envelope" derived from the host cell membrane. The *capsid* is made from proteins encoded by the *viral genome* and its shape serves as the basis for morphological distinction[27]. Virally coded protein subunits will self-assemble to form a *capsid*, generally requiring the presence of the virus genome. Complex viruses code for proteins that assist in the construction of their *capsid*. Proteins associated with nucleic acid are known as *nucleoproteins*, and

the association of viral capsid proteins with viral nucleic acid is called a *nucleocapsid* (**Fig. 1.3**).

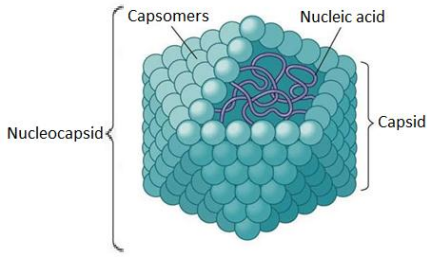

Figure 1.3: *Virion structure.*

The capsid and entire virus structure can be mechanically (physically) probed through *atomic force microscopy*[28-30].

In general, there are four main morphological virus types:

Helical: These viruses are composed of a single type of protomer stacked around a central axis to form a helical structure, which may have a central cavity, or hollow tube (**Fig. 1.4**). This arrangement results in rod-shaped or filamentous virions: these can be short and highly rigid, or long and very flexible. Long helical particles must be flexible in order to prevent forces snapping the structure. The genetic material, generally single-stranded RNA, but ssDNA in some cases, is housed on the inside of the tube, protected from the outside, through a bond into the protein helix by interactions between the negatively charged nucleic acid and positive charges on the protein. Overall, the length of a helical capsid is related to the length of the nucleic acid contained within it and the diameter is dependent on the size and arrangement of capsomers. The well-studied *Tobacco mosaic virus* is an example of a helical virus[31].

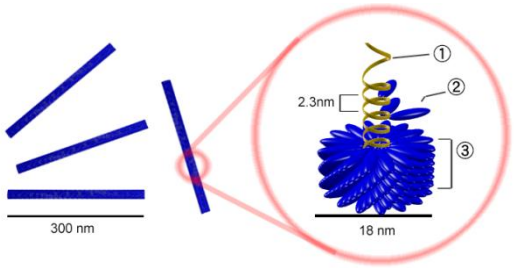

Figure 1.4: *Diagram of a helical capsid*.

Icosahedral: Cubic (=Icosahedral) capsid symmetry results in a spherical appearance of viruses at low magnification but actually consists of capsomers arranged in a regular geometrical pattern, similar to a soccer ball, hence they are not truly "spherical". Capsomers are ring shaped structures constructed from five to six copies of protomers. These associate via non-covalent bonding to enclose the viral nucleic acid, though generally less intimately than helical capsids, and may involve one or more protomers.

Most, if not all, of the polygonal viruses are icosahedral; like a geodesic dome, they are formed by equilateral triangles. Each triangle is composed of protein subunits (capsomeres), often in the form of hexons (multiples of six) that are the building blocks of the capsid. There are 12 vertices (the apical junctions of these triangles), each comprising a penton (five subunits). In order to construct a capsid from repeated subunits, a virus must 'know the rules' which dictate how these are arranged. For an icosahedron, the rules are based on the rotational symmetry of the solid, which is known as *2-3-5 symmetry* (**Fig. 1.5**)[32]:

- An axis of *two-fold* rotational symmetry through the centre of each *edge*.
- An axis of *three-fold* rotational symmetry through the centre of each *face*.
- An axis of *five-fold* rotational symmetry through the centre of each *corner*.

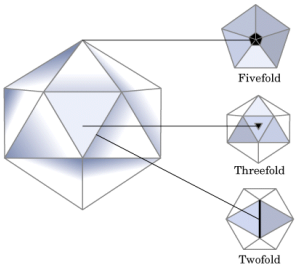

Figure 1.5: *Icosahedral symmetry*[33].

Envelope: Some species of virus envelop themselves in a modified form of one of the cell membranes, either the outer membrane surrounding an infected host cell, or internal membranes such as nuclear membrane or endoplasmic reticulum, thus gaining an outer lipid bilayer known as a viral envelope. This membrane is studded with proteins coded for by the viral genome and host genome; the lipid membrane itself and any carbohydrates present originate entirely from the host. The HIV and influenza virus use this strategy (**Fig. 1.6**). Most enveloped viruses are dependent on the envelope for their infectivity.

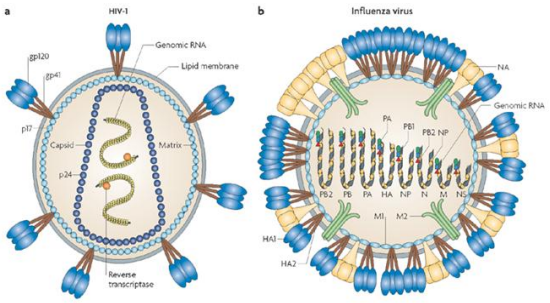

Figure 1.6: *Examples of two enveloped viruses. (a) HIV has an icosahedral capsid which contains two positive-strand RNA copies and (b) Influenza A virus has an helical capsid which contains eight negative-strand RNA segments*[34].

Complex: These viruses possess a capsid that is neither purely helical, nor purely icosahedral, and that may possess extra structures such as protein tails or a complex outer wall. Some bacteriophages, such *as Enterobacteria phage T4* (**Fig. 1.7**) have a complex structure consisting of an icosahedral head

bound to a helical tail, which may have a hexagonal base plate with protruding protein tail fibres. This tail structure acts like a molecular syringe, attaching to the bacterial host and then injecting the viral genome into the cell[27].

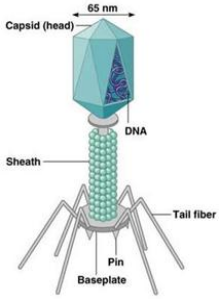

Figure 1.7: *Structural overview of the T4 phage.*

The *poxviruses* are large, complex viruses that have an unusual morphology. The viral genome is associated with proteins within a central disk structure known as a nucleoid. The nucleoid is surrounded by a membrane and two lateral bodies of unknown function. The virus has an outer envelope with a thick layer of protein studded over its surface. The whole virion is slightly pleiomorphic, ranging from ovoid to brick shape[35]. *Mimivirus* is the largest known virus, with a capsid diameter of 400 nm. Protein filaments measuring 100 nm project from the surface. The capsid appears hexagonal under an electron microscope, therefore the capsid is probably icosahedral.

Some viruses that infect *Archaea* have complex structures that are unrelated to any other form of virus, with a wide variety of unusual shapes, ranging from spindle-shaped structures, to viruses that resemble hooked rods, teardrops or even bottles. Other archaeal viruses resemble the tailed bacteriophages, and can have multiple tail structures[36].

1.1.4 Genome

An enormous variety of genomic structures can be seen among viral species; as a group they contain more structural genomic diversity (**Table 1.1**) than plants, animals, archaea, or bacteria. There are millions of different types of viruses; though only about 5,000 of them have been described in detail. A virus has either DNA or RNA genes and is called a DNA virus or a RNA virus respectively. The vast majority of viruses have RNA genomes. Plant viruses tend to have single-stranded RNA genomes and bacteriophages tend to have double-stranded DNA genomes[11,12].

Property	Parameters
Nucleic acid	• DNA • RNA • Both DNA and RNA (at different stages in the life cycle)
Shape	• Linear • Circular • Segmented
Strandedness	• Single-stranded • Double-stranded • Double-stranded with regions of single strandedness
Sense	• Positive sense (+) • Negative sense (-) • Ambisense(+/-)

Table 1.1: *Genomic diversity among viruses.*

Viral genomes are circular, as in the *polyomaviruses*, or linear, as in the *adenoviruses*. The type of nucleic acid is irrelevant to the shape of the genome. Among RNA viruses, the genome is often divided up into separate parts within the virion, in which case it is called *segmented*. Each segment often codes for one protein and they are usually found together in one capsid.

Every segment is not required to be in the same virion for the overall virus to be infectious, as demonstrated by the brome mosaic virus[27].

A viral genome, irrespective of nucleic acid type, is either single-stranded or double-stranded. Single-stranded genomes consist of an unpaired nucleic acid, analogous to one-half of a ladder split down the middle. Double-stranded genomes consist of two complementary paired nucleic acids, analogous to a ladder. Some viruses, such as those belonging to the *Hepadnaviridae*, contain a genome that is partially double-stranded and partially single-stranded.

For viruses with RNA or single-stranded DNA, the strands are said to be ether *positive-sense* (called the plus-strand) or *negative-sense* (called the minus-strand), depending on whether it is complementary to the viral messenger RNA (mRNA). Positive-sense viral RNA is identical to viral mRNA and thus can be immediately translated by the host cell. Negative-sense viral RNA is complementary to mRNA and thus must be converted to positive-sense RNA by an RNA polymerase before translation. DNA nomenclature is similar to RNA nomenclature, in that the *coding strand* for the viral mRNA is complementary to it (−), and the *non-coding strand* is a copy of it (+).

Genome size varies greatly between species. The smallest viral genomes code for only four proteins and have a mass of about 10^6 Daltons; the largest have a mass of about 10^8 Daltons and code for over one hundred proteins[37]. RNA viruses generally have smaller genome sizes than DNA viruses because of a higher error-rate when replicating, and have a maximum upper size limit. Beyond this limit, errors in the genome when replicating render the virus useless or uncompetitive. To compensate for this, RNA viruses often have segmented genomes where the genome is split into smaller molecules, thus reducing the chance of error. In contrast, DNA viruses generally have larger genomes because of the high fidelity of their replication enzymes.

Viruses undergo genetic change by several mechanisms. These include a process called genetic drift where individual bases in the DNA or RNA mutate to other bases. Most of these point mutations are "silent", they do not change the protein that the gene encodes, but others can confer evolutionary advantages such as resistance to antiviral drugs. Antigenic shift occurs when there is a major change in the genome of the virus. This can be a result of recombination or reassortment.

Viruses with segmented genomes, such as influenza virus, have another mechanism for generating diversity: reassortment[38-39].

When an *influenza virus* infects a cell, the individual RNA segments enter the nucleus. There they are copied many times to form RNA genomes for new infectious virions. The new RNA segments are exported to the cytoplasm, and then are incorporated into new virus particles which bud from the cell. If a cell is infected with two different *influenza viruses*, the RNAs of both viruses are copied in the nucleus.

When new virus particles are assembled at the plasma membrane, each of the 8 RNA segments may originate from either infecting virus.

The progeny that inherit RNAs from both parents are called reassortants. One example of the evolutionary importance of reassortment is the exchange of RNA segments between mammalian and avian *influenza viruses* that give rise to pandemic influenza. For example, the 2009 *H1N1* pandemic strain is a reassortant of avian, human, and swine *influenza viruses* (**Fig. 1.8**).

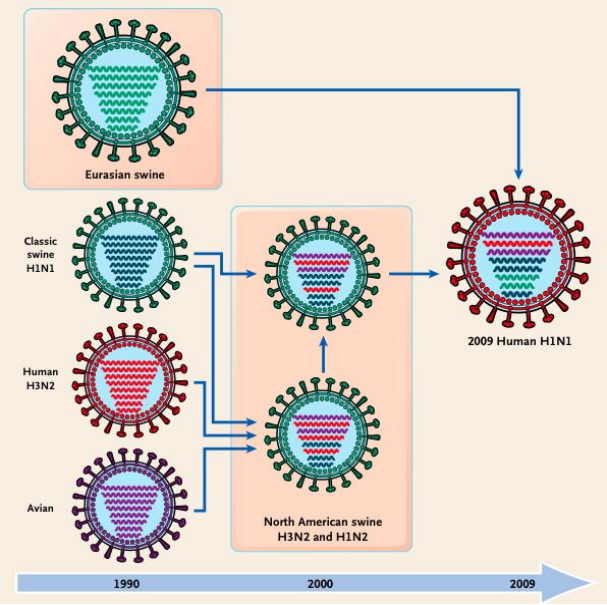

Figure 1.8: *History of Reassortment Events in the Evolution of the 2009 Influenza A (H1N1) Virus.*

Reassortment can only occur between influenza viruses of the same type. Why *influenza A viruses* never exchange RNA segments with *influenza B or C viruses* is not understood. However, the reason is probably linked to the packaging mechanism that ensures that each influenza virion contains at least one copy of each RNA segment[38-40].

Genetic recombination is the process by which a strand of DNA is broken and then joined to the end of a different DNA molecule. This can occur when viruses infect cells simultaneously and studies of viral evolution have shown that recombination has been rampant in the species studied. Recombination is common to both RNA and DNA viruses[41].

1.1.5 Replication cycle

Viral populations do not grow through cell division, because they are acellular. Instead, they use the machinery and metabolism of a host cell to produce multiple copies of themselves, and they assemble in the cell.

The *life cycle of viruses* (**Fig. 1.9**) differs greatly between species but there are six *basic* stages in the life cycle of viruses:

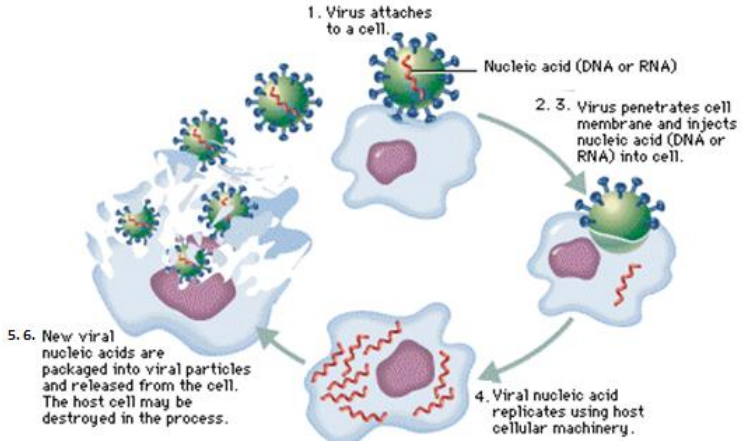

Figure 1.9: *Life cycle of viruses.*

1. ***Attachment*** is a specific binding between viral capsid proteins and specific receptors on the host cellular surface. This specificity determines the host range of a virus. For example, HIV infects only human T cells, because its surface protein, gp120, can interact with CD4 and chemokine receptors on the T cell's surface. This mechanism has evolved to favour those viruses that only infect cells in which they are capable of replication. Attachment to the receptor can induce the viral-envelope protein to undergo changes that results in the fusion of viral and cellular membranes.

2. ***Penetration*** follows attachment; viruses enter the host cell through receptor mediated membrane *fusion* or *endocytosis* (**Fig. 1.10A**). This is often called viral entry. In the case of *fusion* the viral membrane fuses with the cell membrane and the protein capsid is released. Once in the cytoplasm the protein capsid is removed and the viral genome is freed. Depending on the nature of the virus the viral genome may stay in the cytoplasm or it may enter the nucleus before beginning the next stage of

the life cycle. In the case of *engulfment*, o *endocytosis*, the initial adsorption process is the same, but rather than directly fusing with the cell membrane, the cell is stimulated to take-up or engulf the entire eukaryotic virus. Once inside the cytoplasm the enveloped eukaryotic virus is said to be in a vescicle. Subsequently, the two lipid membranes of the vesicle fuse, releasing the capsid covered virus. The capsid is then removed and the viral genome is freed for the next stage of viral replication[4,7]. Some of the non-enveloped viruses like *picornaviruses* and *phages* are capable of directly injecting their genome into the host cell (**Fig. 1.10B**). The infection of plant cells is different from that of animal cells. Plants have a rigid cell wall made of cellulose, so most viruses can only get inside the cells after trauma to the cell wall. However, viruses such as *tobacco mosaic virus* can also move directly in plants, from cell to cell, through pores called plasmodesmata[42].

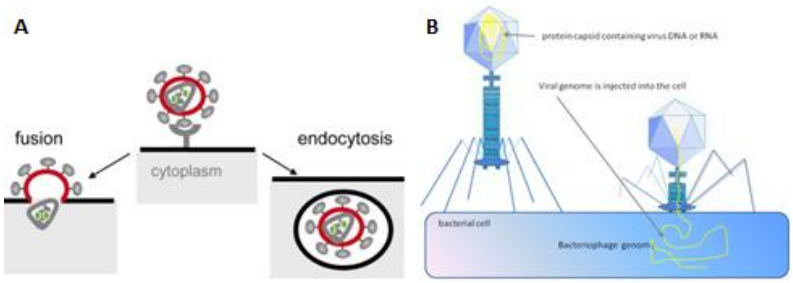

Figure 1.10: *A. Mechanisms of viral penetration: fusion and endocytosis; B. Genome injection in the host cell by phage.*

3. ***Uncoating*** is a process in which the viral capsid is degraded by viral enzymes or host enzymes thus releasing the viral genomic nucleic acid. A key step in uncoating is the acidification of the content of the endosome to a pH of about 5, owing to the activity of a proton pump present in the membrane. The low pH causes rearrangement of coat components, which then expose normally hidden hydrophobic sites. They bind to the lipid bilayer of the membrane, causing the extrusion of the viral core into the

cytosol. For *influenza virus*, the acid-sensitive component is the core HA_2 unit of the haemagglutinin, for *adenoviruses*, it is the penton base. There are four virus uncoating strategies: some enveloped viruses, such as *HIV*, fuse directly with the host cell plasma membrane to release their capsid *(green)* into the cytosol (**Fig. 1.11A**). Other enveloped viruses, such as *influenza virus*, first bind to cell-surface receptors, triggering receptor-mediated endocytosis. When the endosome acidifies, the virus envelope fuses with the endosomal membrane, releasing the nucleocapsid *(blue)* into the cytosol (**Fig. 1.11B**). *Poliovirus*, a nonenveloped virus, binds to a receptor *(green)* on the host cell surface and then forms a pore in the host cell membrane to extrude its RNA genome *(blue)* (**Fig. 1.11C**). *Adenovirus*, another nonenveloped virus, uses a more complicated strategy. It induces receptor-mediated endocytosis and then disrupts the endosomal membrane, releasing part of the capsid into the cytosol. The capsid eventually docks onto a nuclear pore and releases its DNA genome *(red)* directly into the nucleus (**Fig. 1.11D**)[43].

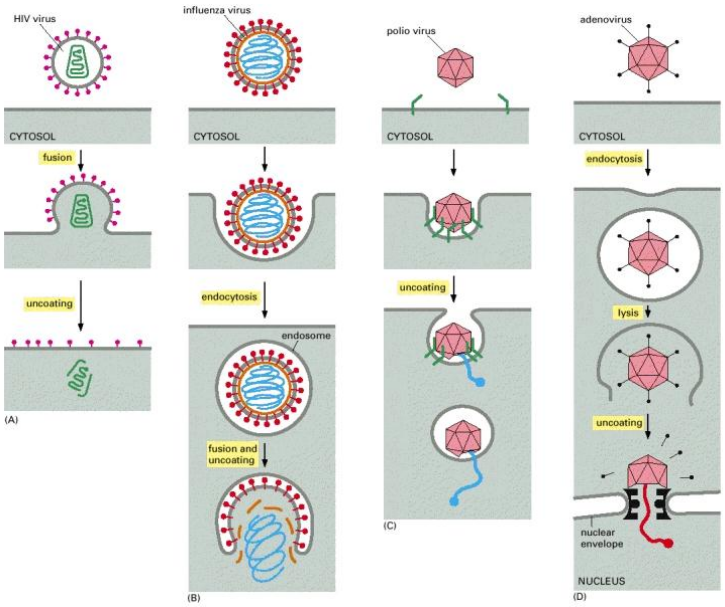

Figure 1.11: *Uncoating strategies.*

4 ***Replication*** involves synthesis of viral messenger RNA (mRNA) for viruses except positive sense RNA viruses, viral protein synthesis and assembly of viral proteins and viral genome replication.

5 **A*ssembly*** of the virus particles, in which post-translational modification of the viral proteins often occurs. In viruses such as *HIV*, this modification (sometimes called maturation) occurs after the virus has been released from the host cell.

6 Viruses are ***released*** from the host cell by *lysis* (a process that kills the cell by bursting its membrane) or *budding* (a process that involves taking a portion of the cell membrane) (**Fig. 1.12A**). Enveloped viruses (e.g., *HIV*) typically are released from the host cell by budding. During this process the virus acquires its envelope, which is a modified piece of the host's plasma membrane. Some viruses undergo a lysogenic cycle (**Fig. 1.12B**) where the viral genome is incorporated by genetic recombination into a specific place in the host's chromosome. The viral genome is then known as a "provirus" or, in the case of bacteriophages a "prophage". Whenever the host divides, the viral genome is also replicated. The viral genome is mostly silent within the host; however, at some point, the provirus or prophage may give rise to active viruses, which lyse their host cells[44].

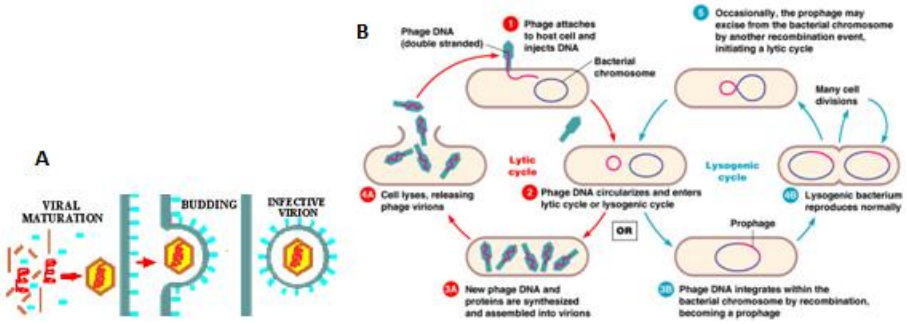

Figure 1.12: *Release strategies: A. Budding; B. Lysis or lysogenesis.*

The genetic material within viruses, and the method by which the material is replicated, vary between different types of viruses:

- **DNA viruses:** The genome replication of most DNA viruses takes place in the cell's nucleus. If the cell has the appropriate receptor on its surface, these viruses enter the cell by fusion with the cell membrane or by endocytosis. Most DNA viruses are entirely dependent on the host cell's DNA and RNA synthesising machinery, and RNA processing machinery. The viral genome must cross the cell's nuclear membrane to access this machinery[45].

- **RNA viruses:** Replication usually takes place in the cytoplasm. RNA viruses can be placed into about four different groups depending on their modes of replication. The polarity (whether or not it can be used directly to make proteins) of the RNA largely determines the replicative mechanism, and whether the genetic material is single-stranded or double-stranded. RNA viruses use their own RNA replicase enzymes to create copies of their genomes.

- **Reverse transcribing viruses:** These replicate using reverse transcription, which is the formation of DNA from an RNA template. Reverse transcribing viruses containing RNA genomes use a DNA intermediate to replicate, whereas those containing DNA genomes use an RNA intermediate during genome replication. Both types use the reverse transcriptase enzyme to carry out the nucleic acid conversion. Retroviruses often integrate the DNA produced by reverse transcription into the host genome. They are susceptible to antiviral drugs that inhibit the reverse transcriptase enzyme, e.g. zidovudine and lamivudine. An example of the first type is HIV, which is a retrovirus. Examples of the second type are the *Hepadnaviridae*, which includes Hepatitis B virus[46].

1.1.6 Classification

Classification seeks to describe the diversity of viruses by naming and grouping them on the basis of similarities. In 1962, André Lwoff, Robert Horne, and Paul Tournier were the first to develop a means of virus classification, based on the Linnaean hierarchical system. This system bases classification on phylum, class, order, family, genus, and species. Viruses were grouped according to their shared properties (not those of their hosts) and the type of nucleic acid forming their genomes. Viruses are mainly classified by phenotypic characteristics, such as morphology, nucleic acid type, mode of replication, host organisms, and the type of disease they cause[47-48].

Currently there are two main schemes used for the classification of viruses: the *ICTV* system and *Baltimore* classification system. Accompanying this broad method of classification are specific naming conventions and further classification guidelines set out by the *International Committee on Taxonomy of Viruses*.

a. ICTV classification

The *International Committee on Taxonomy of Viruses (ICTV)* developed the current classification system and wrote guidelines that put a greater weight on certain virus properties to maintain family uniformity. A unified taxonomy (a universal system for classifying viruses) has been established. The 7th *lCTV* Report formalised for the first time the concept of the virus species as the lowest taxon (group) in a branching hierarchy of viral taxa[49]. However, at present only a small part of the total diversity of viruses has been studied, with analyses of samples from humans finding that about 20% of the virus sequences recovered have not been seen before, and samples from the environment, such as from seawater and ocean sediments, finding that the large majority of sequences are completely novel.

The general taxonomic structure is as follows:

Order (-virales)
Family (-viridae)
Subfamily (-virinae)
Genus (-*virus*)
Species (-*virus*)

So far, six orders have been established by the ICTV: the *Caudovirales, Herpesvirales, Mononegavirales, Nidovirales, Picornavirales, and Tymovirales*. Most notably, species names generally take the form of virus. The establishment of an order is based on the inference that the virus families contained within a single order have most likely evolved from a common ancestor. The majority of virus families remain unplaced. Currently (2009) 6 orders, 87 families, 19 subfamilies, 348 genera, and 2,288 species of virus have been defined[50].

b. Baltimore classification

The *Baltimore* classification of viruses is based on the method of viral mRNA synthesis. The Nobel Prize-winning biologist David Baltimore devised the Baltimore classification system. The ICTV classification system is used in conjunction with the Baltimore classification system in modern virus classification.

Baltimore classification is a classification system that places viruses into one of seven groups depending on a combination of their nucleic acid (DNA or RNA), strandedness (single-stranded (ss) or double-stranded (ds)), Sense, and method of replication (may or may not use reverse transcriptase, RT). Additionally, ssRNA viruses may be either sense (+) or antisense (−). These groups are designated by Roman numerals and discriminate viruses depending on their mode of replication, and genome type.

The replication strategy of the virus depends on the nature of its genome. Viruses can be placed in one of the seven following groups (**Fig. 1.13**)[51]:

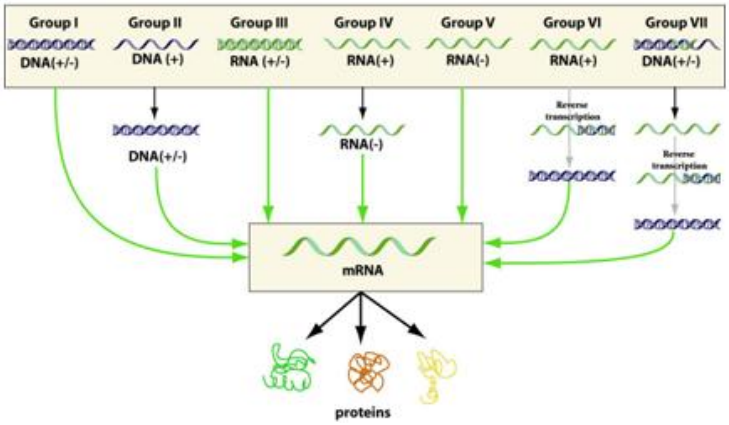

Figure 1.13: *Baltimore classification.*

Viruses belonging to group I and II are DNA viruses (**Table 1.2**).

- **Group I: Double-stranded DNA (dsDNA)**

(*Adenoviruses*; *Herpesviruses*; *Poxviruses*; etc).

Viruses having a dsDNA genome that make mRNA by asymmetric transcription. Some replicate in the nucleus e.g adenoviruses using cellular proteins. *Poxviruses* replicate in the cytoplasm and make their own enzymes for nucleic acid replication.

- **Group II: Single-stranded (+)sense DNA (ssDNA)**

(*Parvoviruses*; *circoviruses*)

Replication occurs in the nucleus, involving the formation of a (-)sense strand, which serves as a template for (+)strand RNA and DNA synthesis.

Virus Family	Examples (common names)	Virion naked/enveloped	Capsid symmetry	Nucleic acid type	Group
1.Adenoviridae	Adenovirus	Naked	Icosahedral	Ds	I
2.Papillomavirus	Papillomavirus	Naked	Icosahedral	ds circular	I
3.Parvoviridae	Parvovirus B19	Naked	Icosahedral	Ss	II
4.Herpesviridae	HSV, VZV, cytomegalovirus, EBV	Enveloped	Icosahedral	Ds	I
5.Poxviridae	Smallpox virus, vaccinia virus	Complex coats	Complex	ds	I
6.Hepadnaviridae	Hepatitis B virus	Enveloped	Icosahedral	Circular, partially ds	VII
7.Polyomaviridae	Polyoma virus, JC virus	Naked	Icosahedral	ds circular	I
8.Circoviridae	Transfusion transmitted virus	Naked	Icosahedral	Ss circular	II

Table 1.2: *DNA viruses.*

Viruses belonging to group III, IV and V are RNA viruses (**Table 1.3**).

- **Group III: Double-stranded RNA (dsRNA)**

(*Reoviruses; Birnaviruses*)

Viruses having a dsRNA genome that make mRNA by asymmetric transcription (**Fig. 1.14A**). Most have multiple pieces of dsRNA, each of which apparently contains the information for the synthesis of a single protein.

- **Group IV: Single-stranded (+)sense RNA ((+)ssRNA)**

(*Picornaviruses*; *Togaviruses*; *Flaviviruses*; *Coronaviruses*; etc)

Viruses having an ssRNA genome that make mRNA of base sequence identical to the genomic RNA. Infect, small amounts of (–)RNA are produced and used as templates to greatly amplify viral (+)RNA, which is encapsidated into new progeny virions (**Fig. 1.14B**).

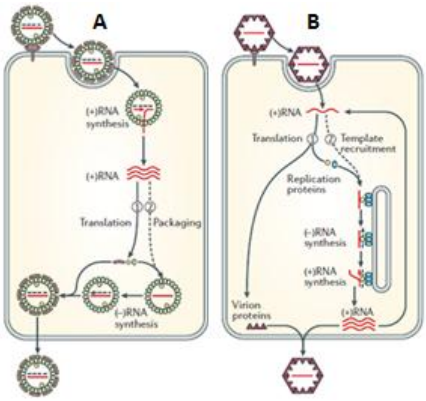

Figure 1.14: *Distinct life cycle of dsRNA (A), (+)RNA viruses(B).*

- **Group V: Single-stranded (-)sense RNA ((−)ssRNA)**

(*Orthomyxoviruses*; *Rhabdoviruses*; etc)

Viruses having an ssRNA genome that make mRNA with a base sequence complementary to the genomic RNA. Must have a virion particle RNA directed RNA polymerase.

Virus Family	Examples (common names)	Virion naked/enveloped	Capsid symmetry	Nucleic acid type	Group
1.Reoviridae	Reovirus, Rotavirus	Naked	Icosahedral	ds	III
2.Picornaviridae	Enterovirus, Rhinovirus, Hepatovirus, Cardiovirus, Poliovirus, Coxsackie	Naked	Icosahedral	ss	IV
3.Calciviridae	Norwalk virus, HEV	Naked	Icosahedral	ss	IV
4.Togaviridae	Rbubella virus	Enveloped	Icosahedral	ss	IV
5.Arenaviridae	Lymphocytic choriomeningitis virus	Enveloped	Complex	ss(-)	V
6.Flaviviridae	Dengue virus, HCV, Yellow fever virus	Enveloped	Icosahedral	ss	IV
7.Orthomyxoviridae	Influenza A, B and C viruses, Isavirus	Enveloped	Helical	ss(-)	V
8.Paramyxoviridae	Measles virus, Mumps virus, RSV	Enveloped	Helical	ss(-)	V
9.Bunyaviridae	California encephalitis virus, Hantavirus	Enveloped	Helical	ss(-)	V
10.Rhabdoviridae	Rabies virus	Enveloped	Helical	ss(-)	V
11.Filoviridae	Ebola virus, Marburg virus	Enveloped	Helical	ss(-)	V
12.Coronaviridae	Corona virus	Enveloped	Helical	ss	IV
13.Astroviridae	Astrovirus	Naked	Icosahedral	ss	IV
14.Bornaviridae	Borna disease virus	Enveloped	Helical	ss(-)	V

Table 1.3: *RNA viruses.*

Viruses belonging to group VII are DNA viruses (**Table 1.2**).

- **VI: Single-stranded (+)sense RNA with DNA intermediate in life-cycle (ssRNA-RT)** (Retroviruses)

Genome is (+)sense but unique among viruses in that it is diploid, and does not serve as mRNA, but as a template for reverse transcription. After cDNA synthesis by reverse transcription, proviral cDNA is integrated into the host chromosome and transcribed to produce (+)RNA (**Fig. 1.15**) that is translated (**1**) and then packaged (**2**) into new virions that are released by budding. *HIV* is a member of this group.

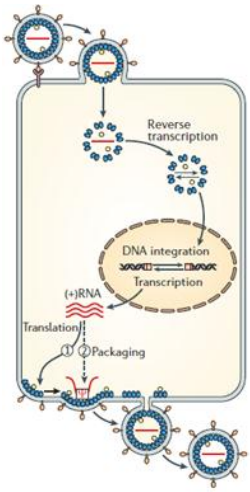

Figure 1.15: *Life cycle of retrovirus.*

- **VII: Double-stranded DNA with RNA intermediate (dsDNA-RT)** (Hepadnaviruses)

This group of viruses also relies on reverse transcription, but unlike the Retroviruses, this occurs inside the virus particle on maturation. Hepadnaviruses replicate through an RNA intermediate which they transcribe back into cDNA using reverse transcriptase. The *hepatitis B virus* can be found in this group.

As an example of viral classification, the chicken pox virus, varicella zoster (VZV), belongs to the order Herpesvirales, family *Herpesviridae*, subfamily *Alphaherpesvirinae*, and genus *Varicellovirus*. VZV is in Group I of the Baltimore Classification because it is a dsDNA virus that does not use reverse transcriptase[5].

1.2 Viruses and human disease

Viruses are of intense interest because many cause serious illness in human or domestic animals and others damage crop plants. During the last century, progress in the control of infectious diseases through improved sanitation, safer water supplies, the development of antibiotics and vaccines, and better medical care have dramatically reduced the threat to human health from these agents, especially in developed countries. The first step in treating viral infection is preventing its occurrence and spread. The use of vaccines has led to effective control of the most dangerous of the viruses. *Smallpox virus* has been eradicated worldwide by means of an ambitious and concerted effort, sponsored by the World Health Organization, to vaccinate all people at risk for the disease. *Poliovirus* and *measles virus* have been eliminated from the Americas by intensive vaccination programs. There is hope that these two viruses will also be eradicated worldwide in the near future. Vaccines exist for the control of many other viral diseases including, among others, *mumps*, *rabies*, *rubella*, *chickenpox*, *shingles*, *influenza*, *hepatitis B*, *hepatitis A*, *yellow fever*, *Japanese encephalitis*, *rotaviral gastroenteritis* and, very recently, *papillomaviral disease* that is the primary cause of cervical cancer. The dramatic decline in the death rate from infectious disease has led to a certain amount of complacency. However, viral diseases continue to plague humans, as do infectious diseases caused by bacteria, protozoa, fungi, and multicellular parasites[52].

There are thousands of viruses, and in humans they cause a wide range of diseases (**Fig. 1.16**).

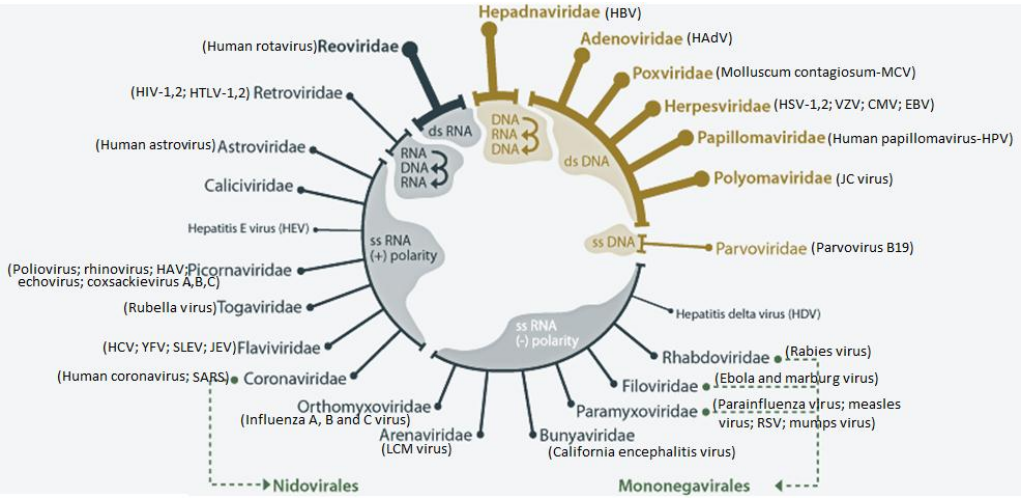

Figure 1.16: *Simplified classification scheme of the main viruses commonly associated with human diseases*[53].

For instance, *rhinoviruses* (Group: IV-(+)ssRNA, family: Picornaviridae, genus: enterovirus, species: *Human rhinovirus A,B,C*) cause colds; *influenza viruses* (Group: V-(-)ssRNA, family: Orthomyxoviridae, genus: *Influenza virus A,B,C*) cause flu; *adenoviruses* (*HAdV*, Group: I-dsDNA, family: Adenoviridae, species: *Human adenovirus A to G*) cause various respiratory problems (mainly species *HAdV-B and C*), conjunctivitis (*HAdV-B and D*) and gastroenteritis (*HAdV-F serotypes 40 and 41*); *rotaviruses* (Group: III-dsRNA Family: Reoviridae, genus: Rotavirus, species: *Rotavirus A-E*) cause gastroenteritis. *Poliovirus* (Group: IV-(+)ssRNA, family: Picornaviridae, genus: enterovirus, species: *human enterovirus C*) can make their way to the spinal cord and cause paralysis, while *coxsackieviruses* (Group: IV-(+)ssRNA, family: Picornaviridae, genus: enterovirus, species: *Human enterovirus A,B)* and *echoviruses* (Group: IV-(+)ssRNA, family: Picornaviridae, genus: enterovirus, species: *Human enterovirus B)* sometimes infect the heart or the membranes surrounding the spinal cord or lungs[52].

Although viruses cause disruption of healthy homeostasis, resulting in disease, they may exist relatively harmlessly within an organism. An example would include the ability of the *herpes simplex virus*, which causes cold sores, to remain in a dormant state within the human body. This is called latency[54] and is a characteristic of the *herpesviruses*. *Herpesviruses* belong to a large virus family, Herpesviridae (Group: I-dsDNA) and there are eight distinct viruses in this family known to cause disease in humans (**Table 1.4**)[55].

Type	Synonym	Subfamily	Primary target cell	pathophysiology	Site of latency
HHV1	Herpes simplex virus-1 (HSV-1)	A	Mucoepithelial	Oral and genital herpes	Neuron
HHV2	Herpes simplex virus-2 (HSV-2)	A	Mucoepithelial	Oral and genital herpes	Neuron
HHV3	Varicella Zoster virus (VZV)	A	Mucoepithelial	Chickenpox and shingles	Neuron
HHV4	Epstein-Barr virus (EBV), lymphocryptovirus	Γ	B cells and epithelial cells	Infectious mononucleosis, lymphoma, leukoplakia	B cell
HHV5	Cytomegalovirus (CMV)	B	Monocyte, lymphocyte and epithelial cells	Infectious mononucleosis, retinitis	Monocyte Lymphocyte
HHV6	Roseolovirus, Herpes lymphotropic virus	B	T cells	Sixth disease	T cells
HHV7	Roseolovirus	B	T cells	Sixth disease	T cells
HHV8	Kaposi's sarcoma-associated herpesvirus (KSHSV), a type of rhadinovirus	Γ	Lymphocyte and other cells	Kaposi's sarcoma, lymphoma,	B cell

Table 1.4: *Human Herpesvirus (HHV) classification.*

For example *Herpes simplex viruses* (*HSV-1,2*) cause cold sores and genital herpes (a sexually transmitted disease); the *Epstein-Barr virus* (*EBV*) and the *cytomegalovirus (CMV)* cause infectious mononucleosis and the *varicella zoster* (*VZV*) virus causes shingles and chickenpox.

Most people have been infected with at least one of these types of herpes virus[56]. However, these latent viruses might sometimes be beneficial, as the presence of the virus can increase immunity against bacterial pathogens, such as *Yersinia pestis*[57].

Other viruses cause a variety of conditions from measles and mumps to hepatitis and AIDS. Viral infections primarily affect respiratory and gastrointestinal system; epithelium, mucous membranes and endothelium of skin, mouth and genitals; lymphoid tissue, liver and other organs and central nervous system (SNC)(**Fig. 1.17**)[58].

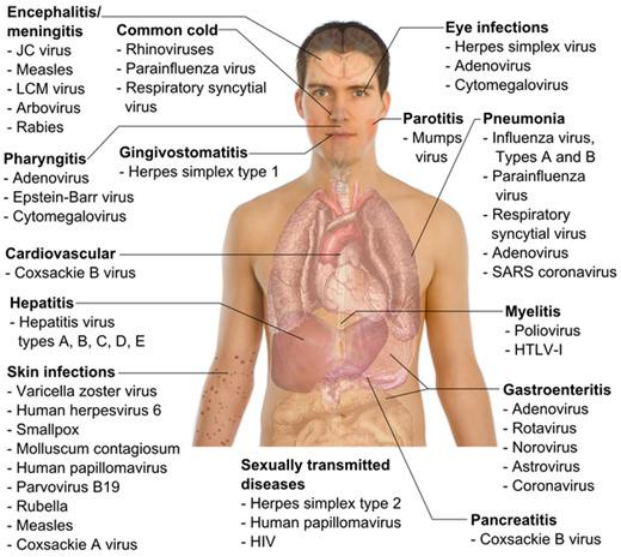

Figure 1.17: *Main types of viral infection and the most notable species involved.*

1.2.1 Infection of oropharynx and respiratory tract

Oropharynx and respiratory tract are the most common sites of infection. Viruses spread through droplets and aerosols, food, water and saliva; through close contact and hands. Similar respiratory symptoms may be caused by many viruses; in contrast, a single virus can cause different symptoms in different people. For example, in some individuals the virus can cause mild upper respiratory infection, in others life-threatening pneumonia.

Symptoms and severity of a viral respiratory illness depend on: virus nature, site of infection (upper or lower respiratory tract), immune status and age of

individual. **Pharyngitis** and other **oropharynx diseases** are common manifestations of viral infection. For example, symptoms such as acute pharyngitis, fever and oral vesicular lesions are characteristic of *coxsackie A virus* (herpangina, hand-foot and mouth disease) and *coxsackie B virus* and *echovirus*. *Herpesviruses* cause local primary infection on oral mucous membrane and face. Latent infection in neurons is followed by a **gingivostomatitis** caused by *herpes virus* and occurs in the form of **herpes labialis**. *Epstein-Barr virus* (*EBV*) and *human herpes virus 6* (*HHV6*) can cause pharyngitis. *Rhinovirus* and *coronavirus* are the predominant cause of the common cold, upper respiratory tract infection.

Both pharingitis and colds can be caused by specific serotypes of *echovirus* and *coxsackievirus*, *adenovirus*, *influenza virus*, *parainfluenza virus* and *respiratory syncytial virus*. Respiratory tract's infections may also degenerate into more serious illnesses. Symptoms of these infections are **bronchitis** (inflammation of bronchioles), **pneumonia** and related conditionats. *Parainfluenza virus* and *respiratory syncytial virus* create more damage to infants and young children, but only cause asymptomatic infections or symptoms of the common cold in adults.

Influenza virus is probably the best known and most feared virus among the common respiratory viruses, because annually you can check the spread of new strains of viruses. The viral agents that cause pneumonia include *adenovirus*, *paramyxovirus* and *varicella-zoster virus* primary infections.

1.2.2 Gastrointestinal infections

Gastrointestinal infections can cause **gastroenteritis**, **diarrhea**, or be asymptomatic. *Norovirus* (*Norwalk virus*), *adenovirus*, *astrovirus*, *rotavirus*, *coronavirus* infect small intestine but not colon, causing damage to the epithelial lining and the intestinal villi and resulting in malabsorption of water

and electrolyte imbalance. *Rotavirus* and *adenovirus 40-41* are the leading cause of infantile gastroenteritis.

1.2.3 Skin infections

Skin viral diseases may be the effect of infections of the mucous membrane or small cuts or skin abrasions (*HSV*), as in the case of a secondary infection after the onset of viremia (*VZV* or *smallpox*) or be the result of an inflammatory response against viral agents (*measles* rash). The classic childhood **exanthems**, accompanied by fever, include exanthema subitum (*HHV6*), erythema infectiosum (*parvovirus B19*) and in unvaccinated children varicella, measles and rubella. *Yellow fever virus (YFV)*, *dengue virus* and other viruses, causing **hemorrhagic fevers**, infect epithelial cells lining the blood vessels and can affect the structure. This produces a hemorrhagic rash with **petechiae** and **ecchymoses**.

1.2.4 Eye infections

Conjunctivitis (pink eye) is a typical feature of many childhood infections, and is caused by specific serotypes of *adenovirus* (*3*, *4a* and *7*), *measles virus* and *rubella virus*. **Keratoconjunctivitis**, caused by *adenovirus* (*8*, *19a* and *37*), *HSV* o *VZV*, affects the cornea and can cause serious damage. *Enterovirus 70* and *coxsackie virus A24* can cause **acute hemorrhagic conjunctivitis**. **Chorioretinitis** is associated with congenital and in immunocompromised persons *CMV* infection.

1.2.5 Organs and tessues infection

Main organs infection can cause significant disease or determine subsequent virus spreading. Symptoms can be the effect of tissues damage or of inflammatory responses. The liver is a major target of many viruses. For example, the **hepatitis** symptoms may be caused by *hepatitis viruses A*, *B*, *C*, *D* and *E* and *yellow fever virus* and these are often associated with infectious

mononucleosis by *EBV* and *CMV* infections. The liver is also the biggest target in disseminated *HSV* infections in infants and children. The heart and other muscles are susceptible to viral infections and the resulting damage. *Coxsackievirus* can cause **myocarditis** or **pericarditis** in infants, children and adults. The *coxsackie B virus* can infect and cause the muscles **pleurodynia** (Bornholm disease). Other viruses (eg *influenza virus* and *CMV*) can infect the heart. Infection of the secretory glands, accessory sex organs and mammary glands causes a contagious spread of the virus (*CMV*, *mumps virus*). For example, **mumps** and epidemic **parotitis** is a viral disease of the human species, caused by the *mumps virus*, whose most typical onset is the painful swelling of the salivary glands (classically the parotid gland). Kidney *CMV* infection and reactivation cause problems in immunocompromised people and are a major cause of failure of kidney transplantation.

1.2.6 Central Nervous System (CNS) infections

Viral infections of the brain and CNS can cause the most serious viral diseases due to CNS importance and to its very limited capacity to repair damage. A virus can spread to the CNS from the blood (*arbovirus*) or macrophages (*acquired human immunodeficiency virus HIV*); from peripheral neurons infection, or it may first infect the skin (*HSV*) or a muscle (*rabies virus*) and then progress to the neurons that innervate the infected area. Virus then infects neurons that express a viral receptor. For example, the temporal lobe is a target in the **encephalitis** by *HSV*, the horn of Ammon in **rabies**, anterior horn of the spinal cord and motor neurons in paralytic **poliomyelitis** (*Enteroviruses*). **Aseptic meningitis** is caused by inflammation and swelling of the meninges that involve the brain and the spinal cord in response to infection by *enteroviruses* (particularly *coxsackievirus* and *echovirus*), *HSV-2*, *mumps virus* or *lymphocytic choriomeningitis virus (LCM virus)*. The disease is usually self-limiting and, unlike bacterial meningitis, resolves without

sequelae unless the virus does not access and infect neurons or brain (**meningoencephalitis**).

Encephalitis and **myelitis** are fatal or cause significant damage and permanent neurological sequelae. *HSV*, *VZV*, *rabies virus*, *California encephalitis virus*, *St. Louis encephalitis virus (SLEV)* and *measles virus* are potential causes of encephalitis. Many *polioviruses* and other *enteroviruses* cause a paralytic disease (myelitis). *HSV* and *VZV* are ubiquitous and usually cause asymptomatic latent infections of the CNS, but can also cause encephalitis. Other neurological syndromes caused by viruses include **HIV dementia**, **Tropical spastic paraparesis** or *human T-lymphotropic virus type I (HTLV-I)*-associated myelopathy, **progressive multifocal leukoencephalopathy** caused by the *papovavirus JC* in immunocompromised people, and **spongiform encephalopathy** (kuru, Creutzfeldt-Jakob syndrome, Gerstmann-Straussler-Scheinker syndrome) that are believed to be caused by prions.

1.2.7 Sexually transmitted diseases

Although sexual transmission is not a very effective way to virus spread, it is the major spread route of *HPV*, *HSV*, *CMV*, *HIV*, *HTLV-1*, *HBV*, *hepatitis C virus (HCV)* and *hepatitis D (HDV)*. *Papillomavirus* and *HSV-2* establish local primary infection causing recurrent disease at the same site. *CMV* and *HIV* enter the bloodstream and infect lymphoid cells, while *HBV* and *HCV* are transported to the liver. These viruses are present in blood, semen and vaginal secretions, through which virus can be transmitted to sexual partners and infants (neonatal or perinatal transmission).

1.2.8 Syndromes with a possible viral etiology

Many diseases cause symptoms or have the epidemiological features or other similar to those of viral infections, or may be the sequelae of viral infections (eg, inflammatory responses to persistent viral infection). These

include **multiple sclerosis**, **Kawasaki disease**, **arthritis**, **diabetes** and **chronic fatigue syndrome**[52]

1.2.9 Chronic and potentially oncogenic infections

Some viruses can cause life-long or chronic infections, where the viruses continue to replicate in the body despite the host's defence mechanisms[59]. Chronic infections are established when the immune system has difficulty in resolving the infection. People chronically infected are known as carriers, as they serve as reservoirs of infectious virus[60]. In populations with a high proportion of carriers, the disease is said to be endemic[61]. In contrast to acute lytic viral infections this persistence implies compatible interactions with the host organism. Persistent viruses may even broaden the evolutionary potential of host species. *CMV* and other *herpesviruses, hepatitis B, C and D viruses* and *retroviruses* cause **chronic productive infections**. *HBV, HCV, EBV, papilloma virus*, and *HTLV-1* are associated with human **tumors**.

Cofactors, chromosomal aberrations, or both, convert a clone of cells, containing a virus, in cancer. *EBV* usually causes **infectious mononucleosis**, but is also associated with **African Burkitt's lymphoma** and **nasopharyngeal carcinoma**, *HTLV-1* is associated with adult **human T cell leukemia**. Many *papillomaviruses (HPV)* cause a simple hyperplasia, characterized by the development of warts; however, many other strains of *HPV* have been linked to cancer in humans (eg, *types 16* and *18* are associated with **cervical cancer**). Chronic infection with *HBV* and *HCV* has been associated with **hepatocellular carcinoma**. *HSV-2* has been associated with **human cervical carcinoma**, most likely as a cofactor[52].

1.3 Antiviral strategies

Effective vaccines have led, or might lead, to the eradication of important viral pathogens, such as smallpox, polio, measles, mumps and rubella. But

other viral diseases, particularly *human immunodeficiency virus (HIV)* and *hepatitis C virus (HCV)*, have so far proved to be intractable to the vaccine approach. The need for effective antiviral drugs is further emphasized by the lack of vaccines for most respiratory-tract virus infections (*adenovirus*, *rhinovirus*, *parainfluenza virus* and *respiratory syncytial virus (RSV)*), the widely occurring *human papilloma viruses (HPV)* and *herpesviruses* (*herpes simplex virus types 1 and 2 (HSV-1,-2)*, *varicellazoster virus (VZV)*, *Epstein–Barr virus (EBV)*, *cytomegalovirus (CMV)*, *human herpesviruses types 6, 7 and 8 (HHV-6, -7, -8)*), and the vast array of *haemorrhagic fever viruses*. And although vaccines have been developed for *hepatitis B virus (HBV)* and *influenza virus types A and B*, their use has not eliminated the need for effective chemotherapeutic agents. Many new antiviral drugs have been licensed in recent years, most of which are used for the treatment of *HIV* infections; of the current repertoire of more than 30 drugs, 16 are anti-*HIV*, 5 are anti-*CMV*, 5 are anti-*HSV* and anti-*VZV*, 1 is anti-*RSV*, 3 are anti-*hepatitis* and 4 are anti-*influenza*. But there is considerable room for improvement, as these compounds are not always efficacious or well tolerated.

The emergence of viral resistance to drugs and drug-related side effects are among the main reasons for further refinement of antiviral drug design and development[62]. The basic strategies that are used to design antiviral drugs include to attack viruses at every stage of their life cycles (**Fig. 1.18**):

1 Entry;
2 Uncoating;
3 Viral components synthesis (through the inhibition of viral enzymes);
4 Assembly;
5 Release phase.

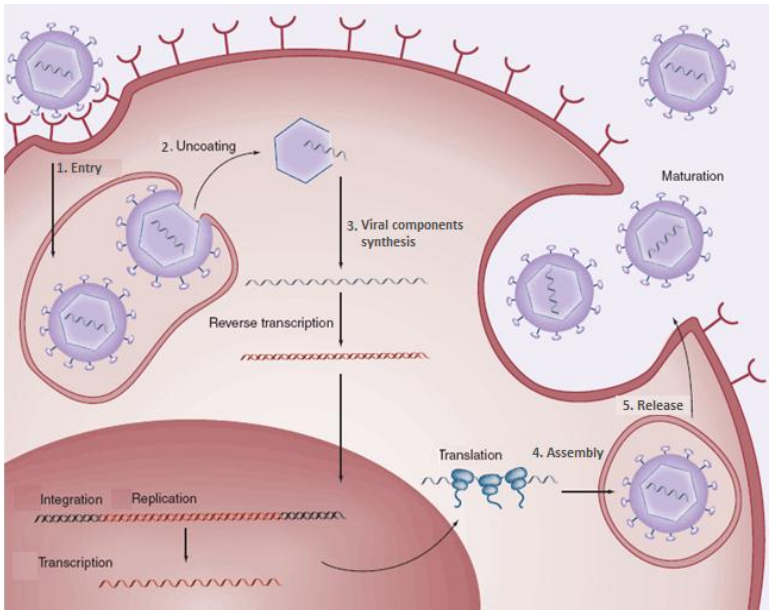

Figure 1.18: *Antiviral strategies*[63].

1.3.1 Entry inhibitors

One anti-viral strategy is to interfere with the ability of a virus to infiltrate a target cell. The virus must go through a sequence of steps to do this, beginning with binding to a specific "receptor" molecule on the surface of the host cell and ending with the virus "uncoating" inside the cell and releasing its contents. Viruses that have a lipid envelope must also fuse their envelope with the target cell, or with a vesicle that transports them into the cell, before they can uncoat. The entry stage of viral replication cycle can be inhibited in two ways:

1. Using agents which act on viral-enveloped proteins. This includes antibodies and synthetic ligands.
2. Using agents which bind to the host cell receptors. This may include natural ligands of the receptor and anti-receptor antibodies.

- **Agents which act on viral-enveloped proteins**

Enveloped proteins or glycoproteins contain oligosaccharide chains (glycans) covalently attached to polypeptide side-chains. Glycoproteins are

often important integral membrane proteins, where they play a role in cell-cell interactions. The N-glycosylation of viral enveloped protein is required for the folding, assembly and infectivity of several viruses.

Belong to this class:

1. *Polyanionic compounds:* For example, polysulphates (such as polyvinylalcohol sulphate, **Fig. 1.19A**), polysulphonates (such as polyvinylsulphonate, **Fig. 1.19B**), polycarboxylates, polynucleotides (such as zintevir, polyoxometalates and negatively charged albumins) have been shown to inhibit HIV replication by preventing virus attachment (adsorption) to the surface of the host cell. All of these negatively charged polymers might be expected to interact with the positively charged amino acids in the V3 loop of the HIV glycoprotein, gp120, which is rich in arginine (R) and lysine (K) residues. In doing so, the polyanions shield the V3 loop and therefore hamper the binding of the HIV virions to heparin sulphate, the primary binding site at the cell surface, before more specific binding occurs with the CD4 receptor on CD4+ cells. Heparan sulphate is widely expressed on animal cells, and is involved in virus–cell binding for a broad array of enveloped viruses, including *HSV* and *dengue virus*. Moreover, these polyanions are not only active against *HIV*, but also against *HSV* and other sexually transmitted disease (STD) pathogens, such as *Neisseria gonorrhoeae* and *Chlamydia trachomatis*[62].

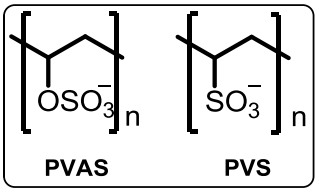

Figure 1.19: *Viral adsorption inhibitors: polyvinylalcohol sulphate (A) and polyvinylsulphonate (B).*

2. *Glycans inhibitors:* Glycans on the viral envelope often have a crucial role in enabling an efficient transmission of the pathogen and/or entry into its susceptible target cells. Some agents interfere with the glycosylation enzymes from the cell, others act by directly binding to the intact glycans on the viral envelope. For example, *MBI-3253* or *Celgosivir* (**Fig. 1.20A**) is an alpha-glucosidase I inhibitor with a potent antiviral activity *in vitro* and *in vivo* against several viruses, including HIV-1, herpes simplex virus (HSV), bovine viral diarrhea virus (BVDV) and HCV. It is currently undergoing phase II development for the treatment of HCV infection. Among agents that interact with the viral-envelope glycans there are *carbohydrate-binding agents (CBAs)*(**Fig. 1.20B**). These compounds have a dual mechanism of antiviral action: first, through direct antiviral activity, by binding to the glycans of the viral envelope and subsequently blocking virus entry, and second, through indirect (additional) antiviral action resulting from the progressive creation of deletions in the envelope glycan shield, thereby triggering the immune system to act against previously hidden immunogenic epitopes of the viral envelope[64-67].

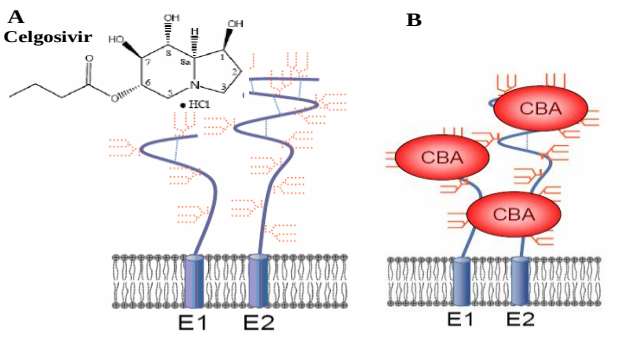

Figure 1.20: *Glycans inhibitors: A. Celgosivir; B. CBAs.*

- **Agents which bind to the host cell receptors**

It is about agents against receptors on the host cell membrane. This interaction results in inhibition of infection during any stage of binding but not in the next phase of post-binding. Belong to this class:

1. *CXCR4 and CCR5 Antagonists:* The chemokine (C-X-C) motif receptor 4 (CXCR4) for T-tropic or X4 HIV strains, and the chemokine (C-C) motif receptor 5 (CCR5) for M-tropic or R5 HIV strains are gp120 co-receptor on the host cell. CXCR4 and CCR5 normally act as the receptors for the C-X-C chemokine, SDF1 (stromalcell- derived factor 1), and the C-C chemokines RANTES (regulated upon activation, normal T-cell expressed and secreted) and MIP1 (macrophage inflammatory protein 1), respectively. The most prominent among the CXCR4 antagonists is the bicyclam *AMD3100* (**Fig. 1.21A**)[62], and the only compound approved by the U.S. Food and Drug Administration (FDA) among the CCR5 antagonists is *Maraviroc* (**Fig. 1.21B**).

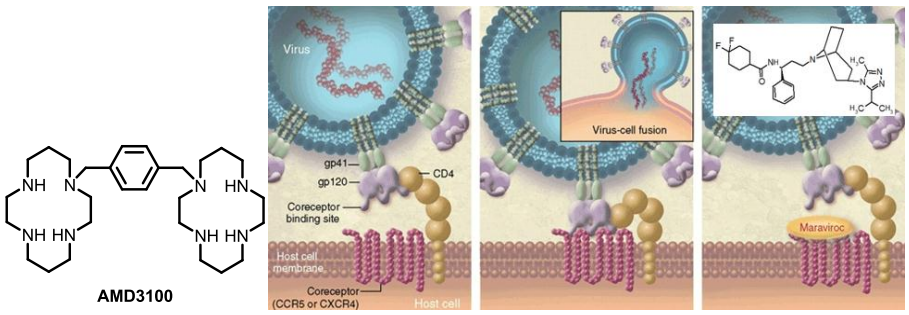

Figure 1.21: *Host cell receptor antagonists: A. AMD3100; B. Maraviroc.*

1.3.2 Uncoating inhibitors

These drugs inhibit the viral genome release and its following replication. Belong to this class:

1. Amantadine *and* rimantadine*:* Have been introduced to combat influenza. Uncoating of viral particles takes place in the host cell endosome. Acidification of the endosome promotes fusion of the viral and endosomal membranes, causing a structural change in the viral hemagglutinin (HA, antigenic glycoprotein on the surface of influenza viruses) and freeing the fusion peptide of its HA2 subunit to interact with the endosome membrane. The concerted structural change of several HA molecules opens up a pore through which the viral RNA passes into the cytosol of the cell (**Fig. 1.22A**).

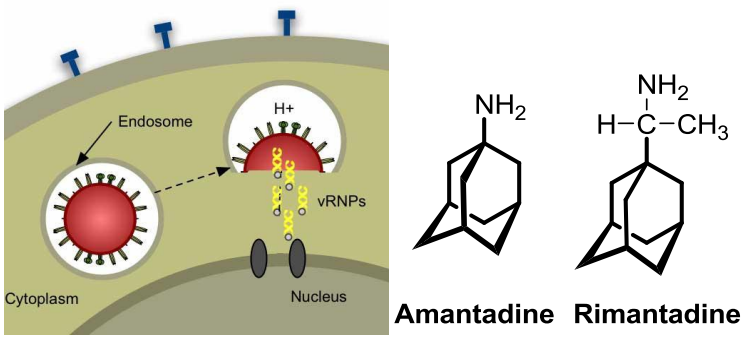

Figure 1.22: *A. Influenza virus uncoating; B. Amantadine and rimantadine structures.*

The precise timing and the location of uncoating depends on the pH-mediated transition of the specific HA molecule involved. The virus-associated M2 ion channel protein allows the influx of H^+ ions into the virion, which disrupts protein-protein interactions, resulting in the release of RNA free of the viral M1 matrix protein. Thus the HA mediated fusion of the viral membrane with the endosomal membrane and the M2-mediated release of the RNA results in the release of the RNA complex into the cytosol. *Amantadine* and *rimantadine* (**Fig. 1.22B**) have been shown to block the ion channel activity of the M2 protein and thus interfere with uncoating[68].

2. *Pleconaril:* Is an antiviral drug being developed by Schering-Plough for prevention of asthma exacerbations and common cold

symptoms in asthmatic subjects exposed to picornavirus respiratory infection. It is active against viruses in the Picornaviridae family, including rhinoviruses, which cause the common cold, and enteroviruses, which can cause diarrhea, meningitis, conjunctivitis, and encephalitis. *Pleconaril* (**Fig. 1.23A**) binds to a hydrophobic pocket in VP1 (**Fig. 1.23B**), the major protein which comprises the capsid (the outer "shell") of picornaviruses. This pocket is similar in most strains of rhinoviruses and enteroviruses. In enteroviruses, this prevents the virus from exposing its RNA, and in rhinoviruses it also prevents the virus from attaching itself to the host cell[69,70].

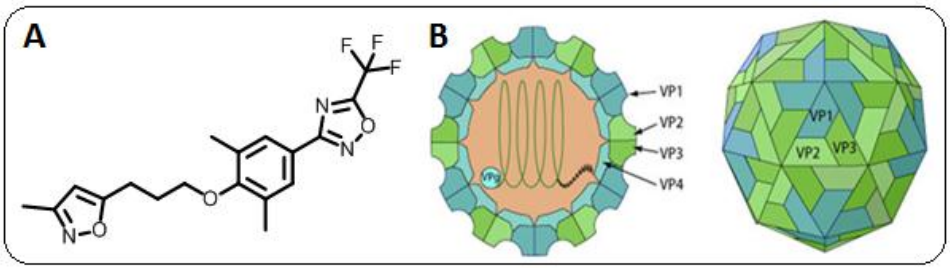

Figure 1.23: *A. Pleconaril structure; B. picornavirus capsid.*

1.3.3 Inhibitors of viral components synthesis

A second approach is to target the processes that synthesize virus components after a virus invades a cell. These inhibitors have the ability to block the function of some viral enzymes preventing some basic steps in the replication process. These inhibitors include:

- **Viral DNA polymerase inhibitors**

Herpesviruses DNA genome can be replicated by the viral DNA polymerase after the latter has been expressed in the virus-infected cell. At present, all the antiviral agents that are available for the treatment of herpesvirus infections are nucleoside analogues (**Fig. 1.24**):

1. *acyclic guanosine analogues*, that is, *acyclovir*, *penciclovir*, *ganciclovir* and their oral prodrud forms *valaciclovir*, *famciclovir* and *valganciclovir*, respectively;
2. *thymidine analogues* such as *brivudin*.

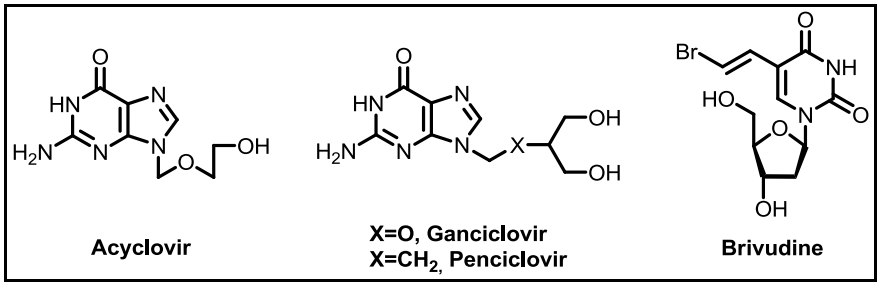

Figure 1.24: *Structures of acyclovir, ganciclovir, penciclovir and brivudine.*

All of these compounds target the viral DNA polymerase, but before they can interact with viral DNA synthesis, they need to be phosphorylated intracellularly to the triphosphate form. The first (and, for *brivudin*, also the second) phosphorylation step is ensured by the HSV- or VZV-encoded thymidine kinase, or the CMV-encoded protein kinase, and is therefore confined to virus-infected cells, which explains the specific antiviral action of the established antiherpetic compounds. Subsequent phosphorylations are achieved by host cellular kinases. In their triphosphate form, the nucleoside analogues interact with the viral DNA polymerase, either as competitive inhibitors or as alternative substrates with respect to the natural substrate (dGTP for the guanosine analogues, dTTP for the thymidine analogues). If the acyclic guanosine analogues act as alternative substrates, their incorporation prevents further chain elongation (**Fig. 1.25**).

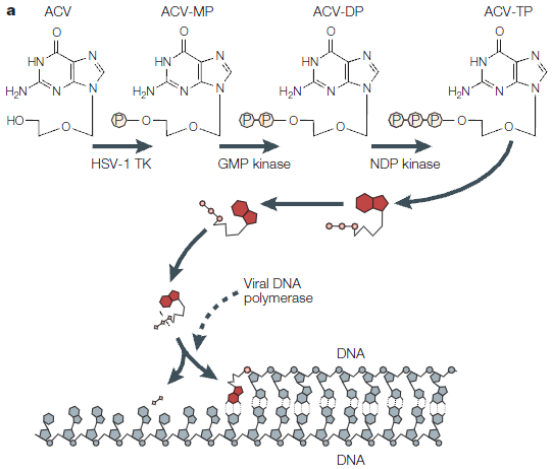

Figure 1.25: *herpesviruses mechanism of action.*

The moderate oral bioavailability of the acyclic guanosine analogues has been improved by formulating them as prodrugs. The success obtained with *acyclovir*, *valaciclovir* and *famciclovir* in the treatment of HSV and VZV infections has impeded further progress in this area. However, *brivudin*, which is considerably more potent than *acyclovir* and *penciclovir* as an anti-VZV agent, represents an important alternative for the treatment of VZV infections[62].

- **Viral RNA polymerase inhibitors**

One of the virus which use RNA polymerase is HCV, a positive-sense single-stranded RNA virus. RNA replication takes places via the viral RNA-dependent RNA polymerase NS5B, which produces a negative-strand RNA intermediate. The negative strand RNA then serves as a template for the production of new positive-strand viral genomes. The HCV polymerase can be viewed as a right hand, where the palm domain contains the active site of the enzyme and where the fingers and the thumb are responsible for the interaction with the RNA. The fingertips are two loops that extend from the fingerdomain and that make contact with the thumbdomain (in the so called

closed conformation). This results in the formation of a tunnel in which the RNA, template as well as the nascent RNA, are contained. In the 'open' conformation, the contact between the finger and the thumbdomain is disrupted; this is the virus inactive conformation[71] (**Fig. 1.26**).

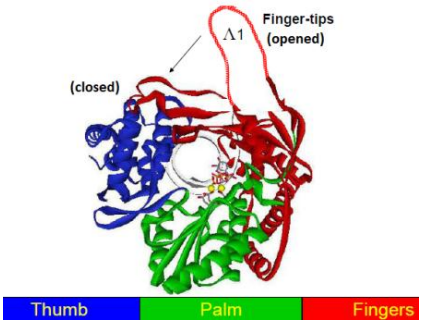

Figure 1.26: *RNA polymerase: opened and closed conformation*[72].

The NS5B RNA dependent RNA polymerase inhibitors are divided into:

1. *Nucleoside inhibitors (NRRIs):* Intracellular phosphorylation of NRRIs (2'-*C* methylcytidine and 2'-*C* methylpurine analogues, **Fig. 1.27**A) to their 5' triphosphate results in the formation of the active inhibitor of the viral polymerase. The compounds are non-obligate chain terminators. RNA elongation may represent the most probable target of 2'-modified nucleotide analogues (**Fig. 1.27B**), because it is more permissive to inhibition than initiation[73].

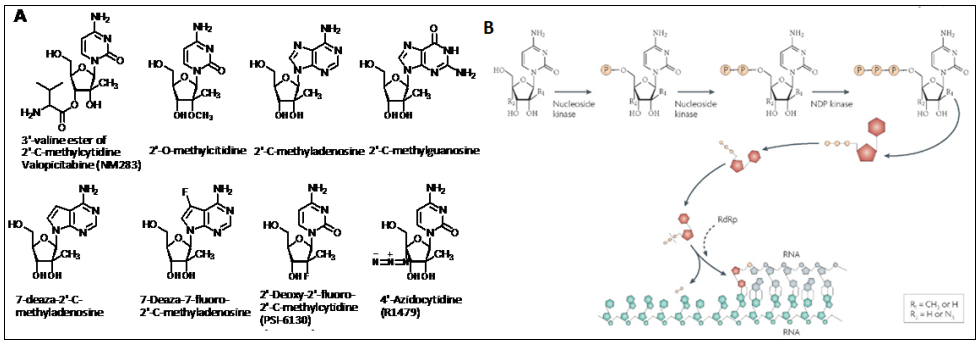

Figure 1.27: *NS5B nucleoside inhibitors: A. Structures; B. Mechanism of action.*

2. *Non-nucleoside inhibitors:* These compounds bind on the surface of the thumbdomain, at a position that is in the "closed" enzyme conformation occupied by one of the fingertips. The binding of the compound to this cavity forces the enzyme in the "open" configuration. A number of structurally unrelated series of non-nucleoside HCV polymerase inhibitors have been reported; these include, but are not limited to, benzimidazoles/diamides (A), disubstituted phenylalaline/thiophene amides (B), benzothiadiazines (C) and benzofurans (D)[71] (**Fig. 1.28**).

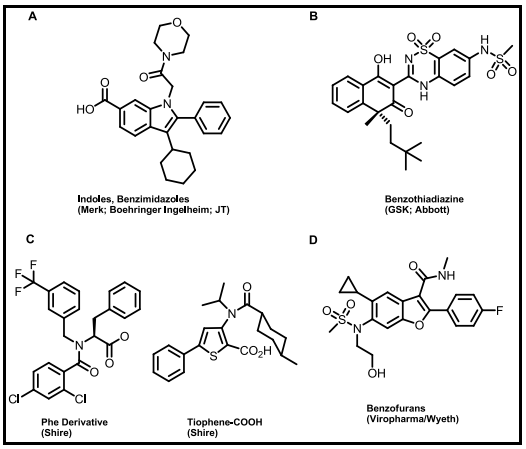

Figure 1.28: *Structures of NS5B non-nucleoside inhibitors.*

- **Reverse transcriptase inhibitors**

Reverse transcriptase (RT) is essential in the replicative cycle of retroviruses, such as HIV, as it synthesizes the proviral DNA, which will then be integrated into the host cell genome and passed on to all of the progeny cells. The RT inhibitors are divided into:

1. *Nucleoside inhibitors:* The substrate (dNTP) binding site of HIV reverse transcriptase (RT) has proved to be an attractive target for HIV nucleoside inhibitors. Six nucleoside analogues have been licensed as anti-HIV drugs: *zidovudine* (*azidothymidine*, *AZT*), *didanosine* (*dideoxyinosine*),

zalcitabine (*dideoxycytidine*), *stavudine* (*didehydrodideoxythymidine*, *d4T*), *lamivudine* (*3′- thiadideoxycytidine*) and *abacavir* (**Fig. 1.29A**), and several others, such as *emtricitabine* and *amdoxovir*, are in advanced development. All of these dideoxynucleoside analogues act according to a similar 'recipe', as exemplified for *AZT*. They must be phosphorylated consecutively inside the host cell by three cellular kinases (a nucleoside kinase, a nucleoside 5′-monophosphate kinase and a nucleoside 5′-diphosphate kinase) to form the corresponding 5′-triphosphate derivative, which can interact, as a chain terminator, with the reverse transcription (RNA→DNA) reaction (**Fig. 1.29B**).

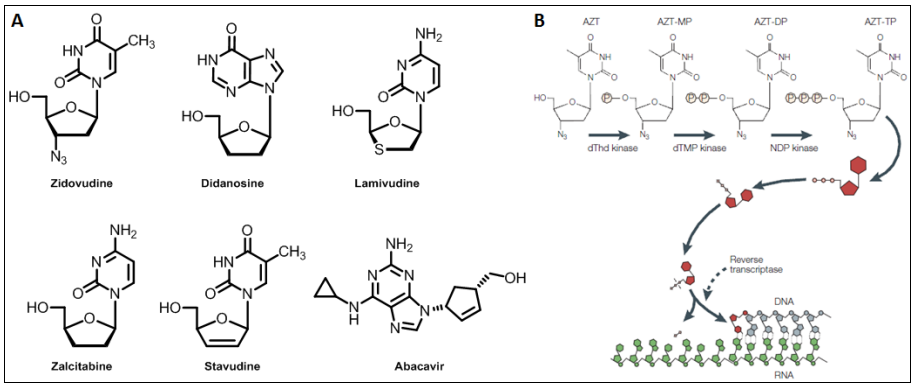

Figure 1.29: *A. Nucleoside inhibitors of RT; B. Mechanism of action.*

2. <u>*Non-nucleoside reverse transcriptase inhibitors, NNRTIs*</u>*:* Interact with an allosteric, non-substrate binding ('pocket') site on HIV-1 RT. At present, only three NNRTIs (*nevirapine*, *delavirdine* and *efavirenz*) have been formally licensed (**Fig. 1.30**), although several others are in the developmental stage[62].

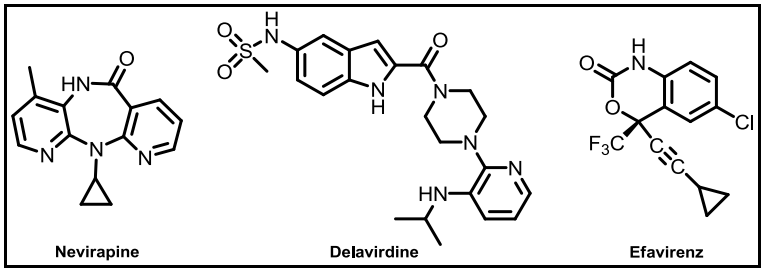

Figure 1.30: *Current clinically used NNRTIs.*

- **Integrase inhibitors**

Gene expression (that is, transcription to viral RNA) of the genome of retroviruses, such as HIV, is not possible without integration of the proviral DNA into the host chromosome (**Fig. 1.31A**). So, the enzyme involved (integrase) has been considered an attractive target for chemotherapeutic intervention. Inhibiting integrase from performing its essential functions therefore blocks stable integration of HIV-1 DNA into the host genome and prohibits the establishment of viral latency within the host cell, preventing high-level HIV-1 replication and infection of new cells by competent virus. At present, the only compounds that qualify as genuine integrase inhibitors are the diketo acids *raltegravir* and *elvitegravir* (**Fig. 1.31B**)[74].

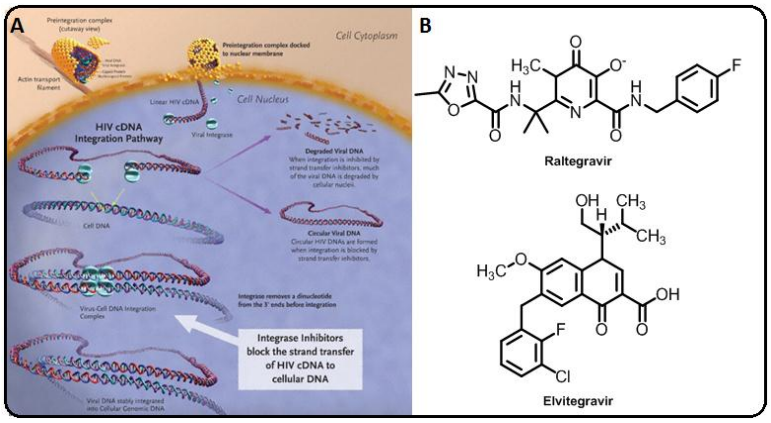

Figure 1.31: *A. Integrase inhibitors: Mechanism of action (A) and structures(B).*

- **Helicase inhibitors**

Helicase are motor proteins that move directionally along a nucleic acid phosphodiester backbone, separating two annealed nucleic acid strands (i.e., DNA, RNA, or RNA-DNA hybrid) using energy derived from ATP hydrolysis. For example, the NS3 HCV region comprises a multifunctional protein that contains a serine protease at the N-terminus (that cleaves the viral polyprotein into functional proteins essential for replication) and a NTP-dependent helicase at the C-terminus. HCV nonstructural protein 3 (NS3) RNA helicase is a promising target for developing new therapeutics. Belong to this class of inhibitors: QU663, a potent new selective inhibitor of the HCV helicase NS3, competing with the nucleic acid substrate without affecting ATPase function, even at high concentrations.

QU663 (**Fig. 1.32**) is one of a new generation of small-molecule nucleotide-mimicking inhibitors which are potential anti-HCV agents. Also 4,5,6,7-tetrabromobenzotriazole (TBBT) (**Fig. 1.32**) hitherto known as a potent highly selective inhibitor of protein kinase 2, is a good inhibitor of the helicase, but not NTPase, activity of hepatitis C virus NTPase/helicase.[75,76]

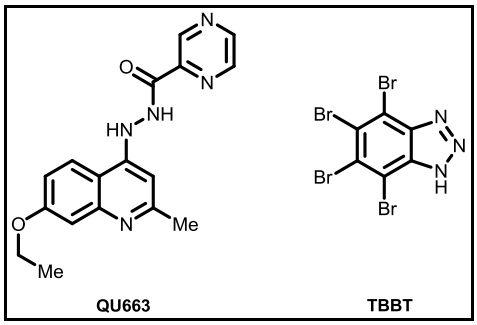

Figure 1.32: *Helicase inhibitors: QU663 and TBBT.*

- **The serine protease inhibitors**

Viral proteases are crucial in the life cycle of many viruses, including retroviruses such as HIV, herpesviruses, picornaviruses such as rhinovirus, and flaviviruses such as HCV. Viral proteases have therefore been favoured as targets for antiviral agents. Proteases cleave newly expressed precursor polyproteins into smaller, mature viral proteins, termed 'functional' (if endowed with enzymatic activity) or 'structural' (if part of the virion structure). For example, protease inhibitors licensed at present for the treatment of HIV infection, namely *saquinavir*, *ritonavir*, *indinavir*, *nelfinavir*, *amprenavir and lopinavir*, share the same structural determinant (**Fig. 1.33A**), a hydroxyethylene core (instead of the normal peptidic linkage) that makes them non-scissile peptidomimetic substrate analogues for the HIV protease. Non-peptidic inhibitors of HIV protease, have cyclic urea, 4-hydroxycoumarin, L-mannaric acid or 4-hydroxy-5,6-dihydro-2-pyrone as the central scaffold instead of the peptidomimetic hydroxyethylene core (**Fig. 1.33A**); for example, *tipranavir*[62].

Among the HCV protease (NS3/4A) inhibitors (**Fig. 1.33B**) there are: the macrocyclic peptidomimetic *BILN-2061* (*ciluprevir*), a non-covalent inhibitor of NS3-4A protease inhibitor (the first HCV protease inhibitor to enter clinical trials); *telaprevir (VX-950)*, a covalent-reversible peptidomimetic inhibitor; *boceprevir (SCH-503034)*, an oral protease inhibitor and *SCH6 (SCH446211)*, a substrate-based inhibitor. Some of these compounds have been forwarded to later stages of development and are now in advanced clinical trials[71,77].

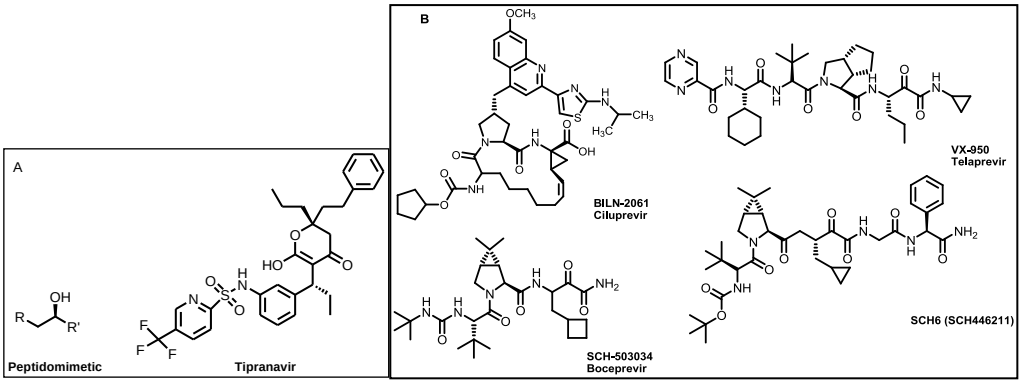

Figure 1.33: *HIV (A) and HCV (B) protease inhibitors.*

1.3.4 Assembly inhibitors

These inhibitors prevent the assembly of viral genome and proteins into mature virus particles. Belong to this class antibiotic *rifampicin* (**Fig 1.34**) that reversibly block the cytoplasmic assembly of vaccinia virus (dsDNA virus). The target of rifampin is a 65-kDa, late structural viral protein, referred to as p65, encoded by the vaccinia virus gene D13L. At inhibiting concentrations, the membranes associated with the viral factories are irregularly shaped, and crescents and spherical, immature particles do not form. These altered structures have been referred to as rifampin bodies. The effects of *rifampin* are rapidly reversible, and within minutes after its removal, the membranes around the *rifampin* bodies acquire their usual convex shape and normal infectious IMVs are formed[78].

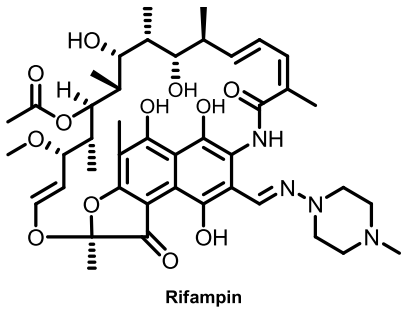

Figure 1.34: *Rifampin structure.*

1.3.5 Release phase inhibitors

The final stage in the life cycle of a virus is the release of completed viruses from the host cell, and this step has also been targeted by antiviral drug developers. Two drugs named zanamivir (Relenza) and oseltamivir (Tamiflu) (**Fig. 1.35**) that have been recently introduced to treat influenza prevent the release of viral particles. Influenza virus (both A and B) has adopted a unique replication strategy by using one of its surface glycoproteins, haemagglutinin, to bind to the target-cell receptor, which contains a terminal sialic acid. The other surface glycoprotein, neuraminidase, cleaves off the terminal sialic acid of the host cell receptor, allowing virus particles to leave the cell after the viral replicative cycle has been completed. The viral neuraminidase is therefore needed for the elution of newly formed virus particles from the cells. In addition, the viral neuraminidase might also promote viral movement through the respiratory tract mucus, thereby enhancing viral infectivity. So, influenza viral neuraminidase has been envisaged as a suitable target for the design of specific inhibitors. Computer-assisted drug design, based on the crystal structure of the influenza viral neuraminidase, led to the identification of *zanamivir* as a specific and potent inhibitor of the enzyme, and of the *in vitro* and *in vivo* replication of both influenza A and B virus. It was tailored to interact with conserved amino-acid residues within the active site of influenza A and B viral neuraminidase and the drug has been licensed for clinical use. *Zanamivir* has to be given topically (by inhalation), owing to its poor oral bioavailability. So an orally bioavailable neuramidase inhibitor, *oseltamivir*, was developed[62].

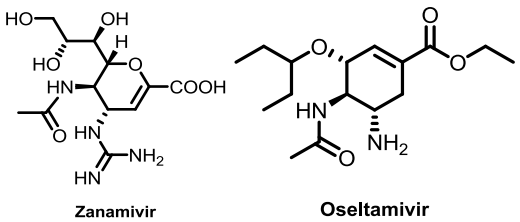

Figure 1.35: *Neuramidase inhibitors.*

1.3.6 Arbidol: A broad-spectrum antiviral compound that blocks viral entry and replication

Many new antiviral drugs have been licensed in recent years, most of which are used for the treatment of HIV infections; of the current repertoire of more than 30 drugs, 16 are anti-HIV, 5 are anti-CMV, 5 are anti-HSV and anti-VZV, 1 is anti-RSV, 3 are anti-hepatitis and 4 are anti-influenza. But there is considerable room for improvement, as these compounds are not always efficacious or well tolerated. The emergence of viral resistance to drugs and drug-related side effects are among the main reasons for further refinement of antiviral drug design and development[62]. The broad-spectrum antivirals are less prone to developing drug resistance but their efficiency is usually a trade-off between some cytotoxicity and anti-viral effects. Given the shortcomings with targeted antivirals, therapeutic regimens have in some cases shifted towards complementing enzyme inhibitors with less specific agents like inhibitors of viral fusion or viral co-receptors. Combination therapy by drugs with different modes of action and resistance profiles could be beneficial for a number of viral infections.

One of antiviral agents that has aroused interest for its broad-spectrum of activity is Arbidol (ARB, **Fig. 1.36**). Arbidol (ethyl-6-bromo-4 [(dimethylamino)methyl]-5-hydroxy-1-methyl-2-[(phenylthio)methyl]-indole-3-carboxylate hydrochloride monohydrate) is an indole compound developed by the Russian Research Chemical Pharmaceutical Institute[79].

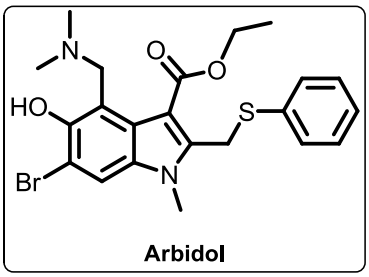

Figure 1.36: *Arbidol structure.*

This indole compound was certified for use in medicine for the prophilaxis and treatment of influenza caused by viruses of antigen types A and B and other acute respiratory viral infections. Beside this, the drug can also be administered for the complex therapy of patients with chronic bronchitis, pneumonia, or a recidivist HSV infection, for prophylaxis of post-operational infections, and for normalization of the immune status of patients, including those after cardiac surgery operations[80].

Arbidol displays a variety of biological effects such as antiviral, anti-carcinogenic, antioxidant, radioprotective and immunostimulative effects, and it is also an interferon-inducer[81]. The mechanism of antitumoral activity of ARB is unknown but some studies have demonstrated that Arbidol has inhibitory effects on the development of a massive tumor induced in mice, probably, via the activation of immunological reactivity. Although Arbidol possesses a number of useful pharmacological properties, the antitumoral, immunomodulating and anti-oxidant aspects of its action are so far inconclusive; whereas its antiviral activity is very interesting.

In fact, it exhibits a wide range and potent antiviral activity against a number of viruses (**Fig. 1.37**) including *influenza A (H1N1, H2N2 and H3N2)*, *B* and *C viruses*, *respiratory syncytial virus (RSV)*, *adenovirus type 7*, *coxsackie B3 virus*, *parainfluenza type 5* and *rhinovirus type 14*, *avian coronavirus*, *infectious bronchitis virus* and *Marek disease virus*, *hepatitis B virus* and *hepatitis C virus*. There are presently no published indications of ARB activity against other medically important viral pathogens like HIV-1, SARS coronavirus or Ebola virus. The extensive list of ARB-sensitive viruses encompasses RNA and DNA viruses, enveloped and non-enveloped viruses and pH-dependent and pH-independent viruses emphasizing a broad spectrum of ARB antiviral activity.

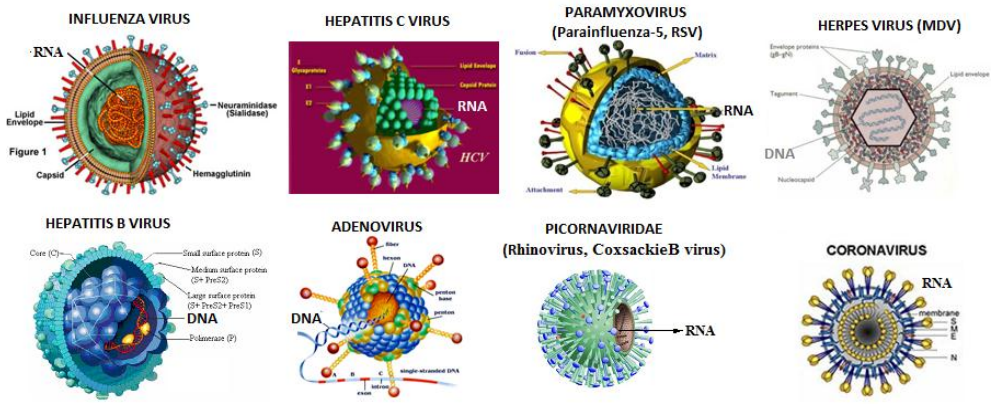

Figure 1.37: *Broad spectrum of ARB antiviral activity.*

The wide spectrum of ARB's activity suggests that ARB targets common critical step(s) in virus – cell interaction.

The anti-viral mechanism involves ARB inhibition of membrane fusion between the virus and the plasma membrane and in some viruses (*Influenza viruses and HCV*) also between the virus and endocytic vesicle membranes, resulting in a block of virus entry into target cells and uncoating[79].

Recent studies conducted on this compound have shown that ARB is an inhibitor of both fusion and replication on *HCV* and it inhibits acute and chronic *HCV* infection. Moreover, it has been shown that ARB inhibits the cell entry of *HCV* pseudoparticles of genotypes 1a, 1b, and 2a in a dose-dependent fashion. It is also conceivable that ARB could inhibit aspects of the *HCV* life cycle that are dependent on cell membranes. For example, ARB antiviral activity toward HCV fusion is due probably to a direct effect of ARB on virus-cell membrane interactions where ARB intercalates into membranes and adopts a consistent orientation with the formation of an 'ARB cage'. This leads to excessive stabilization of cell membranes, which become resistant to HCV fusion. Moreover, ARB-induced inhibition of *HCV* non-structural protein interactions with endoplasmic reticulum (ER) membranes might also contribute to suppression of *HCV* replication. Therefore, in terms of *HCV*

acute infection, the predominant mechanism of action of ARB is likely to be inhibition of fusion; whereas in terms of chronic infection, ARB inhibition of the *HCV* replication complex association with membranes could be the predominant mode of *HCV* suppression.

In conclusion, the inhibitory effect appears to be due to the interaction of ARB with membranes and to subsequent ARB-induced membrane alterations (**Fig. 1.38**), but the nature of the membrane modifications require further study.

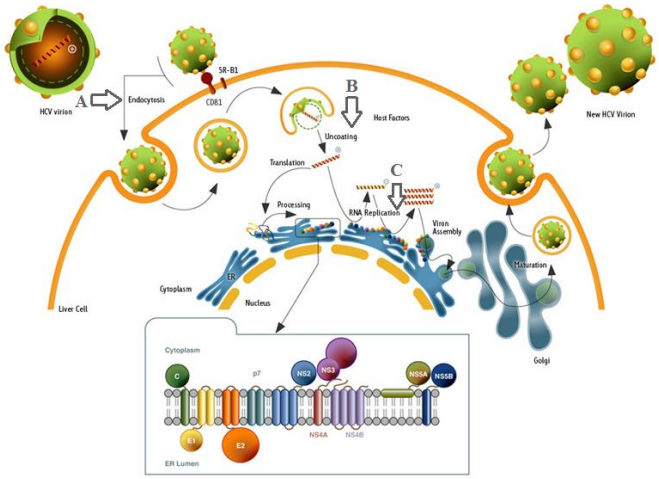

Figure 1.38: *ARB inhibits aspects of the HCV life cycle that are dependent on cell membranes: (A)entry, (B)uncoating, (C)replication.*

In vitro biochemical studies revealed association of ARB with membranelike environments such as detergents and with lipid membranes. This association was particularly prominent at acidic pH which is optimal for viruses-mediated fusion. Several studies have shown that the affinity of ARB for lipid membranes could account for its antiviral actions, together with a differential level of interaction with key motifs in glycoproteins of different viruses.

In fact, a specific effect of ARB on viral glycoproteins themselves cannot be excluded. Therefore, Arbidol might achieve a certain level of specificity toward some viral glycoproteins, in particular, HCV (E1 and E2) and influenza (hemagglutinin) glycoproteins[82-84].

CHAPTER 2

RESULTS AND DISCUSSION

2 AIM OF PROJECT

The present Ph.D. project was divided into different work parts, in a way that helps to understand and define the the goals of this project. In particular:

I) Design, synthesis and characterization of Arbidol analogs using a convenient five-step scheme.

II) Optimization of an alternative scheme, a convenient method to obtain derivatives with different scaffolds in 2-position in one step of reaction.

III) Biological assays on anti-HCV and anti-HSV activity of Arbidol derivatives.

IV) Evaluation of mechanism of Arbidol anti-influenza action.

V) Synthesis and characterization of a P.E.T. radiotracer for tumor hypoxia: *1- (5- [18F] Fluoro-5-deoxy-α-D-arabinofuranosyl) -2-nitroimidazole* or ^{18}F-FAZA.

In addition, V step was made during a sixth-month period in the last year as a Ph.D visiting student at the Aberdeen University (Scotland) and it will be discussed in the next section.

2.1 Synthesis of Arbidol analogs using a convenient five-step scheme

The known biological properties of Arbidol led us to focus on its derivatives as potential antiviral agents. We designed and synthesised several novel ethyl 1H-indole-3-carboxylate derivatives, using ARB as *lead compound*, and we studied then structure-activity relationship.

2.1.1 Design of derivatives

The general design of ARB analogs was guided by the modular composition of this synthetic product. As mentioned in the previous chapter, ARB antiviral activity toward viruses is due probably to a direct effect of ARB on virus-cell membrane interactions, where ARB intercalates into membranes and induces membrane alterations. This leads to excessive stabilization of cell membranes, which become resistant to virus fusion and in some cases (HCV) to virus replication. Its tropism for membranes or membrane like environments is due to ARB's indole-derived structure and to its interaction with lipids via other hydrophobic and aromatic moieties on the molecule (**Fig. 2.1**).
In particular:

- The ***indole ring*** exhibits a preference for membrane interfaces, due to its flat rigid structure and to its aromaticity and establishes cation–π interactions with the positively charged quaternary ammonium lipid headgroups.

- The ***S-phenyl group*** could interact with the hydrophobic fatty acid chains of phospholipids inside the bilayer.

- The ***amino groups*** could bind the phosphate moieties of phospholipids, establishing a salt bridge between two adjacent phospholipid molecules as an ion pair complex. At low pH, these interactions increase for the protonation of the amino groups.

- The ***ester group*** could be a substrate for hydrolysis *in vivo*, leading to intracellular accumulation of the cleaved compound. In light of the above considerations, ARB may be considered a prodrug which is chemically converted into an active drug by cellular metabolic processes[82,83].

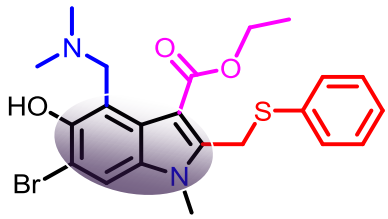

Figure 2.1: *Groups responsible of ARB interaction with membranes.*

In order to maintain antiviral activity we preserved the groups responsible of Arbidol interaction with membranes: indole ring, S-phenyl group, ester group and amino group. In particular, the first series of compounds contains analogs whose structures are closely related to ARB. The indole building block was simplified (**Fig. 2.2**) by:

- elimination of *hydroxy* and *bromo* groups at the 5- and 6-positions of the indole ring;
- shift of *amino group* form 4-position to 5-position to evaluate the influence of the polar group;
- introduction of *different substituents* at the 2- and 5-position of the indole ring to investigate the influence of these variations on antiviral activity.

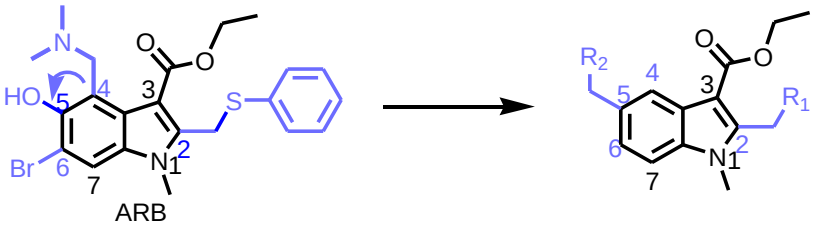

Figure 2.2: *Major changes on lead compound Arbidol.*

In order to examine whether the nature of the amino group could have an effect on the potential anti-HCV activity, we introduced a variety of amine scaffolds, including imidazole, pyrrolidine, dimethylamine, 4-methyl piperazine, morpholine and homopiperazine (**R_2**). In literature, it was demonstrated that the oxidation of sulfide reduced the cellular toxicities and

kept up or increased the antiviral activities[5]; on this basis, we synthesized 8 compounds with phenylsulfonylmethyl groups at the 2-position (**9a$_{1–6}$**).
Subsequently, to investigate the influence of changes to the steric environment and the role of phenylthiomethyl group (**9c$_{1–2}$**) and/or phenylsulfonylmethyl group on the antiviral activity, we introduced the methyl group at the 2-position (**9b$_{1–2}$**). Other changes concerned the introduction of different lipophilic groups at the 2-position such as the o-phenylbenzyl group (**9d$_{1–2}$**) and farnesyl group (**9e$_{1–2}$**) [84]. On the basis of previous data, compounds **9a$_{1–6}$**, **9(b-d)$_{1–2}$**, **9e$_1$** were synthesised, their structures are listed in **Table 2.1**.

Table 2.1: *Structures of compounds 9a$_{1–6}$, 9(b-d)$_{1–2}$, 9e$_1$.*

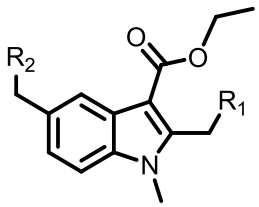

Compound	R_1	R_2
9a$_1$	Phenylsulfonyl	Dimethylamino
9a$_2$	Phenylsulfonyl	Pyrrolidinyl
9a$_3$	Phenylsulfonyl	4-Methyl piperazinyl
9a$_4$	Phenylsulfonyl	Morpholino
9a$_5$	Phenylsulfonyl	Homopiperazinyl
9a$_6$	Phenylsulfonyl	Imidazolyl
9b$_1$	Hydrogen	Dimethylamino
9b$_2$	Hydrogen	Pyrrolidinyl
9c$_1$	Phenylthio	Dimethylamino
9c$_2$	Phenylthio	Pyrrolidinyl
9d$_1$	Phenylbenzyl	Dimethylamino
9d$_2$	Phenylbenzyl	Pyrrolidinyl
9e$_1$	Farnesyl	Pyrrolidinyl

2.1.2 Synthetic approach

In the development and validation of various synthetic schemes for the synthesis of Arbidol derivatives, the molecular diversity was taken into consideration as a fundamental concept as well as the easy implementation. Therefore, to obtain the derivatives we emphasized the importance of decorating the scaffold ethyl 1*H*-indole-3-carboxylate with different building blocks in 2- and 5-position.

The preparation of these derivatives was based on design of a synthetic scheme to obtain products in short reaction times and in high yields. Therefore, **Scheme 1** was designed and optimized.

This scheme has the advantage of providing a common intermediate used in the last step reaction to obtain compounds with different amines in 5-position on indole ring and the same lipophilic group in 2-position.

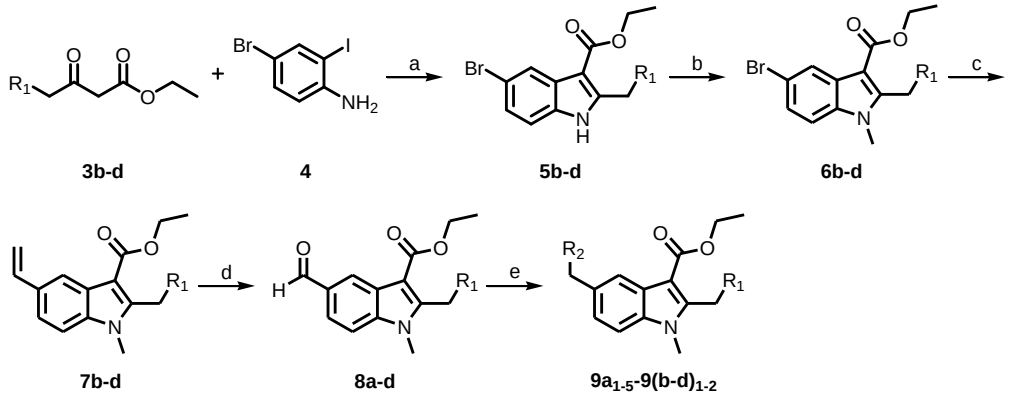

Scheme 1. *Synthesis of target compounds. Reagents and conditions: (a) CuI, BINOL, Cs_2CO_3, DMSO, 50°C, 5–7h, 48–56%; (b) CH_3I, KOH, DMF, 0°C, 1–2h, 92–97%; (c) potassium vinyltrifluoroborate, 6 mol% $PdCl_2$, 18 mol % PPh_3, Cs_2CO_3, THF/H_2O 9:1; 85°C, 20–22 h, 80–86%; (d) Method A: OsO_4, 2,6-lutidine, dioxane, $NaIO_4$ in H_2O, rt, 20min, 90–95%; Method B: OsO_4, $K_3Fe(CN)_6$, K_2CO_3, $Pb(OAc)_4$, Dioxane/H_2O (1:1), 53%; (e) aliphatic amine, acetic acid, THF, $NaB(OAc)_3H$, MW, 100–130 °C, 20min, 75–95%.*

The synthesis of target compounds **$9a_{1–5}$** and **$9(b\text{-}d)_{1–2}$** was achieved using a convenient five-step procedure starting from 4-bromo-2-iodoaniline and appropriate β-keto esters (**3b-d**), as depicted in **Scheme 1**.

Moreover, since β-keto esters **3c**, **3d** and **3e** are not commercially available, these compounds have been synthesized using two synthetic schemes: **Scheme 2** and **Scheme 3**.

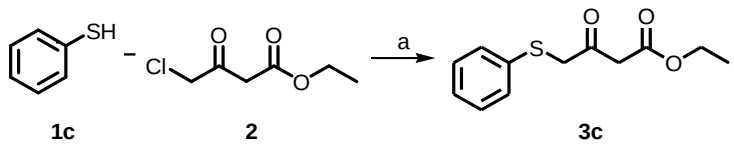

Scheme 2. *Synthesis of ethyl 3-oxo-4-(phenylthio)butanoate 3c. Reagents and condition: (a) KOH, methanol, rt, 6h, 94%.*

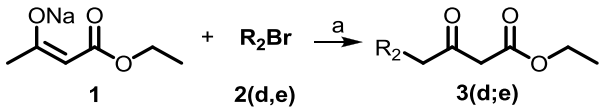

Scheme 3. *Synthesis of 3(d,e) β-keto esters. Reagents and condition: (a) (n-Bu)Li, THF, 0°C,1h, 81-90%.*

In the **Scheme 2**, the thioether **3c** was prepared via etherification of ethyl 4-chloroacetoacetate **2** with thiophenol **1c** (**Scheme 2**).

In the **Scheme 3**, coupling of the dianion (readily prepared by treatment of commercially available sodium ethyl acetoacetate with butyllithium) with brominated compounds R_2Br (**2d** and **2e**) leads to the appropriate β-keto esters **3d** and **3e**. The compound **3e** was used in another synthetic scheme, optimized during the second-third year of my Ph.D period for the synthesis of product **$9e_1$**; instead the other β-keto esters **3c**, **3d** and the commercially available compound **3b** were used in the **Scheme 1**.

The compounds **3b-d** were treated with 4-bromo-2-iodoaniline **4** in a copper-catalyzed Ullmann-type coupling reaction to give the key intermediates **5b–d**. This is the key step in the synthetic scheme because it leads to the synthesis of

the intermediates **5b-d** with indole core and with a substituent R_1 in 2-position. The N-alkylation of compounds **5b–d** with iodomethane using the procedure of Kikugawa afforded in high yields the compounds **6b–d**.

These compounds were subsequently subjected to a Suzuki–Miyaura cross-coupling reaction with potassium vinyltrifluoroborate, affording the intermediates **7b–d** in good yields[84].

Several trials were made before finding the method to obtain compounds **7b-d** with better yields and lower reaction time.

The **Method A** was the first to be tested because it has the advantage to give intermediates **8b-d** with aldehyde group in 5-position, directly from compounds **6b-d**, bypassing the vinylation. Sequential treatment of **6b** with KH and *n*-BuLi followed by the addition of DMF gave 5-formylindole **8b** in 30% yield. The low yield (30%) of this reaction step shifted attention to a vinylation followed by oxidation to aldehyde[86].

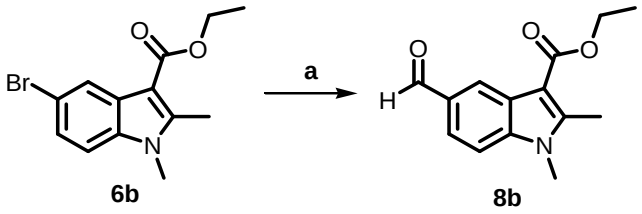

6b **8b**

Method A. *Synthesis of compound 8b. Reagents and conditions: (a) (1) KH (1.13 equiv.), dry ether,0°C, 15min.; (2) n-BuLi (2.13 equiv.), -78°C, 30min.; (3) DMF (2 equiv.), -78°C, 1h, 30%.*

The validation of vinylation was performed in a rigorous manner with an experimental design in which the variation of different parameters was considered, according to methods already described in the literature: nature of substrate carrying vinyl group, stoichiometry of reagents, reagents, solvents, reaction time and temperature. The reaction was carried out using as vinyl boronic acids tributyl(vinyl)stannane or potassium vinyltrifluoroborate (different equivalents), several palladium catalysts such as $Pd(PPh_3)_2OAc$ or

$PdCl_2/PPh_3$, different reaction time and degree. These modifications of reaction conditions are defined in the **Table 2.2** as *method B, C* and *D*[87-88].

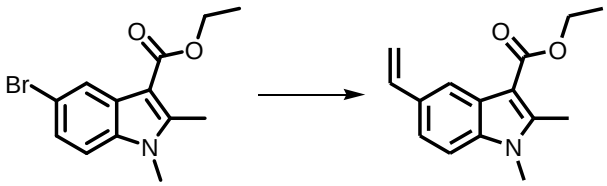

6b **7b**

Method	Reagent	Catalyst	Solvent	°C	Time	Yield
B	tributyl(vinyl)stannane (1.1 equiv.)	$Pd(PPh_3)_2OAc$ (0.025 equiv.)	Toluene	110/ rt	64h	40
C	Potassium vinyltrifluoroborate (1 equiv.)	$PdCl_2/PPh_3/Cs_2CO_3$ 2mol%:6mol%:3equiv	THF/H_2O 9:1	85	22h	60
D	Potassium vinyltrifluoroborate (2.5 equiv.)	$PdCl_2/PPh_3/Cs_2CO_3$ 6mol%:18mol%:3equ.	THF/H_2O 9:1	85	22	80

Table 2.2: *Tested methods of vinylation.*

The best conditions, after these trials, were found and they are those outlined in the *method D*. The application of *method D* on compounds **6b-d** led to the synthesis of compounds **7b-d** in high yields.

The combination of osmium tetroxide and sodium periodate (Lemieux–Johnson oxidation) efficiently achieved both the oxidative cleavage of the vinyl group to an aldehyde group and the oxidation of the sulfide group of compound **7b** to sulfonyl group, thereby yielding the compounds **8(a,b,d)** (*method A*). Synthesis of aldehydic compound **8c** was obtained using a Yamamoto dihydroxylation (*method B*): OsO_4 (0,1 equivalent) as oxidant agent, $K_3Fe(CN)_6$ (3 equivalent) as co-oxidant (to carry out the diol), K_2CO_3 (3 equivalent) as base, Dioxane/H_2O (1:1) as solvent. Then, for the oxidative cleavage we used $Pb(OAc)_4$ (4 equivalent) instead of $NaIO_4$. Lead (IV) acetate was used for the cleavage of the diol in place of $NaIO_4$ which had the disadvantage, in combination with OsO_4, to oxidize also the sulfur group of

phenylthiomethyl group in 2-position[89-90]. In this way we obtained compounds **8c** and **8a** in yield of 53% and 5%, respectively.

Finally, we synthesised the target compounds **$9a_{1–5}$** and **$9(b\text{-}d)_{1–2}$** via a rapid microwave-assisted reductive amination procedure that involves the formation of an imine and subsequent reduction with $NaB(OAc)_3H$ in a one-pot reaction. To obtain compound **$9a_5$**, we used N-Boc protected homopiperazine, which was synthesized according to **Scheme 4**.

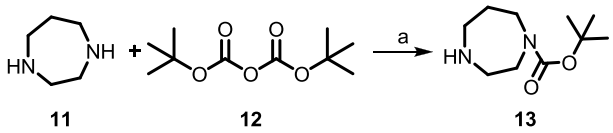

Scheme 4. *Synthesis of N-Boc homopiperazine 13. Reagent and condition: (a) dichloromethane, 0°C, 1h, 88%.*

Imidazole could not be introduced into the 5-position by direct reductive amination with **8a**. Instead, it was realized through a two-step sequence beginning with the reduction of the aldehyde group of compound **8a** to an alcohol group to obtain the intermediate **10a**. This was followed by treatment of **10a** with imidazole and 1,1-carbonyldiimidazole in acetonitrile to generate the derivative **$9a_6$** in good yield (**Scheme 5**)[85].

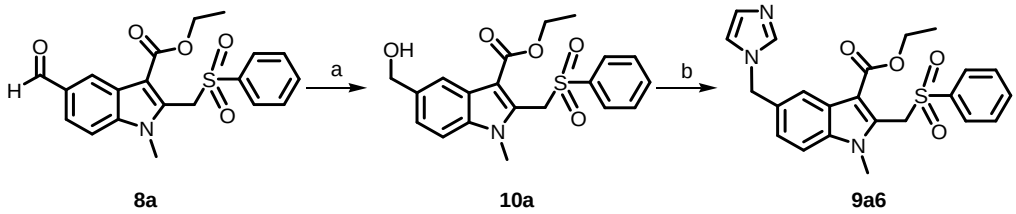

Scheme 5. *Synthesis of compound $9a_6$. Reagents and conditions: (a) $NaBH_4$ in methanol, THF, rt, 1 h, 91%; (b) imidazole, 1,1-carbonyldiimidazole, acetonitrile, reflux, 16 h, 67%.*

Compound **9e$_1$** could not be synthetized with Scheme 1. Therefore, for this synthesis the scheme below was used.

2.2 Alternative synthetic scheme

In order to have greatest speed in the target compounds synthesis, during the second year and the first part of third year, another synthetic scheme was optimized (**Scheme 6**). This scheme, unlike **Scheme 1**, is convenient to obtain derivatives with the same amino group in 5-position on indole ring but different substituents in 2-position.

The starting material of this synthetic scheme is **PABA** (p-amino benzoic acid). In a seven-step synthesis, this compound led to the synthesis of N-methyl 2-iodioaniline replaced in *para*-position with the appropriate amino group (**20**). The latter, interacting with various β-keto esters, will lead to the synthesis of derivatives with different groups in 2-position (R_1). Therefore, we can say that the **Schemes 1** and **6** are both important for the synthesis of derivatives with ethyl 1*H*-indole-3-carboxylic core variously substituted in 2- and 5-position. The **Scheme 1** can be used for the synthesis of derivatives with different amine in 5-position; while the **Scheme 6** can be used for the synthesis of derivatives with different substituents in 2-position.

Really, we used **Scheme 6** to synthesized target compound **9e$_1$**, which has farnesyl group in 2-position and pyrrolidine in 5-position.

In this scheme, **PABA** was subjected to a ioduration to give compound **14** (4-amino-3-iodobenzoic acid)[91], followed by reduction to alcool **15** and then by subsequent oxidation to aldehyde **16**. These steps of reduction and oxidation were made using the reducing agent Lithium aluminium hydride and the oxidant agent Pyridinium dichromate, which oxidizes primary alcohols to aldehydes and secondary alcohols to ketones[92-94].

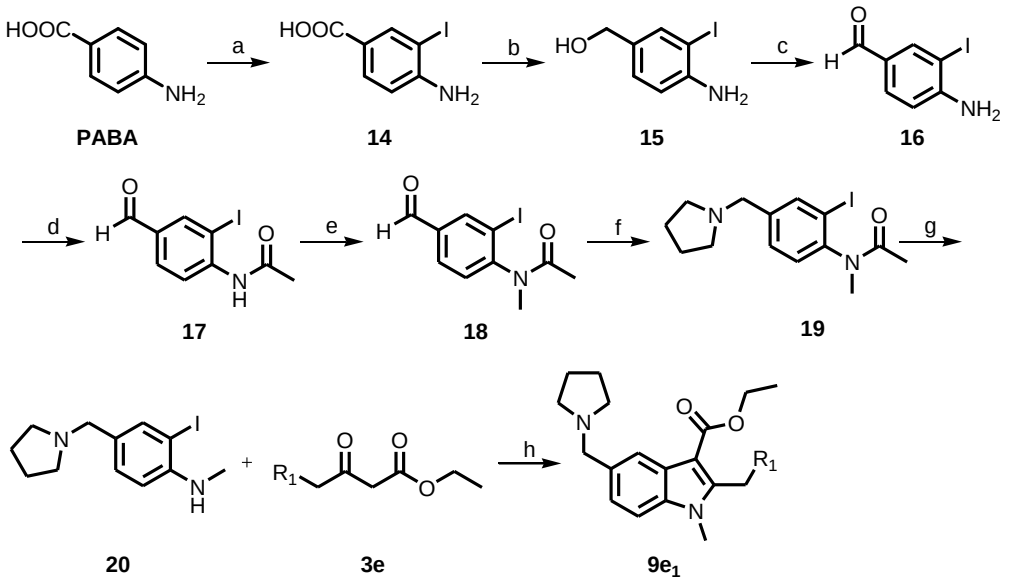

Scheme 6. *Synthesis of target compound 9e₁. Reagents and conditions: (a) $NaIO_4$, NaCl, KI, CH_3COOH/H_2O 9:1, rt, over night, 70%; (b) $LiAlH_4$, Diethyl ether, from 0°C to rt, 16h, 81%; (c) Pyridinium dichromate, DCM, rt, 2h, 80%; (d) Acetic anhydride, DCM, rt, 30h; 87%; (e) NaH, CH_3I, THF, from 0°C to rt, 3h, 75%; (f) Pyrrolidine, CH_3COOH, $NaB(OAc)_3H$, THF, MW, 130 °C, 10min, 85%; (g) NaOH, EtOH, H_2O, reflux, over night, 91%. (h) CuI, BINOL, Cs_2CO_3, DMSO, 50°C, 5–7h, 45%.*

Compound **16** was treated with acetic anhydride to afford the acetylated compound **17** in high yield[95]. The N-methylation using sodium hydride and methyl iodide afforded in good yield compound **18**.

Then it follows a reductive amination on aldehyde to give compound **19** with pyrrolidinyl group in 5-position and a subsequent hydrolysis of amide to afford compound **20**[96].

This compound is precursor of the indole compounds and it was treated with β-keto ester **3e** in a copper-catalyzed Ullmann-type coupling reaction to give final product **$9e_1$** with the farnesyl group in 2-position.

Using different β-keto esters, you can obtain several compounds variously substituted in 2-position. Therefore, the **Scheme 6** is a quick and efficient method for the synthesis of indole compounds with different groups in 2-position while leaving the group in 5-position.

2.3 Biological assays

Compounds **9a$_{1–6}$** and **9b$_{1–2}$** were tested for their antiviral activity against *Hepatitis C virus* (*HCV*) genotype 2a and *Herpes simplex* type 1. Moreover, for all synthesized compounds, it was assessed if they are selective inhibitors of *HCV*.

2.3.1 Anti-HCV analysis

Target compounds **9a$_{1–6}$**, **9b$_{1–2}$** and Arbidol were tested *in vitro* in Huh-7.5 cells for cytotoxicity and anti-HCV activity, specifically, the ability to inhibit the entry and replication of HCV.

For this anti-HCV analysis, a luciferase assay (Bright-Glo Luciferase assay system) was made. This is a convenient assay for reporter gene applications, often used to investigate the replication cycle of different viruses and for identification of compounds with antiviral activity. Synthetic analogs, and their lead Arbidol, were tested using HCV subgenomic particles containing the luciferase gene as reporter gene to infect hepatoma cells. This study evaluated the potency of our inhibitors measuring viral infection indirectly, or rather through estimation of the enzyme activity. Therefore, in the absence of viral inhibitors the infection occurs, the virus enters in the cells, replicates and produces luciferase, whose signal is measured indirectly by indicating the amount of viral particles contained in the cells. In the presence of antiviral drugs, therefore, this signal is inhibited. Moreover, cytotoxicity induced by the test compounds in cultures of cells was also determined. The toxicity of compounds **9a$_{1–5}$** and **9b$_{1–2}$** in Huh-7.5 cells was evaluated by CellTiter-Blue Viability Assay (Promega) a homogeneous, fluorometric method for estimating the number of viable cells present in multiwell plates[85].

The properties of these compounds are summarized in **Table 2.2**.

Table 2.2: *Anti-HCV activity and cytotoxicity of target compounds in vitro.*

Name	Structure	HCV entry (genotype 2a)			HCV replication (genotype 2a)		
		EC_{50}[a] (μM)	CC_{50}[b] (μM)	SI[c]	EC_{50}[a] (μM)	CC_{50}[b] (μM)	SI[c]
Arbidol	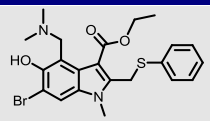	2	12	6	1	15	15
$9a_1$	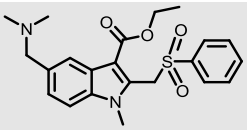	19	>50	>2.6	10	>50	>5
$9a_2$	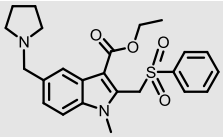	5	>50[d,e]	>10	3	>50[d,e]	>16.7
$9a_3$	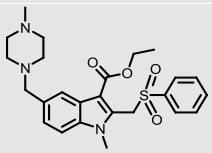	8	>50	>6.3	4	>50	>12.5
$9a_4$	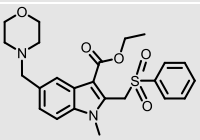	14	>50	>3.6	4	>50	>12.5
$9a_5$	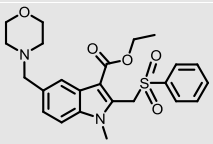	21	>50	>2.4	12	>50	>4.2
$9a_6$	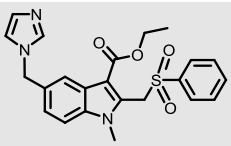	5	23	4.6	15	18	1.2
$9b_1$	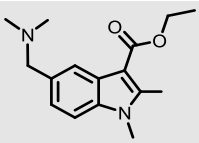	8	>50	>6.3	3	>50	>16.7
$9b_2$	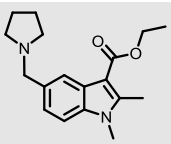	13	>50	>3.8	5	>50	>10

[a] EC50 is 50% effective concentration in Huh-7.5 cells.
[b] CC50 is 50% cytotoxic concentration.
[c] Selectivity index (SI: CC50/EC50).
[d] No cytotoxic activity at 50 μM concentration.
[e] % of inhibition at 100 μM concentration: 95% on entry and 80% on replication.

Several compounds exhibited inhibitory effects on HCV comparable to Arbidol. Compound **9a$_2$** showed the most potent in vitro anti-HCV activity. Its EC_{50} (5 and 3 μM) values in both entry and replication assays were highly comparable to those of Arbidol (2 and 1 μM, respectively). Interestingly, compound **9a$_2$** did not display cytotoxicity at 50 μM concentration, while at 100 μM concentration an inhibition of cell viability of 95% and 80% on entry and replication, respectively, was detected. Therefore, compound **9a$_2$** selectivity indices (>10, >16.7) were higher than those of Arbidol (6, 15).
The analogs **9a$_3$** and **9b$_1$** also exhibited significant efficacy against HCV (structures were listed in **Fig. 2.3**). Their EC_{50} values on entry were 8 and 8 μM and on replication were 4 and 3 μM, respectively, which were higher than the positive control Arbidol. Also in these cases, the selectivity indices of **9a$_3$** and **9b$_1$** on HCV entry (>6.3) and on HCV replication (>12.5, >16.7) were higher than or comparable to those of ARB.

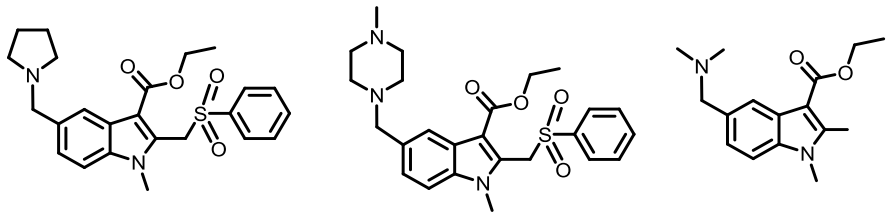

Figure 2.3: *Chemical structures of typical compounds that showed significant anti-HCV activity.*

Compounds **9a$_{1–6}$**, with the same groups in position 1–3 but different ammines in 5-position, showed an IC_{50}, on entry and replication, in the range from 3 to 21 μM concentration. These results suggested that the different amines

introduced at the 5-position had a relatively minor influence on the antiviral activities.

Moreover, the imidazolyl group in compound **$9a_6$** seemed to shift the selectivity toward inhibition of HCV entry, to reduce the potency against HCV replication and to enhance the cytotoxicity.

Compounds **$9b_1$** and **$9b_2$** exhibited strong anti-HCV effects. This revealed that the elimination of the phenylsulfonyl moiety preserved the anti-HCV activity.

These preliminary results demonstrated that the removal of the 6-bromo and 5-hydroxy groups from the indole ring of Arbidol did not have an influence on its anti-HCV efficacy. This implies that these groups might not be the antiviral pharmacophores.

In summary, according to the above results, the following conclusions can be drawn:

1 The elimination of the phenylsulfonyl group at the 2-position seemed to preserve the antiviral activities.
2 Compounds with different amines introduced at the 5-position did not show a wide variation in anti-HCV effects.
3 The 6-bromo and 5-hydroxy groups might not be the pharmacophores responsible for the anti-HCV effects.

Despite several changes made to the Arbidol structure in our derivatives, the antiviral activity was maintained, and the cytotoxicity was reduced[85].

2.3.2 Anti-HSV analysis

Target compounds **$9a_{1–6}$**, **$9b_{1–2}$** and Arbidol were tested *in vitro* in the human keratinocyte (HaCaT) cells for anti-HSV activity.

To evaluate the antiviral activity on HSV type-1 of derivatives, two assays were made: *plaque assay* and *assay for antiviral activity.*

The first assay was performed to choose the best concentration of Arbidol and its analogues to test for the antiviral activity. In the *plaque assay,* Human

Keratinocyte cells (HaCat) were treated with Arbidol and derivatives at different concentration (12, 6, 3 and 1 μM) for 3 h. As positive control a treatment with acyclovir 10 μM was used. The cells were then washed with PBS and infected with HSV-1 at MOI (low multiplicity of infection) of 0.001 PFU (plaque-forming units)/ cell. After 1 h of incubation at 37 °C (adsorption period), the unadsorbed virus was removed and the plaque number calculated.
All substances at all concentrations tested showed a reduction of PFU (the number of particles able to form plaques and so infectious particles) compared to that obtained in the untreated infected cell. The best concentration resulted 3 μM used for all the other experiments. At this concentration Arbidol and compounds **9b$_2$**, **9b$_1$** and **9a$_2$** showed the best anti-HSV activity with a reduction of infectivity (**Fig. 2.4**), vs the untreated infected cells, of about: 42%, 35%, 46% and 49%, respectively. The other target compounds did not show a substantial antiviral activity with a reduction of infectivity under 35%.

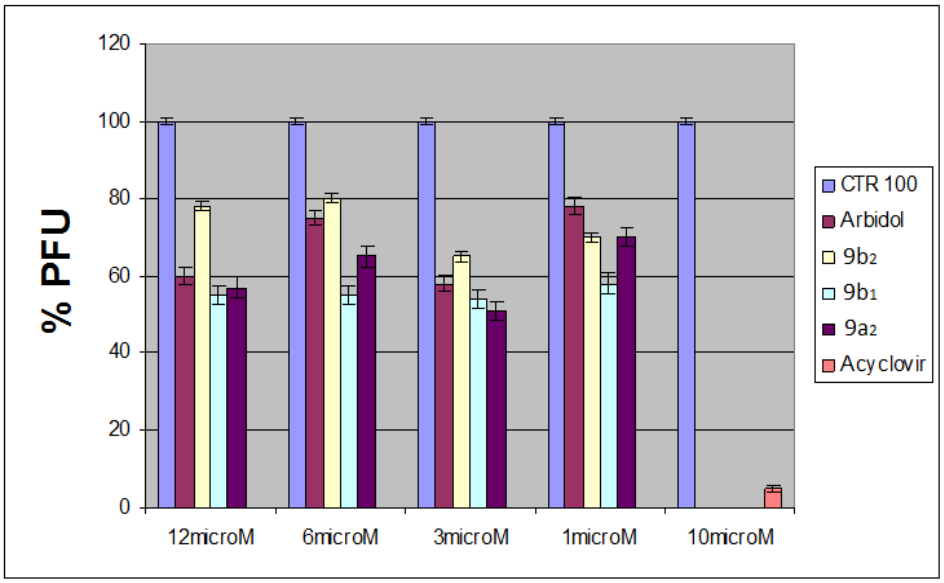

Figure 2.4: *Plaque assay.*

The *assay for antiviral activity* was made in order to identify which phase of HSV-1 replication (preadsorption/adsorption or post-adsorption period) was affected by Arbidol and its analogues.

Therefore, it was evaluated the virus yield detected after 24 and 48 h from the infection of keratinocyte cultures with HSV-1, treated or not with Arbidol and derivatives at 3 μM. In three different set of experiment the molecules were added 1) 3h befor /during infection (preadsorption/adsorption), 2) during infection (adsorption) and 3) during post infection (post-adsorption) period**.**

In this assay, good results (**Fig. 2.5**) were obtained *pretreating* keratinocytes for three hours and adding the molecules *during the adsorption* period.

Data represent the virus yield detected at 24 and 48h after infection in the presence or absence of ARB and derivatives. Values indicate the percent of inhibition of virus production in treated cells compared to untreated infected controls (PFU%).

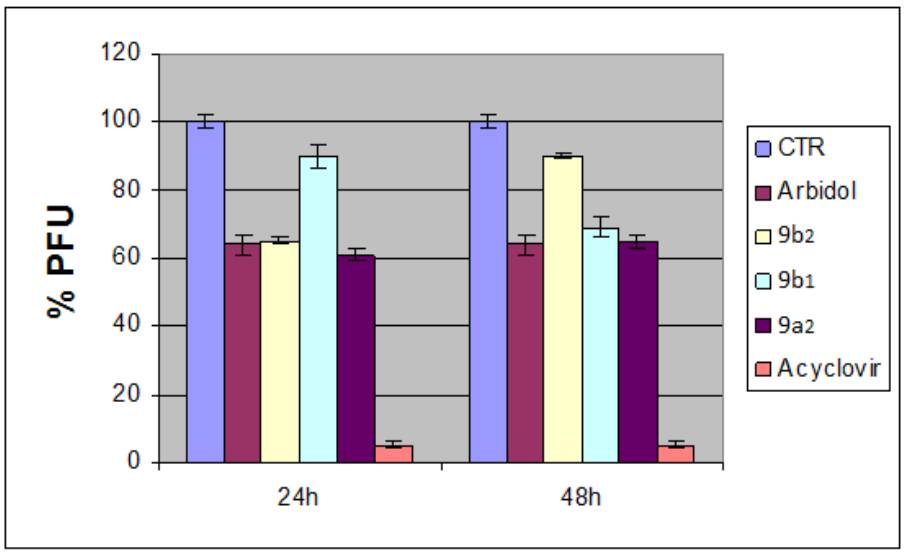

Figure 2.5: *Assay of antiviral activity.*

This proves that Arbidol analogues work in the first step of HSV replication cycle (entry).

In the other experimental conditions there are no obvious differences between treated and untreated infected controls. This proves no activity of compounds on the HSV replication. Therefore, some Arbidol analogues have a good and, in two compounds, higher anti-HSV-1 activity than lead compound (**9b**$_1$ and **9a**$_2$). Moreover, the most active compounds on HSV-1 have the best activity also on HCV. This reveals that Arbidol derivatives, such as the lead compound, have a broad antiviral spectrum.

2.3.3 Evaluation of the selective anti-HCV activity

An evaluation of the selective antiviral activity of compounds **9a$_{1–6}$**, **9(b-d)$_{1–2}$** and Arbidol on the replication of Hepatitis C virus (genotype 1b, Con1 strain) in Huh cells (subtype 5-2) was made. To assess whether synthesized compounds and/or Arbidol can be retained as selective inhibitors of HCV replication, a replicon system was used.

To fully understand the results obtained with this assay, a short explanation on replicon system should be made.

The HCV replicon system is a piece of viral RNA (replicon) that self-replicates in the host cell without the need of infecting cells and also not producing new infectious virus particles (it is a virus particle-free system). This multiplication of the replicon is extremely dependent on the good health of the host cell.

The cell viability is shown with the green line. In detail, a compound can be retained as a selective inhibitor (**Fig. 2.6**) of the replication of HCV when:

1. It produces an EC_{90};
2. It inhibits the HCV replicon >50% (preferably >90%) at a concentration where the green curve is at 95-100%;
3. The SS (selectivity surface = the surface delineated by the green, red and 50% horizontal) should be as high as possible, meaning >30 or so.

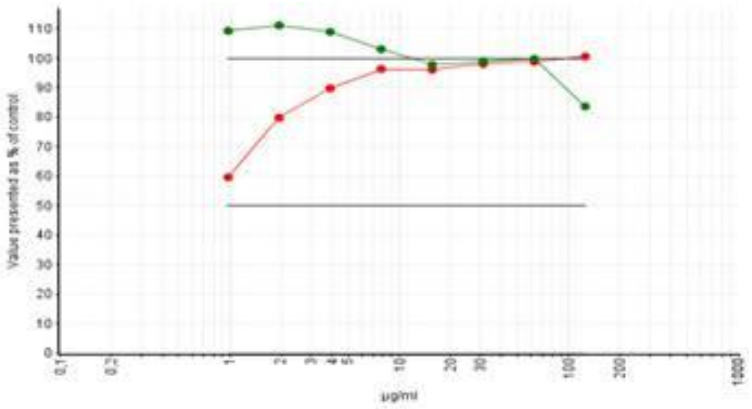

Figure 2.6: *Example of how the curve looks for a selective inhibitor of HCV replication.*

After a detailed screening, it was revealed that none of the compounds can be retained as selective inhibitor of HCV replication in the replicon system.

In fact, what you can see is that for all of compounds, the green line goes down with increasing concentration of compound. This can be seen also in the lead compound Arbidol (**Fig. 2.7**).

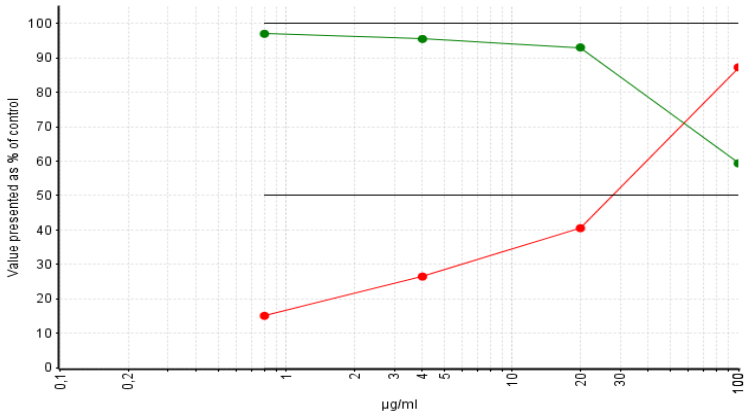

Figure 2.7: *Diagram of Arbidol in the selectivity assay: a maximum of 71% inhibition is observed at 72.3 ug/ml. This compound is not a selective inhibitor of virus replication.*

Moreover, none of compounds produce an EC_{90} and all results are summarized in **Table 2.3**.

Table 2.3: *Selective antiviral activity of target compound on HCV replication.*

Compound	Unit	CC_{50}	EC_{50}	EC_{90}	SI	SS	TI	%Inh.	at []
Arbidol	µg/ml	>100	27.7	ND	>3.61	>6.52	>3.63	71	72.3
$9a_1$	µg/ml	45.7	8.21	ND	5.57	11.8	8.83	79.7	23
$9a_2$	µg/ml	18.2	6.01	ND	3.03	4.5	2.17	68.7	13.2
$9a_3$	µg/ml	17.6	8.96	ND	1.96	2.46	0.72	66.8	15.2
$9a_4$	µg/ml	53	10.7	ND	4.95	12.8	8.92	79.4	37.2
$9a_5$	µg/ml	44.6	10.9	ND	4.07	9.58	5.84	80.9	19.4
$9a_6$	µg/ml	31.1	7.94	ND	3.92	6.2	3.68	74.3	16.4
$9b_1$	µg/ml	14.3	5.44	ND	2.64	3.58	1.51	67	12.1
$9b_2$	µg/ml	30.5	8.52	ND	3.58	5.85	3.24	73	16.2
$9c_1$	µg/ml	2.58	<0.8	ND	>3.22	>11.2	>5.72	79.6	1.65
$9c_2$	µg/ml	4.28	<0.8	ND	>5.36	>10.7	>7.82	74.9	2.59
$9d_1$	µg/ml	<0.8	<0.8	<0.8	ND	ND	ND	96.2	20
$9d_2$	µg/ml	<0.8	<0.8	<0.8	ND	ND	ND	100	100

ND= not determined.
CC50= 50% Cytostatic/Cytotoxic Concentration (concentration at which 50% adverse effect is observed on the host cell).
EC50= 50% Effective Concentration (concentration at which 50% inhibition of virus replication is observed).
EC90= 90% Effective Concentration (concentration at which 90% inhibition of virus replication is observed).
SI= Selectivity Index (CC50/EC50).
SS= Selectivity Surface (integrated surface delineated by the green curve, the red curve and the 50% horizontal).
TI= Therapeutical Index (SS * 10logSI).

For two compounds, exactly **$9d_1$** and **$9d_2$**, we had an extreme case in which the green curve is at the bottom (the cells are death) and the red one at the top (**Fig. 2.8**). In this case the virus replicon cannot replicate because its replication is highly dependent on the viability of the host cell itself.

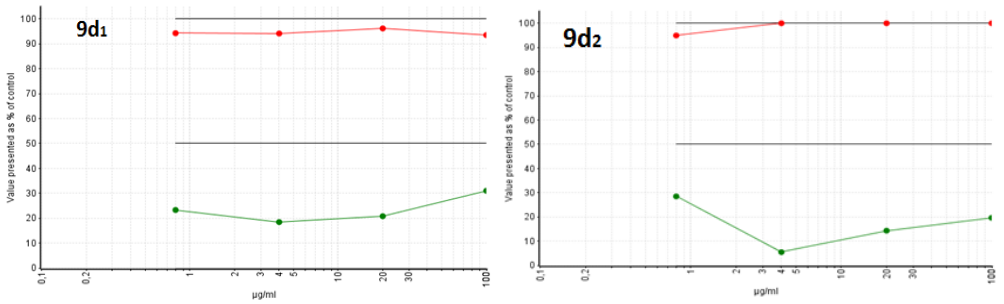

Figure 2.8: *Diagrams of compounds $9d_1$ and $9d_2$ in the selectivity assay: extreme cases in which all cells are death.*

It's also interesting to note that compounds **$9c_{1\text{-}2}$** (not yet tested in the above assays), although not selective replication inhibitors, have an EC_{50} lower than the other compounds (**Fig. 2.9**), including the lead compound. Moreover, unlike other compounds, these have an inhibitory activity even at low concentrations when the cell viability is high .

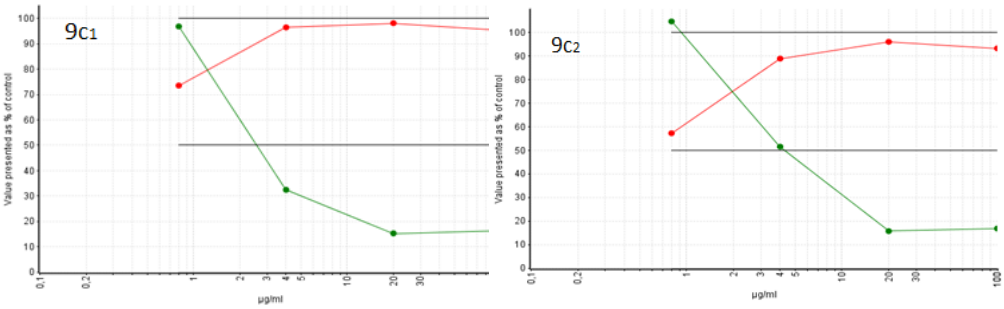

Figure 2.9: *Diagrams of compounds $9c_{1\text{-}2}$ in the selectivity assay. At low concentrations (<1µg/ml) we have high green line and high red line.*

Through these results, we demonstrated that Arbidol and derivatives are not HCV selective inhibitors, but their anti-HCV activity, also as replication inhibitors, is due to a nonspecific mechanism, such as the interaction with the membranes.

2.4 Evaluation of mechanism of Arbidol anti-influenza action

As previously mentioned, Arbidol is a broad-spectrum antiviral agent lunched in Russia for the prophylaxis and treatment of influenza A and B. It acts in the early stages of the replication cycle of these viruses, such as membrane fusion between virus and host cell (which occurs at pH 7.4) and between the virus and endosome (which occurs at pH 5 and it is responsible for the release of the viral genome). There are also experimental evidence that ARB does not affect viral neuraminidase (NA, a surface protein of influenza virus) activity or viral transcription/translation and nor does ARB inhibit adsorption. Influenza virus haemagglutinin (HA, other surface protein) mediates viral envelope fusion with endosomal membranes. Fusion requires HA conformational changes that occur only at acidic pH; these changes lead to the exposure of the N-terminal fusion peptide contained in the HA2 subunit of HA, permitting its interaction with the target endosomal membrane (**Fig. 2.10**).

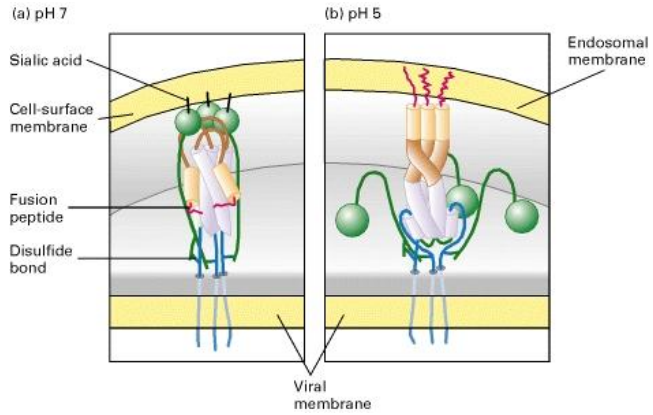

Figure 2.10: *HA conformations: a) At a pH of 7.0, the N-terminus of each HA_2 subunit is tucked into a crevice in the spike. This is the normal HA conformation when a viral particle encounters the surface of a host cell. b) At the pH of 5.0 within an endocytic vesicle, HA undergoes several conformational changes that cause a major rearrangement of the subunits. As a result, the three HA_2 subunits twist together into a three-stranded coiled-coil rod that protrudes more than 13 nm outward from the viral membrane with the fusion peptides at the tip of the rod*[97].

ARB affects early post-adsorption stages of virus replication with possible involvement of the second surface viral protein, the haemagglutinin (HA). Arbidol could act increasing influenza virus HA stability and preventing low pH induced HA transition to its fusogenic state, thus blocking infection at the viral fusion stage.

To support this hypothesis there are recent data in literature in which ARB-resistant mutants, selected from the most sensitive reassortant, possessed single amino acid substitutions in the HA2 subunit which caused an increase in the pH of fusion and the associated conformational change in HA. Moreover, Xray crystallography structure analysis, that reveals how ARB stabilizes the HA molecule, have not yet been made[79,98].

To evaluate the interaction of Arbidol with the N-terminal hydrophobic fusion domain of Haemagglutinin (HA), during second year of my Ph.D period the peptide host-guest (P20H6) was synthesized and *Circular dichroism* studies were made.

2.4.1 Synthesis of host-guest peptide (P20H10)

In the host-guest peptide (P20H6), the fusion domain (guest) was linked via a flexible linker to a very polar, solubilizing (host) peptide to remove the strong tendency of the domains to aggregate in solution and in membrane environments.

The fusion domain of HA in the form of host-guest peptide P20H6 has the following sequence: GLFGAIAGFIENGWEGMIDGGGKKKK, in which multiple lysine residues increase the solubility of the peptides and facilitate binding to negatively charged membranes[99].

The synthesis of peptide (P20H6) was made with techniques of Solid Phase Peptide Synthesis (SPPS). This synthetic strategy provides for the anchorage of the growing peptide chain to an insoluble polymeric support (resin) with

linkers, which are anchored covalently to the first amino acid through the free carboxyl group, leaving the amino group properly protected.

The general principle of SPPS is the repetition of cycles of deprotection and coupling: the amino group of the first residue, anchored to the resin is unprotected and reacts with the free carboxyl of a new amino acid, also amino-protected. In this way, the peptide remains "attached" to the support for the duration of the cycles of synthesis, allowing you to replace the intermediate steps of purification by simple washing and filtration.

At the end of synthesis, the compound is removed from the media and they are removed once protections introduced on the groups in side chain. This type of technique has several advantages compared to the synthesis in solution. First, it allows to overcome the problems arising from the possible insolubility of peptide intermediates in organic solvent used. Secondly, it allows easy removal of excess reagents and by products by simple washing and filtration after completion of each reaction, because the peptide is completely insoluble in all synthetic stages.

The synthesis is performed in a single reactor, this will avoid loss of material and obtain high yields in the final products, utilizing large excesses of reagents to drive reactions to completion. Disadvantages are represented by the lack of methods for quantification in real-time of reactions. Moreover the yield of the single reactions must be kept as close as possible to 100%. It is evident that the purity of the final product will be higher when greater is the yield of individual reactions cyclically repeated to assemble the peptide.

Modeling kinetics of deprotection and condensation reactions are very complex because the pores of the particles of support are gradually obstructed by the growing chains. These chains, in turn, tend to assume an ordered structure in space resulting in mutual interactions and then they aggregate hiding the reactive terminal; in addition, as a result of inter-chain interactions,

the structure of the porous matrix may collapse, drastically reducing the rate of diffusion of reagents and solvents through the matrix.

Given the multiple benefits that this method of synthesis has, a large number of resins has been developed. The choice of solid support and appropriate protecting and activating groups is made on the basis of the amino acid sequence to be synthesized. The resin must meet certain requirements, such as ease of reaction with the acid group of the first amino acid and stability, which must maintain the conditions for removing protecting groups. This suggests that, if, for example, the protecting group is basic-labile, the resin must be acid-labile.

Among the resins available the choice fell on Rink-amide, a polystyrene resin copolymerized with 2% of divinylbenzene (DVB).

Latter aims to create cross-links to make the resin insoluble in organic solvents. The level of crosslinking can not exceed 2% to not harden the resin, which should be swellable like a sponge when wet by the solvent to allow easy movement of the reagents inside. The resin used is derivatized with the linker group (**Figure 2.11**), which have NH_2 group protected with Fmoc group N-(9-Fluorenylmethyloxycarbonyl).

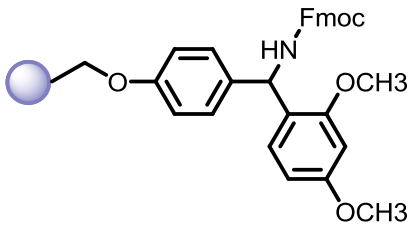

Figure 2.11: *Rink amide resin linker.*

Moreover, this resin is acid-labile, so it is stable in basic conditions. This means that it is not affected by changes in the conditions of removal of protecting groups of amino function in the amino acids considered,

representing 9-fluorenylmethyloxycarbonyl (Fmoc). So it can be done in basic environment for piperidine.

In addition, it is necessary to use amino acids protected with groups in the side chains and to remove them only in highly acidic conditions, used during the terminal phase of cleavage, with which, peptide is removed from the resin with acidolysis (**Fig. 2.12**) with trifluoroacetic acid **(**TFA).

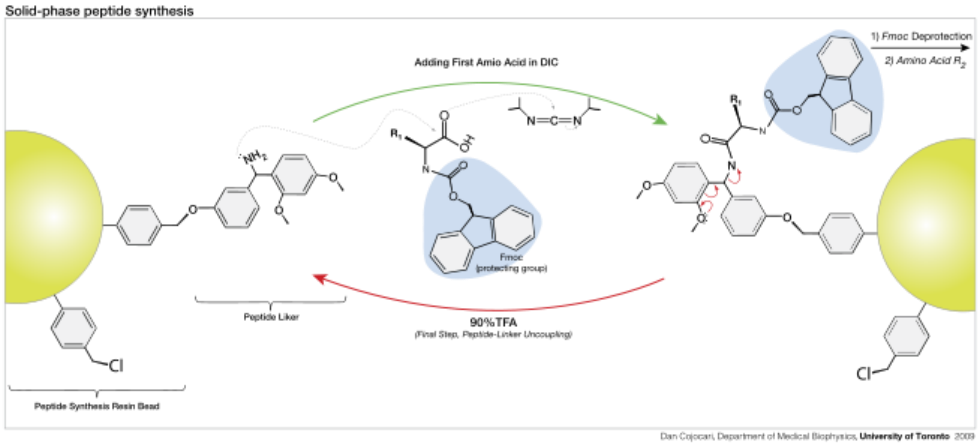

Figure 2.12: *Solid-phase peptide synthesis and acidolysis with TFA.*

The first operation performed was the solvation of the resin in DMF (N, N-dimethylformamide). This operation has the aim to expand the resin, and make more accessible the reaction sites. Subsequently it was necessary to remove the Fmoc group to release the amino function of the linker, which is essential for the next reaction; the removal was done using a solution of 25% piperidine in DMF, as the subsequent steps of deprotection of the amino group of the growing chain.

The first amino acid, Fmoc-Lys-(Boc)-OH as well as the following, were then coupled according to standard protocols of solid phase peptide synthesis.

The coupling was carried out using as coupling agents salts of uronic such as HOBT (*N*- Hydroxybenzotriazole) and HBTU (O-Benzotriazole-N,N,N’,N’-

tetramethyl-uronium-hexafluoro-phosphate) in presence of a tertiary base, DIPEA (*N,N*-Diisopropylethylamine). In some cases we used DCC (*N,N'*-Dicylohexylurea) instead of HBTU (**Fig. 2.13**).

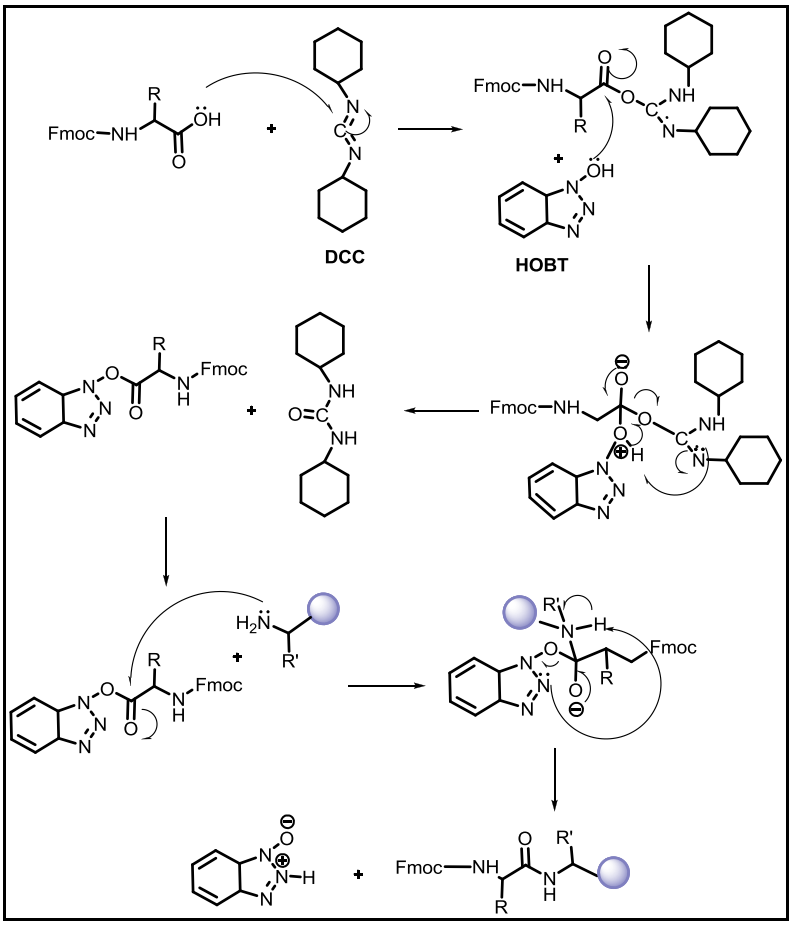

Figure 2.13. *Activation of amino acids through training active esters and coupling.*

The N^{α}-Fmoc group of each amino acid was removed by 25% piperidine in DMF (**Fig. 2.14**). The amino acid sequence was thus assembled by alternating cycles of deprotection with cycles of coupling.

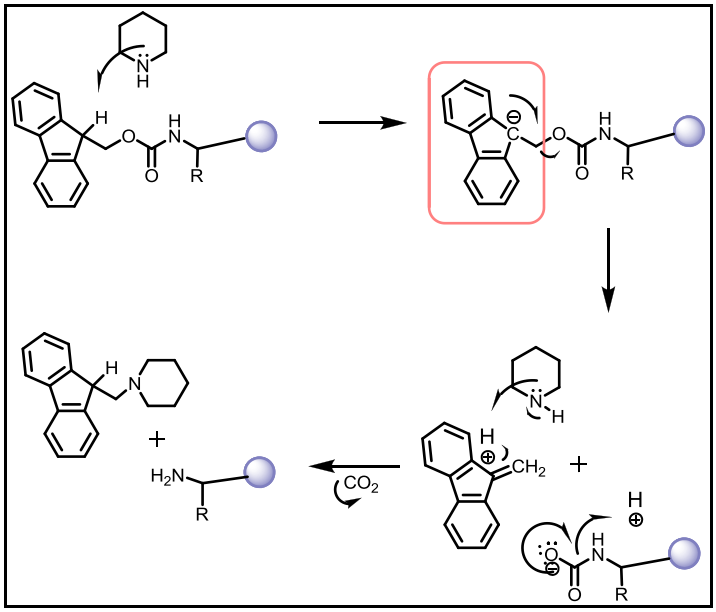

Figure 2.14. *Removing of Fmoc.*

After each coupling, to determine the completeness, and after each deprotection, to verify the complete removal of the Fmoc protecting group, the Kaiser test was done. The separation of the final peptide from the resin and simultaneous removal of other protecting groups in the side chain were performed using a mixture of TFA (trifluoroacetic acid) 90%, TIPS (Triisopropylsilane) 5% and H_2O 5% (**Fig. 2.15**).

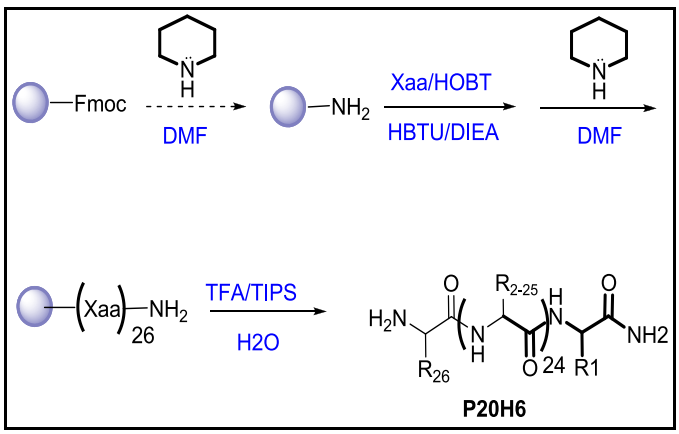

Figure 2.15. *Diagram of synthesis of peptide.*

The resin was removed from the solution by filtration and the crude peptide was obtained by precipitation in diethyl ether in cold, giving a white powder. The crude peptide obtained was purified on reversed phase preparative RP-HPLC column and chemical-physical properties and purity of these peptidomimetics were assessed by ESI / MS and RP-HPLC.

2.4.2 Circular dichroism studies

Circular dichroism (CD) refers to the differential absorption of left and right circularly polarized light. This phenomenon is exhibited in the absorption bands of optically active chiral molecules. CD spectroscopy has a wide range of applications in many different fields.

This technique allows to measure the variation of the polarization after passage of light through a chiral substance. In the circular dichroism circularly polarized light is used. This can be dextrorotatory (R) or left-handed (L) and the interaction with a chiral center involves more interaction with the component L or R. Due to the interaction with the molecule, the electric field vector of the light traces out an elliptical path after passing through the sample. The ellipticity is the parameter measured in CD spectroscopy.

The main components of a used CD spectropolarimeter are: a light source that sends light to a monochromator. The monochromatic radiation reaches the linear polarizer and emerges as linearly polarized radiation.

Two radiations of this type affect a modulator electro, giving rise to a circularly polarized light and this affects the sample. From the sample, the light exits as elliptically polarized and heads toward the detector. After the detector, an amplifier / signal processor and recorder are contained.

Graphs are obtained by the rotation and they, when properly interpreted, provide useful information about the molecule conformation. The CD spectrum of proteins can reveal important characteristics of their secondary structure.

CD spectra can be readily used to estimate the fraction of a molecule that is in the alpha-helix conformation, the beta-sheet conformation, the beta-turn conformation, or some other (e.g. random coil) conformation (**Fig. 2.16**).

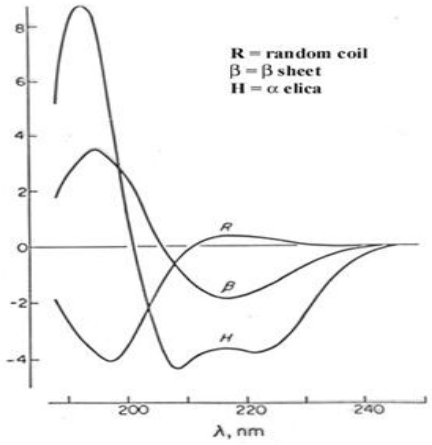

Figure 2.16: *Diagram of peptide conformations (α, β and random coil).*

These fractional assignments place important constraints on the possible secondary conformations that the protein can be in. CD cannot, in general, say where the detected alpha helices are located within the molecule or even completely predict how many there are. Despite this, CD is a valuable tool, especially for showing changes in conformation. It can, for instance, be used to study how the secondary structure of a molecule changes as a function of temperature, of the concentration, of denaturing agents or of agents that interact with protein.

Circular dichroism (CD) experiments were performed at 25°C on a 810-Jasco spectropolarimeter using a quartz cuvette with a path length of 1 mm.

CD spectra were performed on peptide in H_2O at 200 μM concentration, at pH 5 and 7, in lysophosphatidylcholine micelles (LPC), with or without Arbidol. In addition, the estimation of the secondary structure composition was carried out using the algorithm K2D by DichroWeb.

CD spectra, in **figure 2.17** and **2.18**, shows peptide curve at pH 5 and 7, in LPC micelles, alone and in the presence of Arbidol in the molar ratio of 1:1 and 1:5 peptide/Arbidol (the choice of the molar ratio 1:5 peptide/Arbidol is due to peptide molecular weight that is about 5 times higher than those of Arbidol).

Figure 2.17 shows that the CD spectra of peptide, alone and at pH 5, is an alpha helix (100%). After addition of Arbidol in molar ratio 1:1, the peptide adopts an alpha helix of 90%. Finally, a transition from alpha helix to β sheet (90%) occurs after an increase of Arbidol concentration, in particular using a molar ratio 1:5 peptide/Arbidol.

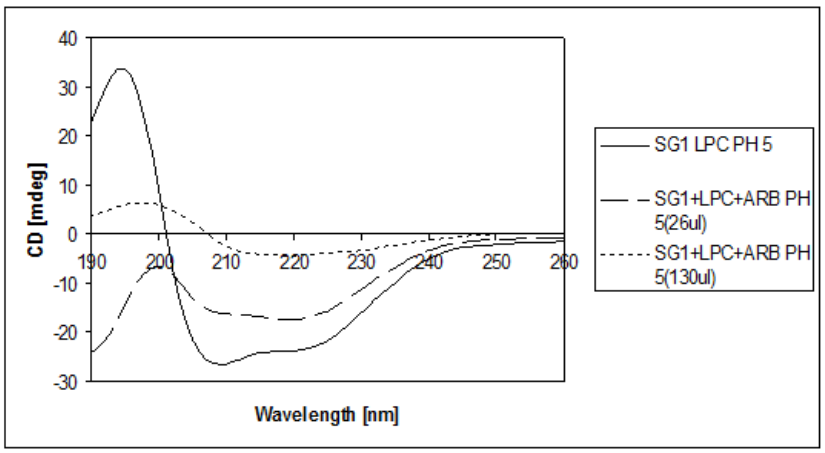

Figure 2.17: *Circular dichroism of peptide P20H6 (SG1) in LPC at pH 5, alone and in molar ratio 1:1 and 1:5 with Arbidol.*

Figure 2.18 shows that the CD spectra of peptide, alone and at pH 7, is an α-helix (100%). When Arbidol is in molar ratio 1:1 with peptide, the peptide curve still adopts an α-helical conformation (100%). Moreover, the addition of Arbidol in higher concentration, using a molar ratio 1:5 peptide/Arbidol, leads to a transition to a more disordered conformation (40% alpha helix and 60% random coil).

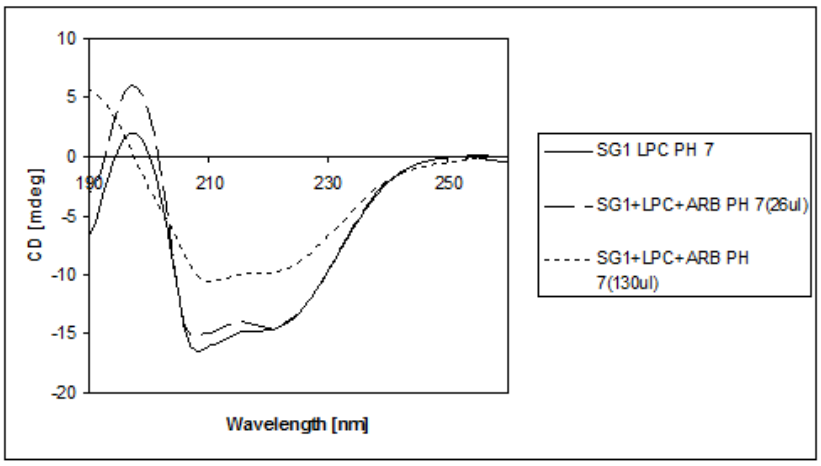

Figure 2.18: *Circular dichroism of peptide P20H6 (SG1) in LPC at pH 7, alone and in molar ratio 1:1 and 1:5 with Arbidol.*

From this first studies we can deduct that Arbidol interacts with the haemagglutinin fusion domain at pH5 and 7, through changes in the secondary structure of peptide.

In addition, the prominent interaction is at fusiogenic pH in which we have a transition from α-helix to β sheet and this transition is directly linked to the increase of Arbidol concentration.

Moreover, other CD studies were performed to assess if the changes in the secondary structure of peptide were due to the presence of bromine in the Arbidol molecule and not to its antiviral activity. Therefore, CD spectra on peptide were made at pH 5 and 7, and in presence of another compound with bromine on its structure, 4-Br-2-iodoaniline (**Fig. 2.19-2.20**).

CD spectra of peptide in presence of this brominated molecule showed not significant changes in the secondary structure of peptide. In fact, in both pH of 5 and 7, peptide curve was always an α-helix (100%) such as in the only peptide.

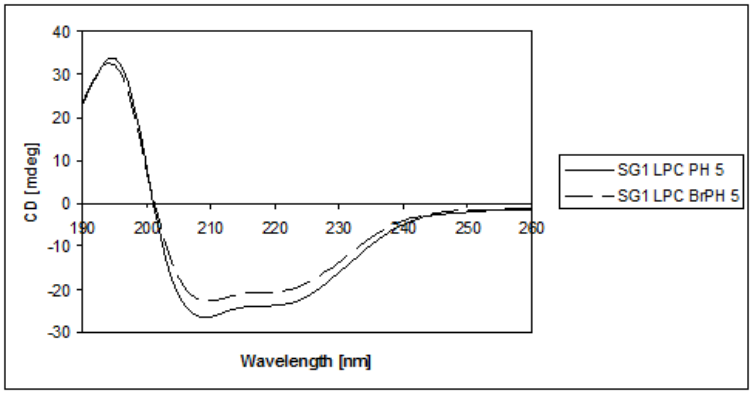

Figure 2.19: *Circular dichroism of peptide P20H6 (SG1) at pH 5 in LPC, alone and in presence of 4-Br-2-iodoaniline.*

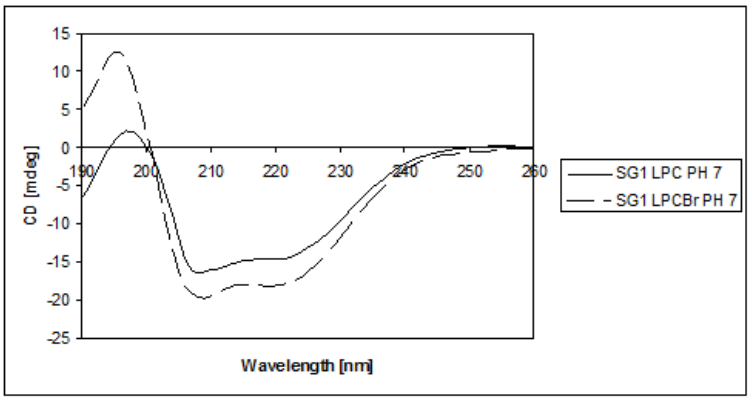

Figure 2.20: *Circular dichroism of peptide P20H6 (SG1) at pH 7 in LPC, alone and in presence of 4-Br-2-iodoaniline.*

CHAPTER 3

SYNTHESIS OF A P.E.T. RADIOTRACER FOR TUMOUR HYPOXIA: ^{18}F-FAZA

3 INTRODUCTION

During the last year of my Ph.D., I spent six months at the University of Aberdeen where I worked to the synthesis of a PET (Positron Emission Tomography) radiotracer for tumour hypoxia: the *[^{18}F]1-α-D-(5-Fluoro-5-deoxyarabinofuranosyl)-2-nitroimidazole*, known as ^{18}F-FAZA.

The ^{18}F-FAZA is currently the gold standard for PET Imaging of diseases characterized by hypoxia (solid tumours, ischemia, stroke), but), but it is not routinely used and synthesized in Scotland. The work done is an important starting point for the introduction of ^{18}F-FAZA in Scotland with the aim of using it in clinical imaging and research.

In particular, following a detailed bibliography research on this compound and its synthesis, that is not fully reported, and a subsequent optimization of the synthetic scheme used, the ^{18}F-FAZA precursor was obtained: *1-α-D-[5'-O-Toluenesulfonyl-2',3'-Di-Oacetylarabinofuranosyl]-2-nitroimidazole* (DAcTs-AZA).

Before explaining the chemistry, it is appropriate to provide a wider overview on tumour hypoxia and radiotracers used in PET, in a way that helps to understand and define the goals of this project.

3.1 Tumour hypoxia

Tissue hypoxia results from an inadequate supply of oxygen (O_2) that compromises biological functions. Structural and functional abnormalities of the tumour vasculature, together with altered diffusion conditions inside the tumour, seem to be the main causes of tumour hypoxia.

Evidence from experimental and clinical studies points to a role of tumour hypoxia in tumour propagation, resistance to therapy and malignant progression. The prevalence of hypoxic areas is a characteristic feature of

locally advanced solid tumours and has been described in a wide range of human malignancies, including cancer of the breast, uterine cervix, vulva, head and neck, prostate, rectum, and pancreas as well as in brain tumours, soft tissue sarcomas and malignant melanomas.

Up to 50–60% of locally advanced solid tumours may exhibit hypoxic and/or anoxic tissue areas that are heterogeneously distributed within the tumour mass. These hypoxic areas result from an imbalance between oxygen supply and consumption which is caused by abnormal structure and function of the microvessels (**Fig 3.1**) supplying the tumour (causing acute hypoxia), increased diffusion distances between the nutritive blood vessels and the tumour cells (causing chronic hypoxia), and reduced O_2 transport capacity of the blood due to the presence of disease- or treatment-related anaemia.

Recent studies have demonstrated a clear relevance of this hypoxic microenvironment to tumour-associated metabolic alterations, which are tightly linked to the biology of the tumour[103].

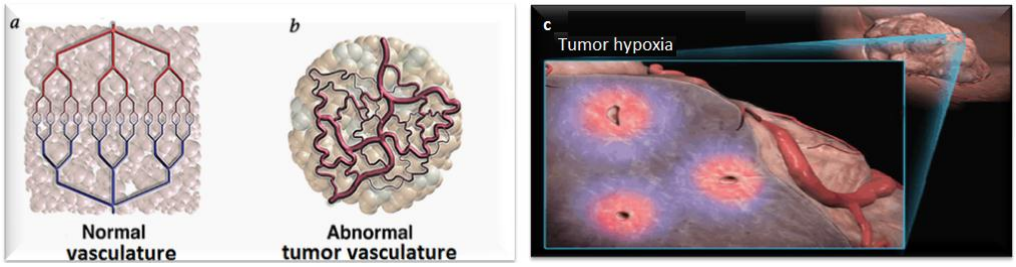

Figure 3.1: *Normal vasculature (a), abnormal tumour vasculature (b) and chronic tumour hypoxia (c).*

Hypoxic cells are viable, oxygen deficient, cells that are generally 2.5 to 3-fold more radioresistant than well-oxygenated cells to the cytotoxic effects of ionizing radiation (oxygen effect).

Hypoxia develops in many solid tumours, leading to the induction of adaptive genomic transcriptional and post-translational changes that promote the

establishment of an aggressive phenotype which induces metastatic potential, promotes angiogenesis and supports local disease progression.

Inadequate angiogenesis and compression of blood and lymphatic vessels in rapidly proliferating tumour cells change the composition and structure of the extracellular matrix (ECM), which effectively reduces perfusion of the tumour and, consequently, decreases the delivery of the drugs to the hypoxic area.

Since hypoxic tumour cells have an aggressive and treatment-resistant phenotype, they respond poorly to radiotherapy (external beam radiotherapy; XRT) and are major determinants of XRT failure.

In this respect, tumour hypoxia has been associated with an aggressive tumour phenotype, poor response to radiotherapy and chemotherapy, increased risk of invasion and metastasis, and worse prognosis in advanced squamous cell carcinoma of the cervix, head and neck, and soft-tissue sarcomas.

This necessitates early identification of hypoxic tumour cells and aggressive, innovative treatment to combat their rapid progression and the resultant poor prognosis[104].

Many of the adaptations to tumour hypoxia seem to be orchestrated by the transcription factor hypoxia-inducible factor (HIF)-1, which has been verified as a master regulator of oxygen homeostasis under hypoxic conditions.

Its oxygen-dependent activity is regulated in a delicate interplay between several factors in which a family of prolyl hydroxylase domain-containing proteins or PHDs, the von Hippel-Lindau (VHL) tumour suppressor protein (pVHL) and an E3 ubiquitin ligase complex, amongst many others, play an important role (**Fig. 3.2**).

The HIF-1 pathway mediates critical hypoxic adaptations by the induction of target genes involved in glucose metabolism, angiogenesis, erythropoiesis and apoptosis.

These target genes include vascular endothelial growth factor (VEGF), facilitative glucose transporters (GLUTs), hexokinases (HKs), erythropoietin (EPO), carbonic anhydrase IX (CAIX), etc.

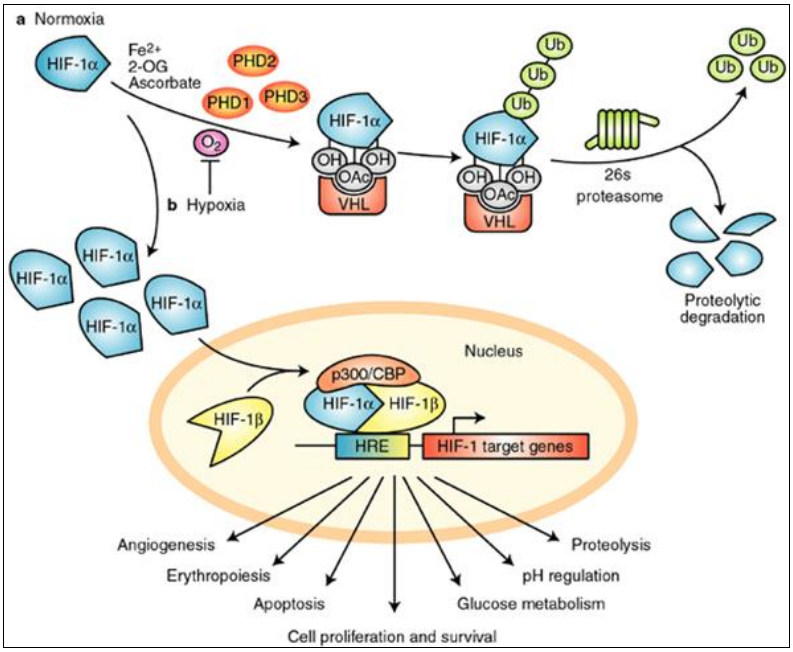

Figure 3.2: *HIF-1α regulation by proline hydroxylation: (a) In normoxia, hypoxia-inducible factor (HIF)-1α is hydroxylated by proline hydroxylases (PHD1, 2 and 3) in the presence of O_2, Fe^{2+}, 2-oxoglutarate (2-OG) and ascorbate. Hydroxylated HIF-1α (OH) is recognised by pVHL (the product of the von Hippel–Lindau tumour suppressor gene), which, together with a multisubunit ubiquitin ligase complex, tags HIF-1α with polyubiquitin; this allows recognition by the proteasome and subsequent degradation. Acetylation of HIF-1α (OAc) also promotes pVHL binding. (b) In response to hypoxia, proline hydroxylation is inhibited. VHL is no longer able to bind and target HIF-1α for proteasomal degradation, which leads to HIF-1α accumulation and translocation to the nucleus. There, HIF-1α dimerises with HIF-1β, binds to hypoxia-response elements (HREs) within the promoters of target genes and recruits transcriptional co-activators such as p300/CBP for full transcriptional activity. A range of cell functions are regulated by the target genes, as indicated. Abbreviation: CBP, CREB-binding protein; Ub, ubiquitin*[105].

The resulting adaptive changes in the proteome and genome of the tumour cells are believed to lead to more aggressive clones which are better adapted to survive in their compromised situation. Subsequent selection and clonal

expansion of these clones lead to a more adapted and aggressive tumour cell population.

As noted above, the presence of tumour hypoxia appears to impair the effectiveness of common anticancer therapies like radiotherapy (RT) and chemotherapy.

Hypoxia-induced radioresistance is multifactorial. Besides the above-mentioned proteomic and genomic changes that most likely contribute to resistance by increasing the number of mutated cells that are more resistant to apoptosis and by causing upregulation of several stress proteins, the main reason for radioresistance is the intrinsic dependence of RT on oxygen to cause damage to the tumour cell. For damage to be inflicted on tumour cells by ionizing radiation, the presence of oxygen is necessary because it mediates DNA damage through formation of free radicals by interaction of ionizing radiation with intracellular water. Hypoxia has also been shown to reduce chemotherapeutic efficacy by causing cells within hypoxic regions to cycle more slowly and by providing a selection mechanism for cells with reduced susceptibility for apoptosis. Additionally, due to limited drug penetration within solid tumours, hypoxic regions are often protected from the cytotoxic effects of chemotherapeutic agents further reducing drug efficacy.

All these mechanisms together ensure that tumour hypoxia is a negative prognostic factor. In order to predict outcome and identify patients with a worse prognosis and/or patients that would benefit from appropriate treatments, in vivo measurement of tumour hypoxia is required.

A variety of invasive and noninvasive approaches have been developed to measure tumour oxygenation including: *oxygen-sensitive electrodes* and *hypoxia marker techniques*[103].

3.1.1 Invasive measurement of tumour hypoxia

At present, the gold standard for direct in vivo determination of tumour oxygenation is a commercially available oxygen electrode, commonly referred to as the *Eppendorf electrode*.

However, this technically demanding procedure has a number of drawbacks and limitations like its sensitivity for sampling errors, its invasive nature and the fact that only easily accessible tumours can be studied (e.g., those in the oral cavity). In addition, a system that allows the tracking of the electrode during measurements has not been developed.

Therefore the search for a non-invasive assay for tumour hypoxia continues[103].

3.1.2 Non-invasive measurement of tumour hypoxia

These techniques use various labels that can be detected by different methods such as positron emission tomography (PET), single photon emission computed tomography (SPECT), magnetic resonance imaging (MRI), autoradiography and immunohistochemistry. Moreover, in the detection of tumour hypoxia the most encouraging results have been obtained using radiotracers that selectively accumulate in hypoxic tumours and which can be applied together with functional PET or SPECT imaging[106].

SPECT is similar to PET in its use of radioactive tracer material and detection of gamma rays. In contrast with PET, however, the tracer used in SPECT emits gamma radiation that is measured directly, whereas PET tracer emits positrons which annihilate with electrons up to a few millimetres away, causing two gamma photons to be emitted in opposite directions (**Fig. 3.3**)[107].

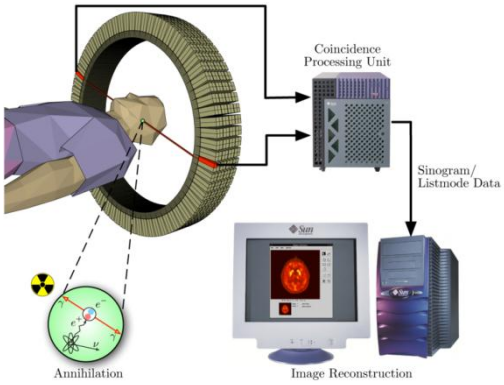

Figure 3.3: *Schema of a pet acquisition process.*

There are several prerequisites to which the ideal non-invasive hypoxic marker should comply:

1. It should be specific for hypoxia and thus distinguish normoxia, hypoxia and anoxia or necrosis.
2. It should image acute and chronic hypoxia and possibly distinguish between both.
3. It should be simple, non-toxic, fast, easy to perform and allow repeated measurements.
4. It should be lipophilic to have a homogeneous biodistribution in all tissues including tumours but at the same time hydrophilic to have a faster elimination, thus allowing larger tumour to normal tissue ratio of radioactivity.
5. It should have little hypoxia-independent degradation in vivo leading to non-specific tracer metabolites and/or little aspecific tissue binding, so that only oxygen-specific retention mechanisms determine the amount of tracer that is temporarily or permanently trapped.
6. It should reflect intracellular pO2 rather than blood flow or some consequence of subsequent biochemistry.
7. It should be sensitive at pO2 levels relevant to tumour therapy.
8. It should offer the ability to quantify.

Unfortunately, none of the present hypoxia tracers available completely fulfils these requirements.

Although SPECT is more commonly used than PET, and, in particular, it has a number of practical advantages that include ready availability at low cost, and versatile chemistry, the superior spatial resolution and more accurate quantitation with PET makes the latter a better candidate for detection of tumoural hypoxia. In addition, radiation exposure of normal tissues is less due to the short half-life of its radioisotopes, such as fluorine-18 (^{18}F)[103].

Fluorine-18, a radioactive isotope of fluorine first produced by Snell is currently the positron-emitting radioisotope of choice for the development of radiopharmaceuticals for positron emission tomography (PET), one of the most powerful nuclear medicine imaging technique in man. Reasons for such an interest for fluorine-18 are related to the physical and nuclear properties of this radioisotope: its half-life (109 min), its positron decay (97%) and positron weak energy (635 keV maximum, 2.3 mm range in matter), are particularly advantageous in term of resolution and dosimetry. During the last years, a significant number of articles have reported the use of fluorine-18 for the synthesis of new labelled tracers and their in vivo studies, in particular in man as illustrated by the wide clinical use in oncology of: [^{18}F]FDG and two nitroimidazole compounds, [^{18}F]FMISO and [^{18}F]FAZA[107].

- ***[^{18}F]FDG (2-deoxy-2-[18F]fluoro-D-glucose)***

In PET imaging, ^{18}F-FDG (**Fig. 3.4**) can be used for the assessment of glucose metabolism in the heart, lungs, and the brain. [^{18}F]FDG-PET is a non-invasive functional imaging method that is routinely used for cancer detection, staging and monitoring of response in several tumour types. Most cancer cells have increased glycolysis rates, accompanied by overexpression of glucose transmembrane transporters (GLUTs) and hexokinases (HKs) compared to normal cells. GLUTs assist in transporting glucose into the cell. Cellular

glucose becomes phosphorylated by HKs resulting in its retention inside the cell. ^{18}F-FDG is taken up by cells, phosphorylated by hexokinase (whose mitochondrial form is greatly elevated in rapidly-growing malignant tumours), and retained by tissues with high metabolic activity, such as most types of malignant tumours. As a result FDG-PET can be used for diagnosis, staging, and monitoring treatment of cancers, particularly in Hodgkin's disease, non-Hodgkin's lymphoma, colorectal cancer, breast cancer, melanoma, and lung cancer. It has also been approved for use in diagnosing Alzheimer's disease.

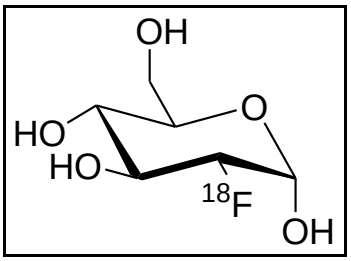

Figure 3.4: *Structure of ^{18}FDG.*

FDG, as a glucose analog, is taken up by high-glucose-using cells such as brain, kidney, and cancer cells, where phosphorylation prevents the glucose from being released again from the cell, once it has been absorbed. The 2' hydroxyl group (—OH) in normal glucose is needed for further glycolysis (metabolism of glucose by splitting it), but FDG is missing this 2' hydroxyl. Thus, in common with its sister molecule 2-deoxy-D-glucose, FDG cannot be further metabolized in cells. The ^{18}F-FDG-6-phosphate formed when ^{18}F-FDG enters the cell thus cannot move out of the cell before radioactive decay. As a result, the distribution of ^{18}F-FDG is a good reflection of the distribution of glucose uptake and phosphorylation by cells in the body.

After ^{18}F-FDG decays radioactively, however, its 2'-fluorine is converted to $^{18}O^{-}$, and after picking up a proton H^{+} from a hydronium ion in its aqueous environment, the molecule becomes glucose-6-phosphate labeled with

harmless nonradioactive "heavy oxygen" in the hydroxyl at the 2' position. The new presence of a 2' hydroxyl now allows it to be metabolized normally in the same way as ordinary glucose, producing non-radioactive end-products.
Because the uptake of [^{18}F]FDG during FDG PET imaging relies largely on the expression of proteins that are under control of HIF-1, the degree of [^{18}F]FDG uptake by tumours might indirectly reflect the level of hypoxia. Reports trying to relate [^{18}F]FDG uptake with tumour hypoxia have, however, given inconsistent results. *In vitro* studies have suggested that FDG should be accumulated in hypoxic cancer cells compared to normoxic cancer cells because of changed metabolism. However, in vivo experiments (pre-clinical and clinical) have given conflicting results when showing a correlation between the uptake of [^{18}F]FDG and the existence of hypoxia in tumours[103].
PET imaging of [^{18}F]FDG will highlight all zones presenting a variation of the glucidic metabolism, in particular in tumours whose energetic metabolism is exacerbated at time of proliferation. [^{18}F]FDG is not however the universal tumour marker and there are limitations to its effectiveness for cancer studies, as success is very dependent on the location and homogeneity of the tumour[107,108].

- ***Nitroimidazole compounds***

One promising non-invasive approach to assess hypoxia is to utilize appropriately-labelled radiosensitizers which will bind to oxygen-deficient tissues, but not to normally-oxygenated tissues. Selective binding of reactive reduction intermediates of nitroimidazole radiopharmaceuticals to the macromolecular fraction of hypoxic tissues has been porstulated to be the basis for concentrating these compounds in target (hypoxic) tissues.
These compounds are reduced into reactive intermediary metabolites by intracellular reductases in a process which is directly related to the level of oxygenation/hypoxia. This causes a gradient which is favourable for detection

of hypoxic cells. In particular, 2-Nitroimidazoles can undergo a series of oxygen-reversible single-electron reductions in hypoxic environments, forming reactive oxygen radicals[103].

The nitro-radical anion produced in the first reduction step is very reactive toward oxygen, leaving no substrate for the second step of the reduction process. In contrast, an environment of low oxygen concentration induces further reductive reactions that ultimately lead to the formation of either reactive products that are able to covalently bind to cell components or charged species that diffuse slowly out of the tissues. The reactive products observed during this multi-step process include nitroso (2e-), hydroxylamine (4e-), and amine (6e-) derivatives. When the fragmentation of the imidazole ring occurs, reactive portions of the molecule, such as glyoxal, bind to macromolecular components of cells in tissues and tumors.

In particular, metabolites obtained covalently bind to thiol groups of intracellular proteins and thereby accumulate within viable hypoxic cells.

When labelled with a PET tracer, these chemicals can be detected using PET imaging methods.

The ideal nuclear medicine marker should have a partition coefficient (lipid/water solubility) which promotes rapid and nearly equal distribution to body tissues so that the quantity of marker which becomes bound to cells, especially in tumors, will be an approximate inverse image of intracellular oxygen concentration.

Several nitroimidazole compounds with different properties and labelled with different PET radionuclides have been described, in particular two have showed a selectivity for tumour hypoxia and have been thoroughly evaluated in clinical studies[109-111].

a)[^{18}F]FMISO ([^{18}F]1-(2-nitro-1-imidazolyl)-3-fluoro-2-propanol)

[^{18}F]FMISO (**Fig. 3.5**) is the most widely used and investigated hypoxia marker and has been validated in multiple studies both in humans and animals. Studies using [^{18}F]FMISO have demonstrated variable, but significant levels of hypoxia in several tumour types.

In addition, [^{18}F]FMISO PET imaging has been used as a prognostic indicator in several other studies.

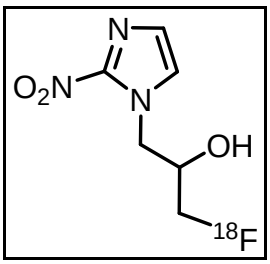

Figure 3.5: *Structure of [^{18}F]FMISO.*

In a number of studies, [^{18}F]FMISO uptake was compared with [^{18}F]FDG uptake. Most of these studies demonstrated the feasibility and utility of [^{18}F]FMISO PET imaging to identify tumour hypoxia, whereas [^{18}F]FDG PET imaging seemed less suitable for this purpose. A number of studies compared [^{18}F]FMISO uptake with invasive Eppendorf electrode pO2 measurements. In some of these studies, [^{18}F]FMISO uptake in renal cell carcinoma and head and neck cancer correlated well with pO2 measurements from polarographic needle oxygen electrodes, confirming the use of [^{18}F]FMISO PET to measure tumour hypoxia.

Other studies also compared uptake of [^{18}F]FDG and [^{18}F]FMISO in patients with head and neck cancer. They found no correlation between [^{18}F]FDG uptake and pO2 measurements, whereas an association between [^{18}F]FMISO uptake and pO2 measurements existed. Further comparison of [^{18}F]FDG and

[^{18}F]FMISO indicated that no correlation exists between both tracers as both represent different tumour characteristics.

It has, however, failed to gain wider acceptance for routine clinical application because of a number of limitations such as: (1) slow accumulation in hypoxic tumours; (2) a low target to background ratio due to high non-specific binding resulting from its relatively high lipophilicity; and (3) significant non-oxygen dependent metabolism leading to a considerable amount of radioactive metabolite products[103].

However, the utility of ^{18}FMISO is limited by the fact that one has to wait several hours after tracer application for clearance from the normoxic background tissue. This is a major deficiency, given the short half-life of radioisotope (110 min). In addition, clearance via the hepatobiliary and intestinal systems adds to the radiation dose to the patient, when compared to renally cleared tracers.

It therefore warrants the development of a more hydrophilic congener of ^{18}FMISO that overcomes these limitations without compromising its sensitivity in detecting hypoxic tissue: ^{18}FAZA[106].

b) [^{18}F]FAZA ([^{18}F]1-α-D-(5-Fluoro-5-deoxyarabinofuranosyl)-2-nitroimidazole)

The optimal hypoxia-selective reductive binding potential and faster clearance properties of several radioiodinated sugar-coupled 2-nitroimidazoles, in comparison to non-sugared azomycins, led to their clinical advancement as imaging radiodiagnostics. Exploitation of the shorter half-life of F-18 (110 min) and the superior image resolution of PET formed the basis to develop ^{18}F-labeled 1-a-D- (5-deoxy- 5-fluoroarabino furanosyl)- 2-nitroimidazole ([^{18}F]-FAZA).

[^{18}F]-FAZA (**Fig. 3.6**) is currently being used in several tumor hypoxia based clinical diagnostic studies. Radiolabeled FAZA, radiodiagnostic used extensively in the nuclear medicine community, is C-5' substituted azomycin nucleosides; it has free hydroxyl groups at C-2' and C-3', a strongly electron-withdrawing nitro group at the C-5 imidazole position and the fluorine atom in FAZA is located at C-5'; as a primary alkyl fluoride that it is prone to in vivo hydrolysis[104].

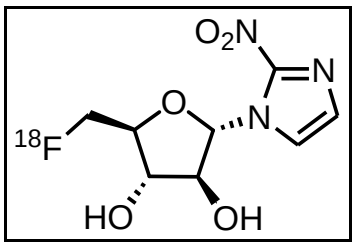

Figure 3.6: *Structure of ^{18}F-FAZA.*

The molecule 1-α-D-(5-deoxy-5-[^{18}F]-fluoroarabinofuranosyl)-2-nitroimidazole (^{18}F-FAZA) was invented and developed at the Cross Cancer Institute (Edmonton, Alberta). It is a 2-nitroimidazole-based molecule that undergoes reductive metabolism under hypoxic conditions, forming highly reactive intermediates that consequently bind to macromolecular cellular components.

Preclinical studies have shown that ^{18}F-FAZA is rapidly cleared from the circulation and nonhypoxic tissues, and is excreted mainly via the renal pathway, thereby providing more favourable tumour-tobackground (T/B), tumour-muscle (T/M) and tumour-blood (T/B) ratios in most anatomical regions. Moreover, its faster clearance from the body results in shorter waiting times after tracer application and perhaps a lower radiation exposure. In contrast, ^{18}F-FMISO, that is more lipophilic agent, is cleared primarily through the hepatobiliary route and undergoes nonspecific lipoidal uptake in the brain,

liver and other organs, thereby interfering with the image quality in the region of interest.

The in vitro as well as the in vivo experiments indicated that ^{18}F-FAZA is an excellent marker for tumour hypoxia, whereas ^{18}F-FDG is not.

Given the potential advantages of ^{18}F-FAZA for imaging hypoxia, a phase I/II study was performed to demonstrate the safety of the ^{18}F-FAZA drug product manufactured jointly by the Edmonton PET Centre and the Edmonton Radiopharmaceutical Centre, and to determine the general biodistribution pattern of this PER in patients with HNSCC, small-cell lung cancer (SCLC) or non-small-cell lung cancer (NSCLC), malignant lymphoma, or high-grade gliomas (astrocytoma and glioblastoma multiforme), GBM.

This study suggested that ^{18}F-FAZA may be a very useful radiopharmaceutical to image hypoxia in the tumour types selected. Especially the high uptake by gliomas was encouraging. Given the good imaging properties, including acceptable T/B ratios in the tumour categories studied, ^{18}F-FAZA could be considered as a very promising agent for assessing the hypoxic fraction of these tumour types[112].

^{18}F-FAZA is a PET radiotracer that is currently being used in human cancer patients in several cancer hospitals to develop improved treatment plans by assessing the presence of hypoxia in solid tumors and correlate the hypoxia levels with the treatment response. ^{18}F-FAZA has been indicated to be a superior clinical agent due to its superior central compartment clearance in comparison to ^{18}F-FMISO and is clinically being studied to see the chemotherapeutic effect of tirapazamine, a radiosensitizer[113].

3.2 Synthesis of [^{18}F]FAZA

As mentioned above, the aim of my Ph.D. visiting period was to perform the synthesis of the ^{18}F-FAZA precursor with the view of introducing ^{18}F-FAZA as a hypoxia radiotracer in Scotland. Unfortunately, the current method to synthesise FAZA is not very efficient.

Original synthetic pathway for FAZA is uneconomical and lengthy since it involves expensive reagents, and a multi-step process that requires several days of reaction, purification of the intermediate products. This lowers the overall chemical yield of FAZA (~12%) and results in tremendous time and reagents' loss[113]. In addition, this synthesis is not particularly well detailed in the literature. Therefore, after a careful bibliography research on ^{18}F-FAZA synthesis and its subsequent optimization, the **Scheme 1** was used for the synthesis of *1-α-D-[5'-O-Toluenesulfonyl-2',3'-Di-Oacetylarabinofuranosyl]-2-nitroimidazole* (DAcTs-AZA), the ^{18}F-FAZA precursor.

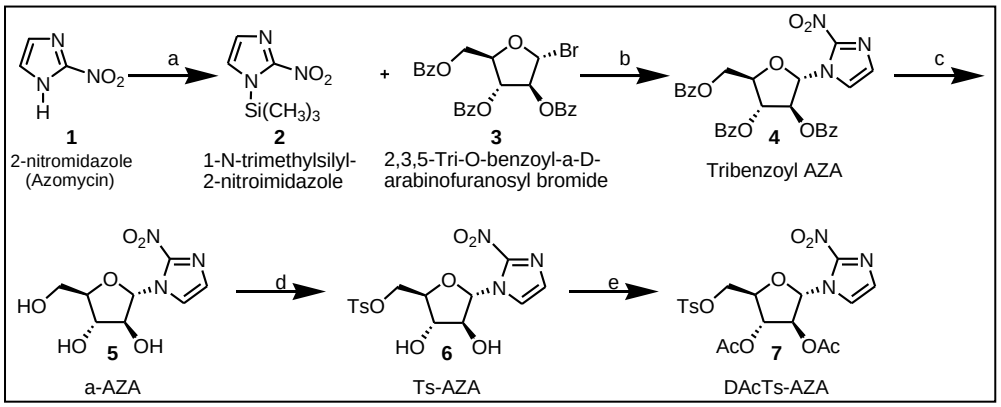

Scheme 1. *Synthesis of ^{18}F-FAZA. Reagents and conditions: (a) hexamethyldisilazane (HMDS), ammonium sulfate, reflux, 4h; (b) mercuric cyanide, anhydrous acetonitrile, 50°C, 16h, 40%; (c) NH_3 in CH_3OH, 10 h at 0°C, all weekend at rt, 90%; (d) 4-Tosyl chloride, anhydrous pyridine over KOH, 5°C, 48h, 60%; (e) acetic anhydride, , anhydrous pyridine , overnight, rt, 88%.*

In **Scheme 1** 2-nitroimidazole (Azomicin, **1**) was treated with Hexamethyldisilazane (HMDS) and a catalytic amount of ammonium sulfate to give its *N*-1-trimethylsilyl derivative (**2**). After removal of HMDS excess under complete exclusion of moisture and under high vacuum, compound **2** was subjected to a stereoselective mercuric cyanide-assisted coupling with the respective bromosugar (**3**) to afford 1-(α-D-2,3,5-Tri-*O*-benzoylarabinofuranosyl)-2-nitroimidazole (α-tribenzoyl AZA, **4**)[114]. The formation of the nucleoside product **4** was confirmed by comparison of its physical and spectroscopic data with those reported in the literature.

In this reaction, interaction of the protective group at C-2' hydroxyl plays a significant role in determining the final conformation of the coupled base.

In theory, nucleophilc substitution should occur with the inversion of configuration but by coupling of 1-α-bromo-2,3,5-tri-O-benzoyl arabinofuranose with 1-trimethylsilyl-2-nitroimidazole resulted in the exclusive formation of α-coupled product as expected according to the trans rule (double Walden inversion), whereby the benzoyl carbonyl group in the 2'-ara configuration facilitates this mechanism. In particular, intramolecular involvement of the β-plane electrons with electropositive C-1 creates steric hindrance to nucleophilic approach of 2-nitroimidazole from the α-face and results in the exclusive formation of α-azomycin tribenzoylarabinofuranoside (α-Tribenzoyl AZA). Moreover, the use of benzyl-or substituted silyl-(non-carbonylated) groups instead of benzoyl protective groups avoids this retention of configuration.

Subsequently, a deprotection of compound **4** was performed in the presence of NH_3/methanol (2M solution) and α-AZA (**5**) was obtained. For this step, the originally described procedure was modified[115]. In fact, according to the standard method, we obtained mainly the 1-(2-benzoyl-α-D-arabinofuranosyl)-2-nitroimidazole (monobenzoyl AZA, **Fig. 3.7**) and only a few milligrams of AZA (21% of yield).

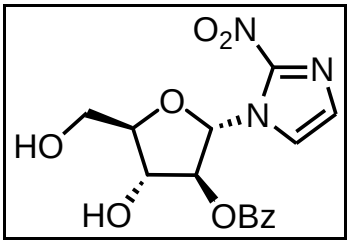

Figure 3.7: *Structure of monobenzoyl AZA.*

To increase the yield of this step of reaction, a variation of some parameters was made (**Table 3.1**), in particular: volume of NH_3/Methanol 2M solution and reaction time.

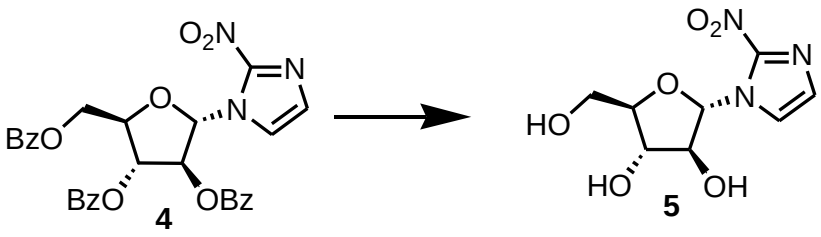

Method	mL NH_3/MeOH (for 0.054 mmol of 4)	TIME to °C	TIME to rt	Yield
A (described)	4	10h	6h	21
B	6	10h	24h	50
C	6	10h	50h	90

Table 3.1: *Tested methods of deprotection.*

The optimal conditions identified by means of these trials are outlined in the *method C*. Then, the application of this method on compound **4** led to the synthesis of compound **5** in 90% yield.

A subsequent tosylation by combining the alcohol **5** with 4-toluenesulfonyl chloride in an aprotic solvent, such as pyridine, afforded 1-α-D-[5'-O-Toluenesulfonyl-arabinofuranosyl-2-nitroimidazole (Ts-AZA, **6**).

Using the condition showed in literature, the product Ts-AZA was obtained in a very low yield (8%) because the starting material **5** did not react.

Therefore, several trials were made for identifying the optimal conditions for the formation of compound **6**.

The validation of tosylation was performed in a rigorous manner in which the variation of different parameters was considered: stoichiometry of reagents, catalyst, distillation of solvent, reaction time and temperature. The different reaction conditions are defined in the **Table 3.2** as *method A-D.*

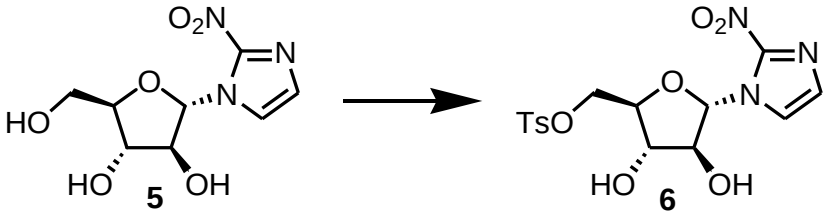

Method	4-Tosyl chloride (equiv.)	AZA (equiv.)	Catalyst	Solvent (pyridine)	TIME h	°C	Yield
A (described)[14]	1	1.4	/	Dry	4	-10	8
B	1	1	DMAP[117]	Dry	6+42	-10/5	9
C	1	1	/	dried over KOH	42	5	27
D	1.5	1	/	dried over KOH	42	5	60

Table 3.2: *Tested methods of tosylation.*

The best conditions were therefore identified (*method D*): 4-Tosyl chloride (1.5 equiv.) was added to a precooled (5°C) solution of AZA (1.0 equiv.) in anhydrous pyridine (dried over KOH). The temperature was maintained to 5°C, and the reaction was complete in nearly 42h, affording Ts-AZA (**6**) in 60% yield.

Finally, we synthesized DAcTsAZA (**7**) via acetylation with acetic anhydride, according to the described procedure[116]. ^{1}H-NMR and Mass characterization was made to confirm the synthesis of the precursor of ^{18}F-FAZA: 1-α-D-[5'-O-Toluenesulfonyl-2',3'-Di-Oacetylarabinofuranosyl]-2-nitroimidazole.

To perform clinical studies with [^{18}F]FAZA, the optimal synthesis conditions in a labeling procedure with good yields and high reproducibility, will be performed in the John Mallard Scottish PET centre at the *Aberdeen Royal Infirmary*. For this purpose, the described nucleophilic substitution reaction of no-carrier-added [^{18}F]fluoride with 1-(2,3-di-O-acetyl-5-O-tosyl-a-D-arabinofuranosyl)-2-nitroimidazole as precursor was chosen as a general protocol.

In particular, [^{18}F]Fluoride will be produced at the PETtrace cyclotron by irradiation of enriched [^{18}O]water via the ^{18}O(p,n) ^{18}F nuclear reaction.

Then, the synthesis of 1-(5-[18F]fluoro-5-deoxy-a-D-arabinofuranosyl)-2-nitroimidazole ([^{18}F]FAZA) will take place by nucleophilic substitution and subsequent hydrolysis (**Fig. 3.8**).

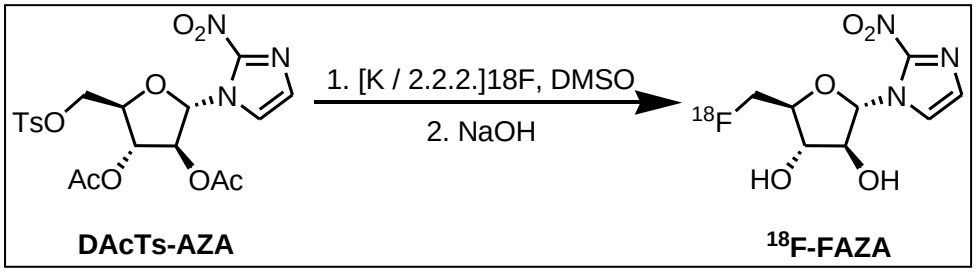

Figure 3.8: *Synthesis of [^{18}F]FAZA.*

The procedure will be performed by means of an automated, commercially available module (**Fig. 3.9**) for highly reliable production of [^{18}F]FAZA in amounts sufficient for clinical studies. As showed in literature, the automated synthesis affords ^{18}F-FAZA in an overall radiochemical yield of 20.773.5%[118].

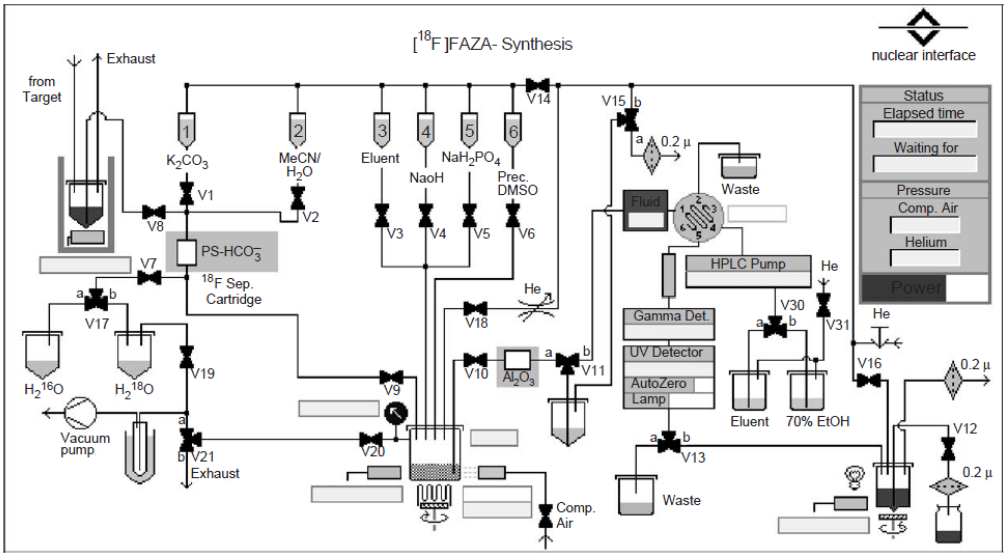

Figure 3.9: *Scheme for the automated synthesis of [^{18}F]FAZA.*

CONCLUSIONS

The present work was divided into several sections. In the early years the known broad-spectrum antiviral properties of Arbidol, led us to focus on its derivatives as potential antiviral agents. Therefore, we designed and synthesized several novel ethyl 1H-indole-3-carboxylate derivatives, using ARB as *lead compound.* In order to maintain antiviral activity we preserved the groups responsible of Arbidol interaction with membranes, eliminated those that were not considered pharmacophores (*hydroxy* and *bromo* groups at the 5- and 6-positions of the indole ring) and introduced different building blocks in 2- and 5-position. On this basis two synthetic schemes were validated: the Scheme 1 can be used for the synthesis of derivatives with different amine scaffolds in 5-position; the Scheme 6 can be used for the synthesis of derivatives with different substituents in 2-position. Biological assays on first compounds **9a$_{1–6}$** and **9b$_{1–2}$**, against *Hepatitis C virus* (*HCV*) genotype 2a and *Herpes simplex* type 1, demonstrated that ARB derivatives have anti-HCV and anti-HSV activity comparable to and, in some cases, even better than those of lead Arbidol. In particular, it was demonstrated that synthesized compounds are fusion inhibitors on both viruses and also inhibitors of HCV replication. Furthermore, it was also shown that all synthesized compounds are not selective inhibitors of HCV replication (genotype 1b, Con1 strain).

Subsequently, the attention was focused to study the mechanism of Arbidol anti-influenza action and the interaction of ARB with the N-terminal hydrophobic fusion domain of Haemagglutinin (HA, a surface viral protein of influenza virus) was evaluated. Therefore, the peptide host-guest (P20H6) was synthesized using techniques of Solid Phase Peptide Synthesis (SPPS) and *Circular dichroism* studies were made. From these studies we demonstrated that Arbidol interacts with the haemagglutinin fusion domain at pH5 and 7, through changes in the secondary structure of peptide. In addition, the

prominent interaction was at fusiogenic pH in which we had a transition from α-helix to β sheet with increasing of ARB concentration.

At the end of my Ph.D. project, I spent six months at the University of Aberdeen where I worked to the synthesis of a PET (Positron Emission Tomography) radiotracer for tumour hypoxia: the *[^{18}F]1-α-D-(5-Fluoro-5-deoxyarabinofuranosyl)-2-nitroimidazole*, known as ^{18}F-FAZA. ^{18}F-FAZA is currently the gold standard for PET Imaging of diseases characterized by hypoxia (solid tumours, ischemia, stroke), but it is not routinely used and synthesized in Scotland. The work done is an important starting point for the introduction of ^{18}F-FAZA in Scotland with the aim of using it in clinical imaging and research. In particular, the ^{18}F-FAZA precursor was synthesized: *1-α-D-[5'-O-Toluenesulfonyl-2',3'-Di-Oacetylarabinofuranosyl]-2- nitro imidazole* (DAcTs-AZA). This precursor will be used for the radiochemical synthesis of ^{18}F-FAZA in the J. Mallard Scottish PET Centre at the University of Aberdeen.

Currently, in regard to Arbidol derivatives tests are in progress to evaluate anti-HCV and anti-HSV activity of last synthesized compounds **9(c-d)$_{1-2}$** and **9e$_1$**. Moreover, to evaluate the antiviral spectrum of synthesized compounds against other viruses (influenza virus, HBV, etc) and to assess whether these compounds, such as Arbidol, interact with the N-terminal fusion hydrophobic domain of Haemagglutinin (HA, surface protein of influenza virus), circular dichroism studies and other biological assays will be performed.

The positive biological results obtained and the new results will be the basis for a rational study of a second series of compounds that will analyze in a rigorous manner the structure-activity relationships.

CHAPTER 4

EXPERIMENTAL PART

4.1 CHEMISTRY

4.1.1 Material and methods

Synthesis in solution of Arbidol derivatives and reaction intermediates. Microwave experiments were performed in a CEM Discover monomode reactor (CEM Corp., Matthews, NC). All reactions were conducted in a specially adapted cylindrical Pyrex vessel. All reagents were analytical grade and purchased from Sigma–Aldrich (Milano, Italy). Flash chromatography was performed on Carlo Erba silica gel 60 (230–400 mesh; Carlo Erba, Milan, Italy). TLC was carried out using plates coated with silica gel 60F 254 nm purchased from Merck (Darmstadt, Germany). Melting points were determined in open capillary tubes on an Electrothermal 9100 apparatus and are uncorrected. ^{1}H NMR spectra were registered on a Bruker AC 300. Chemical shifts are reported in ppm. All target compounds were assessed for purity by analytical high performance liquid chromatography (HPLC) using an Agilent 1100 series instrument equipped with a UV detector monitoring at 254 nm, HP Chem Station software, and a Waters C18 RP-column (5 µm, 300 mm x 3.9 mm). All target compounds were found to have >95% purity.

Mass spectra (MS) were taken in ESI mode on a Finnigan LCQ Deca ion trap instrument. Microanalyses were carried out on a Carlo Erba 1106 elemental analyzer. Compound 3a was synthesised in accordance with the literature Procedures[119-120].

Peptide Synthesis. N^{α}-Fmoc-protected natural amino acids, Rink-amide resin, HBTU, DCC, HOBt were purchased from Fluka–Sigma–Aldrich (Milan, Italy). Peptide synthesis solvents and reagents and CH_3CN for HPLC were reagent grade and were purchased from Riedel–Sigma–Aldrich (Milan, Italy) and used without further purification.

Peptide was synthesized according to the solid-phase approach using standard Fmoc methodology in a manual reaction vessel.

Peptide was purified with (RP-HPLC) using a Phenomenex, Jupiter C-18 (250x4,60 mm, 5 μm, 300 Å) column and a concentration gradient of CH_3CN/H_2O with 0.1% of TFA (flow rate 2 ml/min). Molecular weight was determined with a Finnigan™ LCQ™ Deca electrospray ionization/ion trap mass spectrometer.

Synthesis in solution of 18-FAZA precursor and reaction intermediates. All reagents were analytical grade and purchased from Sigma–Aldrich (UK). 2-Nitroimidazole was purchased from Merck (UK). Flash chromatography was performed on silica gel Geduran® Si 60 (0.040-0,0630) mesh (Merck UK). TLC was carried out using glass plates coated with silica gel 60F 254 nm purchased from Merck (UK). ^{1}H and ^{13}C NMR spectra were registered on a Varian 400-MR. Mass spectra (MS) were taken in ESI mode on Thermo Surveyor TSQ Quantum. LC-MS analysis were performed on an Agilent 1200 LC-MS system.

4.1.2 General procedure for the synthesis of compounds 3d-e

The sodium salt of ethyl acetoacetate (20 mmol) was dissolved in THF (40 mL) distilled and cooled to 0 °C, and n-butyllithium (2.0 M in cyclohexane, 21.0 mmol) was added dropwise. After 30 min 2-phenylbenzyl bromide **2d** or farnesyl bromide **2e** (10 mmol) was added to the solution of dianion and stirring was continued for 30 min at 0 °C. The mixture was then poured into a cold saturated solution of potassium hydrogen phosphate and extracted with ether. The combined organic layers were washed with water, dried over Na_2SO_4, filtered, and concentrated. The residue was purified by flash chromatography (n-hexane/ EtOAc, 9:1) to give **3d–e**.

4.1.2.1 Ethyl 3-oxo-5-((2-phenyl)phenyl) pentanoate (3d). Slightly yellow oil (90%); ^{1}H NMR ($CDCl_3$): δ 1.29 (t, J = 7.1 Hz, 3H, -OCH$_2$C*H*$_3$); 2.68 (t, 2H, -COC*H*$_2$CH$_2$-); 2.93 (t, 2H, -COCH$_2$C*H*$_2$-); 3.31 (s, 2H, -CO-C*H*$_2$-CO-); 4.12 (q, J=7.2 Hz, 2H, -OC*H*$_2$CH$_3$); 7.14-7.48 (m, 9H, -Ph*H*-Ph*H*).

4.1.2.2 Ethyl 7,11,15-trimethyl-3-oxohexadeca-6,10,14-trienoate (3e). Slightly yellow oil (81%); ^{1}H NMR ($CDCl_3$): δ 1.29 (t, J = 7.1 Hz, 3H, -OCH$_2$C*H*$_3$); 1.61 (m, 9H, -C*H*$_3$ farnesyl) 1.71 (s, 3H, -C*H*$_3$ farnesyl); 2 (m, 8H, C*H*$_2$ farnesyl); 2.32 (q, 2H, -C*H*$_2$CH$_2$CO-); 2.62 (t, 2H, -CH$_2$-C*H*$_2$-CO-); 3.41 (s, 2H, -CO-C*H*$_2$-CO); 4.2 (q, J=7.2 Hz, 2H, -OC*H*$_2$CH$_3$); 5.1 (m, 3H, =C*H*-).

4.1.3 General procedure for the synthesis of compounds 5b–d

A mixture of 4-bromo-2-iodoaniline (20 mmol), ethyl acetoacetate **3b** or 3-oxo-4 (phenylthio)butanoate **3c** or ethyl 3-oxo-5-((2-phenyl)phenyl) pentanoate **3d** (22 mmol), CuI (2 mmol), BINOL (4 mmol) and Cs_2CO_3 (20 mmol) in DMSO (35 ml) was stirred at 50 °C for 5–7 h under an atmosphere of nitrogen. After this time, the mixture was partitioned between ethyl acetate and saturated NH_4Cl. The organic layer was washed with brine, dried over sodium sulphate and concentrated in vacuo. The residue was purified by flash chromatography over silica gel to give **5b-d**.

4.1.3.1 Ethyl 5-bromo-2-methyl-1H-indole-3-carboxylate (5b). Elution with toluene/EtOAc (95:5) afforded **5b** (52%) as gray-green powder; mp: 163–165 °C; ^{1}H NMR ($CDCl_3$): δ 1.5 (t, J = 7.2 Hz, 3H, –OCH$_2$C*H*$_3$); 2.75 (s, 3H, –C*H*$_3$); 4.45 (q, J = 7.2 Hz, 2H, –OC*H*$_2$CH$_3$); 7.2 (d, 1H, –Φ*H*); 7.35 (dd, J = 8.55, 1.75 Hz, 1H, –Φ*H*); 8.28 (s, 1H, –Φ*H*); 8.38 (s, 1H, –N*H*); MS: m/z 282.1, 284.1 [MH$^+$].

4.1.3.2 Ethyl 5-bromo-2-((phenylthio)methyl)-1H-indole-3-carboxylate (5c). Elution with n-hexane/EtOAc (95:5) afforded **5c** (56%) as yellow powder; mp: 142–144 °C; ^{1}H NMR ($CDCl_3$): δ 1.47 (t, J = 7.2 Hz, 3H, –OCH_2CH_3); 4.42 (q, J = 7.2 Hz, 2H, –OCH_2CH_3); 4.80 (s, 2H, –CH_2-sulfonyl–); 7.18 (d, 1H, –Φ*H*); 7.20–7.5 (m, 6H, –Φ*H* and –Ph*H*); 8.20 (s, 1H, –Φ*H*); 8.8 (s, 1H, –N*H*); MS: m/z 390.0, 392.0 [MH^+].

4.1.3.3 Ethyl 5-bromo-2-((phenylphenyl)ethyl)-1H-indole-3-carboxylate (5d). Elution with benzene/chloroform (7:3) afforded **5d** (48%) as white powder; ^{1}H NMR ($CDCl_3$): δ 1.5 (t, J = 7.1 Hz, 3H, -OCH_2CH_3); 3.08 (t, 2H, -CH_2CH_2-Ph-Ph); 3.25 (t, 2H, -CH_2CH_2-Ph-Ph); 4.40 (q, J = 7.2 Hz, 2H, -OCH_2CH_3); 7.05 (d, 1H, -Φ*H*); 7.20-7.5 (m, 10H, -Ph*H*–Ph*H* and -Φ*H*); 8.20 (s, 1H, -Φ*H*); MS: m/z 448.0, 450.0 [MH^+].

4.1.4 General procedure for the synthesis of compounds 6b-d

To a stirred solution of compound **5b** or **5c** or **5d** (9 mmol) in DMF (40 mL) at 0 °C was added freshly powdered potassium hydroxide (10 mmol). After stirring the mixture for 30 min at 0 °C, methyl iodide (13.5 mmol) was added dropwise with vigorous stirring. After 1 h, the reaction mixture was diluted with diethyl ether and washed with saturated NaCl solution. The organic layer was dried (Na_2SO_4), and the solvent was removed in vacuo to yield **6b-d**.

4.1.4.1 Ethyl 5-bromo-1,2-dimethyl-1H-indole-3-carboxylate (6b). Brown powder (92%); mp: 98–100 °C; ^{1}H NMR ($CDCl_3$): δ 1.5 (t, J = 7.2 Hz, 3H, –OCH2C*H*$_3$); 2.83 (s, 3H, –C*H*$_3$); 3.77 (s, 3H, –NC*H*$_3$); 4.45 (q, J = 7.2 Hz, 2H, –OCH_2CH_3); 7.2 (d, 1H, –ΦH); 7.35 (dd, J = 8.55, 1.75 Hz, 1H, –ΦH); 8.28 (s, 1H, –ΦH); MS: m/z 296.1, 298.1 [MH+].

4.1.4.2 Ethyl 5-bromo-1-methyl-2-((phenylthio)methyl)-1H-indole-3-carboxylate (6c). White powder (97%); mp: 109–111 °C; ^{1}H NMR ($CDCl_3$): δ 1.45 (t, J = 7.2 Hz, 3H, –OCH$_2$C*H*$_3$); 3.70 (s, 3H, –NC*H*$_3$); 4.35 (q, J = 7.2 Hz, 2H, –OC*H*$_2$CH$_3$); 4.78 (s, 2H, –C*H*$_2$-sulfonyl–); 7.18 (d, 1H, –Φ*H*); 7.20–7.5 (m, 6H, –Φ*H* and –Ph*H*); 8.23 (s, 1H, –Φ*H*); MS: m/z 404.0, 406.0 [MH+].

4.1.4.3 Ethyl 5-bromo-1-methyl-2-((phenylphenyl)ethyl)-1H-indole-3-carboxylate (6d). White powder (87%); ^{1}H NMR ($CDCl_3$): δ 1.5 (t, J = 7.1 Hz, 3H, -OCH$_2$C*H*$_3$); 3.0 (s, 3H, -N-C*H*$_3$); 3.08 (t, 2H, -CH$_2$C*H*$_2$-Ph-Ph); 3.25 (t, 2H, -C*H*$_2$CH$_2$-Ph-Ph); 4.40 (q, J = 7.2 Hz, 2H, -OC*H*$_2$CH$_3$); 7.05 (d, 1H, -Φ*H*); 7.20-7.5 (m, 10H, -Ph*H*–Ph*H* and –Φ*H*); 8.20 (s, 1H, -Φ*H*); MS: m/z 462.1, 464.1[MH$^+$].

4.1.5 General procedure for the synthesis of compounds 7b-d

A solution of potassium vinyltrifluoroborate (8 mmol), $PdCl_2$ (0.2 mmol), PPh_3 (0.6 mmol), Cs_2CO_3 (9.6 mmol), and compound **6b** or **6c** or **6d** (3.2 mmol) in THF/H2O (9:1) (24 mL) was heated at 85 °C and stirred for 20–22 h. Then, the reaction mixture was cooled to room temperature and diluted with H_2O, followed by extraction with dichloromethane. The solvent was removed in vacuo, and the crude product was purified by silica gel chromatography to give compounds **7b-d**.

4.1.5.1 Ethyl 1,2-dimethyl-5-vinyl-1H-indole-3-carboxylate (7b). Elution with n-hexane/ EtOAc (9:1) afforded **7b** (92%) as yellow powder; mp: 51–53 °C; ^{1}H NMR ($CDCl_3$): δ 1.5 (t, J = 7.2 Hz, 3H, –OCH$_2$C*H*$_3$); 2.83 (s, 3H, –C*H*$_3$); 3.77 (s, 3H, –NC*H*$_3$); 4.45 (q, J = 7.2 Hz, 2H, –OC*H*$_2$CH$_3$); 5.23 (d, J = 11.18 Hz, 1H, C*H*$_2$=CH–); 5.7 (d, J = 17.54, 1H, C*H*$_2$=CH–); 6.87 (dd, J = 17.10, 10.74 Hz, 1H, CH$_2$=C*H*–); 7.25 (d, 1H, –Φ*H*); 7.45 (dd, J = 8.55, 1.75 Hz, 1H, –Φ*H*); 8.20 (s, 1H, –Φ*H*); MS: m/z 244.0 [MH+].

4.1.5.2 Ethyl 1-methyl-2-((phenylthio)methyl)-5-vinyl-1H-indole-3-carboxylate (7c). Elution with n-hexane/ EtOAc (9:1) afforded **7c** (97%) as yellow powder; mp: 103–105 °C; ^{1}H NMR ($CDCl_3$): δ 1.42 (t, J = 7.2 Hz, 3H, –OCH$_2$C*H*$_3$); 3.70 (s, 3H, –NC*H*$_3$); 4.35 (q, J = 7.2 Hz, 2H, –OC*H*$_2$CH$_3$); 4.78 (s, 2H, –C*H*$_2$-sulfonyl–); 5.23 (d, J = 10.96 Hz, 1H, C*H*$_2$=CH–); 5.7 (d, J = 11.54 Hz, 1H, C*H*$_2$=CH–); 6.87 (dd, J = 17.87, 10.74 Hz, 1H, CH$_2$=C*H*–); 7.25 (d, 1H, –ΦH); 7.35–7.5 (m, 6H, –ΦH and –PhH); 8.20 (s, 1H, –ΦH); MS: m/z 352.0 [MH$^+$].

4.1.5.3 Ethyl 1-methyl-2-((phenylphenyl)ethyl)-5-vinyl-1H-indole-3-carboxylate (7d). Elution with toluene/petroleum ether (9:1) afforded **7d** (90%) as white powder; ^{1}H NMR ($CDCl_3$): δ 1.5 (t, J = 7.1 Hz, 3H, -OCH$_2$C*H*$_3$); 3.0 (s, 3H, -N-C*H*$_3$); 3.08 (t, 2H, -CH$_2$C*H*$_2$-Ph-Ph); 3.25 (t, 2H, -CH$_2$CH$_2$-Ph-Ph); 4.40 (q, J = 7.2 Hz, 2H, -OC*H*$_2$CH$_3$); 5.20 (d, 1H, C*H*$_2$=CH-); 5.78 (d, 1H, C*H*$_2$=CH-); 6.87 (dd, 1H, CH$_2$=C*H*-); 7.05 (d, 1H, -Φ*H*); 7.20-7.5 (m, 10H, -PhH–Ph*H* and –Φ*H*); 8.20 (s, 1H, -Φ*H*); MS: m/z 410.2 [MH$^+$].

4.1.6 General procedure for the synthesis of compounds 8(a,b,d)

OsO_4 (0.1 mmol) was added to a stirred mixture of **7b** or **7c** (1 mmol) and 2,6-lutidine (2 mmol) in dioxane (26 mL). The mixture turned from colorless to black in 1 min. Sodium periodate (4 mmol) in water (6 mL, warmed to dissolve) was added. A gray precipitate was immediately formed. The mixture was stirred for 20 min, then extracted with water and dichloromethane. The organic layers were combined, dried, filtered and concentrated. The residue was purified by flash chromatography over silica gel to yield **8(a,b,d)**.

4.1.6.1 Ethyl 5-formyl-1-methyl-2-((phenylsulfonyl)methyl)-1H-indole-3-carboxylate (8a). Elution with n-hexane/ EtOAc (7:3) afforded **8a** (95%) as gray-white powder; mp: 136–138 °C; ^{1}H NMR ($CDCl_3$): δ 1.3 (t, J = 7.2 Hz, 3H, –OCH$_2$C*H*$_3$); 4.03 (s, 3H, –NC*H*$_3$); 4.15 (q, J = 7.2 Hz, 2H, –OC*H*$_2$CH$_3$); 5.33 (s, 2H, –C*H*$_2$-sulfonyl–); 7.45–7.75 (m, 6H, –Φ*H* and –Ph*H*); 7.95 (d, 1H, –Φ*H*); 8.56 (s, 1H, –Φ*H*); 10.12 (s, 1H, –CO*H*); MS: m/z 386.1 [MH$^+$].

4.1.6.2 Ethyl 5-formyl-1,2-dimethyl-1H-indole-3-carboxylate (8b). Elution with n-hexane/ EtOAc (7:3) afforded **8b** (92%) as beige powder; mp: 118–120 °C; ^{1}H NMR ($CDCl_3$): δ 1.5 (t, J = 7.2 Hz, 3H, –OCH2C*H*$_3$); 2.83 (s, 3H, –C*H*$_3$); 3.77 (s, 3H, –NC*H*$_3$); 4.45 (q, J = 7.2 Hz, 2H, –OC*H*$_2$CH$_3$); 7.45 (d, 1H, –Φ*H*); 7.88 (dd, J = 8.55, 1.75 Hz, 1H, –Φ*H*); 8.67 (s, 1H, –Φ*H*); 10.12 (s, 1H, –CO*H*); MS: m/z 246.1 [MH$^+$].

4.1.6.3 Ethyl 5-formyl-1-methyl-2-((phenylphenyl)ethyl)-1H-indole-3-carboxylate (8d). Elution with dichloromethane/petroleum ether (7:3) afforded **8d** (90%) as white powder; ^{1}H NMR ($CDCl_3$): δ 1.5 (t, J = 7.1 Hz, 3H, -OCH$_2$C*H*$_3$); 3.0 (s, 3H, -N-C*H*$_3$); 3.08 (t, 2H, -CH$_2$C*H*$_2$-Ph-Ph); 3.25 (t, 2H, -C*H*$_2$CH$_2$-Ph-Ph); 4.40 (q, J = 7.2 Hz, 2H, -OC*H*$_2$CH$_3$); 7.45 (d, 1H, -Φ*H*); 7.75-7.9 (m, 10H, -Ph*H*–Ph*H* and –Φ*H*); 8.67 (s, 1H, -Φ*H*); 10.12 (s, 1H, -CO*H*); MS: m/z 412.1 [MH$^+$].

4.1.7 General procedure for the synthesis of compounds 8c

$K_3Fe(CN)_6$ (25 mmol), K_2CO_3 (25mmol) and OsO_4 (0.83 mmol) were added to a solution of **7c** (8.3 mmol) in dioxane /water (1:1; 120 mL). After 30 min. $Pb(OAc)_4$ (33.3 mmol) was added to the reaction and stirred all night at room temperature. The reaction was quenched by the addition of solid Na_2SO_3 and saturated $NaHSO_3$, and extracted with ethyl acetate. The combined organic extracts were washed with brine, dried over Na_2SO_4 and concentrated

and purified by flash chromatography (petroleum ether/ethyl acetate, 9.1) to provide **8c** (53%) as white solid.

^{1}H NMR ($CDCl_3$): δ ^{1}H NMR ($CDCl_3$): δ 1.3 (t, J = 7.2 Hz, 3H, –OCH_2CH_3); 3.71 (s, 3H, –NCH_3); 4.3 (q, J = 7.2 Hz, 2H, –OCH_2CH_3); 4.72 (s, 2H, –CH_2-sulfur–); 7.39–7.65 (m, 6H, –Φ*H* and –Ph*H*); 7.75 (d, 1H, –Φ*H*); 8.12 (s, 1H, –Φ*H*); 10.12 (s, 1H, –CO*H*); MS: m/z 354.1 [MH^+].

4.1.8 General procedure for the synthesis of compounds $9a_{1–2}$

Compound **8a** (0.04 g, 0.1 mmol), dimethylamine or pyrrolidine (0.12 mmol), acetic acid (0.06 mL, 1.02 mmol) and $NaB(OAc)_3H$ (0.05 g, 0.21 mmol) were, in that order, added to dry THF (4 mL). The mixture was irradiated with microwaves for 10 min at 130 °C. Additional amine (0.12 mol) and $NaB(OAc)_3H$ (0.05 g, 0.21 mmol) were added, and the mixture was irradiated at 130 °C for 5 min. This gave 100% conversion to product. The reaction mixture was filtered and concentrated. The residue was dissolved in methanol (1.5 mL) and concd HCl (0.5 mL) and irradiated using microwaves at 100 °C for 5 min. The mixture was filtered and purified by flash chromatography over silica gel (benzene/methanol, 9:1) to give the desired compounds $\mathbf{9a_{1–2}}$.

4.1.8.1 Ethyl 5-((dimethylamino)methyl)-1-methyl-2-((phenyl sulfonyl)methyl)-1H-indole-3-carboxylate ($9a_1$). Sandy powder (0.033 g, 78%); mp: 205–208 °C; ^{1}H NMR ($CDCl_3$): δ 1.45 (t, J = 7.2 Hz, 3H, –OCH_2CH_3); 2.45 (s, 6H, –$N(CH_3)_2$); 3.82 (s, 2H, –CH_2N<); 3.95 (s, 3H, –NCH_3); 4.05 (q, J = 7.2 Hz, 2H, –OCH_2CH_3); 5.25 (s, 2H, –CH_2-sulfonyl–); 7.3–7.75 (m, 7H, –Φ*H* and –Ph*H*); 8.0 (s, 1H, –Φ*H*); MS: m/z 415.0 [MH+].

4.1.8.2 Ethyl 1-methyl-2-((phenylsulfonyl)methyl)-5-((pyrrolidin-1yl) methyl)-1H-indole-3-carboxylate (9a$_2$). Beige powder (0.039 g, 87%); mp: 118–120 °C; ^{1}H NMR ($CDCl_3$): δ 1.3 (t, J = 7.2 Hz, 3H, –OCH$_2$C*H*$_3$); 1.87 (s, 4H, –pyrrolidinyl *H*); 2.73 (s, 4H, –pyrrolidinyl *H*); 3.82 (s, 2H, –C*H*$_2$N<); 3.95 (s, 3H, –NC*H*$_3$); 4.05 (q, J = 7.2 Hz, 2H, –OC*H*$_2$CH$_3$); 5.25 (s, 2H, –C*H*$_2$-sulfonyl–); 7.3–7.75 (m, 7H, –Φ*H* and –Ph*H*); 8.0 (s, 1H, –Φ*H*); MS: m/z 441.0 [MH$^+$].

4.1.9 Synthesis of N-Boc homopiperazine 13

To a solution of dichloromethane (45 mL) and homopiperazine **11** (1.84 g, 18 mmol), maintained at 0 °C using an ice bath, was added dropwise a di-tert-butyldicarbonate solution 12 (2 g, 9 mmol in 18 mL dichloromethane). The mixture was stirred for an additional 1 h then was filtered.

The filtrate was concentrated to dryness. Water (27 mL) was added to the resulting oil, and the mixture was filtered. The filtrate was saturated with potassium carbonate and extracted with diethyl ether (3 x 13 mL). The solvent was dried over sodium sulfate and concentrated to dryness, yielding 13 (1.58 g, 88%).

4.1.10 General procedure for the synthesis of compounds 9a$_{3–5}$

Compound **8a** (0.04 g, 0.1 mmol), 4-methylpiperazine or morpholine or 1-BOC-homopiperazine (0.15 mmol), acetic acid (0.06 mL, 1.02 mmol) and $NaB(OAc)_3H$ (0.055 g, 0.24 mmol) were, in that order, added to dry THF (4 mL). The mixture was irradiated with microwaves for 10 min at 130 °C. Additional amine (0.15 mol) and $NaB(OAc)_3H$ (0.055 g, 0.24 mmol) were added, and the mixture was irradiated at 130 °C for 5 min. This gave 100% conversion to product. The reaction mixture was filtered and concentrated. The residue was dissolved in methanol (1.5 mL) and conc. HCl (0.5 mL) and irradiated using microwaves at 100 °C for 5 min. The mixture was filtered and

purified by flash chromatography over silica gel to give the desired compounds **9a$_{3–5}$**.

4.1.10.1 Ethyl 1-methyl-5-((4-methylpiperazin-1-yl)methyl)-2-((phenylsulfonyl)methyl)-1H-indole-3-carboxylate (9a$_3$). Elution with benzene/MeOH (9:1) afforded **9a$_3$** (0.045 g, 94%) as a brownish-yellow powder; mp: 94–96 °C; ^{1}H NMR ($CDCl_3$): δ 1.3 (t, J = 7.2 Hz, 3H, –OCH_2CH_3); 2.57 (s, 3H, 4-CH_3 of piperazinyl); 2.75–3.05 (m, 8H, 8H of piperazinyl); 3.75 (s, 2H, –CH_2N<); 3.95 (s, 3H, –NCH_3); 4.05 (q, J = 7.2 Hz, 2H, –OCH_2CH_3); 5.25 (s, 2H, –CH_2-sulfonyl–); 7.3–7.7 (m, 7H, –Φ*H* and –Ph*H*); 7.95 (s, 1H, –Φ*H*); MS: m/z 470.1 [MH^+].

4.1.10.2 Ethyl 1-methyl-5-(morpholinomethyl)-2-((phenylsulfonyl) methyl)-1H-indole-3-carboxylate (9a$_4$). Elution with benzene/MeOH (95:5) afforded **9a$_4$** (0.039 g, 85%) as an rose powder; mp: 109–111 °C; ^{1}H NMR ($CDCl_3$): δ 1.3 (t, J = 7.2 Hz, 3H, –OCH_2CH_3); 2.53 (s, 4H, 4*H* of morpholino); 3.65 (s, 2H, –CH_2N<); 3.75 (s, 4H, 4*H* of morpholino); 3.95 (s, 3H, –NCH_3); 4.05 (q, J = 7.2 Hz, 2H, –OCH_2CH_3); 5.25 (s, 2H, –CH_2-sulfonyl–); 7.3–7.7 (m, 7H, –Φ*H* and –Ph*H*); 7.95 (s, 1H, –Φ*H*); MS: m/z 457.0 [MH^+].

4.1.10.3 Ethyl 5-((1,4-diazepan-1yl)methyl)-1-methyl-2-((phenyl sulfonyl) methyl)-1H-indole-3-carboxylate (9a$_5$). Elution with benzene/MeOH/NH_4OH (9:1:0.25) afforded **9a$_5$** (0.04 g, 83%) as a white powder; mp: 98–100 °C; ^{1}H NMR (CD_3OD): δ 1.3 (t, J = 7.2 Hz, 3H, –OCH_2CH_3); 2.0 (s, 1H, –N*H* of homopiperazine); 2.1 (m, 2H, 2*H* of homopiperazine); 2.95 (t, 2H, 2*H* of homopiperazine); 3.1 (t, 2H, 2*H* of homopiperazine); 3.35 (t, 4H, 4*H* of homopiperazine); 3.90 (s, 3H, –NCH_3); 4.0 (s, 2H, –CH_2N<); 4.15 (q, J = 7.2 Hz, 2H, –OCH_2CH_3); 5.4 (s, 2H, –CH_2-

sulfonyl–); 7.4–7.75 (m, 7H, –Φ*H* and –Ph*H*); 8.05 (s, 1H, –Φ*H*); MS: m/z 470.1 [MH^+].

4.1.11 Synthesis of ethyl 5-(hydroxymethyl)-1-methyl-2-((phenylsulfonyl) methyl)-1H-indole-3-carboxylate (10a)

To an ice-cooled solution of the corresponding aldehyde **8a** (0.12 g, 0.3 mmol) in THF (1.5 mL) was added $NaBH_4$ (0.029 g, 0.75 mmol) in methanol (3.8 mL). Then, the resulting mixture was stirred at rt for 1 h. After complete conversion, the solvent was distilled off under reduced pressure. Then, water was added, and the resulting mixture was extracted with ethyl acetate. The combined organic phases were washed with brine, dried over Na_2SO_4 and evaporated under reduced pressure. The desired product was purified by chromatography on silica gel (hexane/EtOAc 6:4) to give **10a** (0.106 g, 91%) as white solid; mp: 172–174 °C; ^{1}H NMR ($CDCl_3$): δ 1.3 (t, J = 7.2 Hz, 3H, –OCH_2CH_3); 2.0 (s, 1H, –CH_2OH); 3.97 (s, 3H, –NCH_3); 4.05 (q, J = 7.2 Hz, 2H, –OCH_2CH_3); 4.82 (s, 2H, –CH_2-sulfonyl–); 5.28 (s, 2H, –CH_2OH); 7.4–7.75 (m, 7H, –Φ*H* and –Ph*H*); 8.05 (s, 1H, –Φ*H*); MS: m/z 388.1 [MH^+].

4.1.12 Synthesis of ethyl 5-((1H-imidazol-1-yl)methyl)-1-methyl-2-((phenyl sulfonyl)methyl)-1H-indole-3-carboxylate ($9a_6$)

To a solution of compound **10a** (0.06 g, 0.15 mmol) in acetonitrile (1.5 mL) was added CDI (0.127 g, 0.75 mmol) and imidazole (0.021 g, 0.3 mmol). The resulting solution was heated to reflux for 16 h. After cooling to ambient temperature, the reaction mixture was diluted with water and extracted with ethyl acetate. The combined organic phases were washed with brine, dried over Na_2SO_4 and evaporated under reduced pressure. The desired product was purified by chromatography on silica gel (dichloromethane/methanol, 98:2) to obtain **$9a_6$** (0.044 g, 67%) as a pearl-white powder; mp: 95–97 °C; ^{1}H NMR ($CDCl_3$): δ 1.3 (t, J = 7.2 Hz, 3H, –OCH_2CH_3); 3.97 (s, 3H, –NCH_3); 4.05 (q, J

= 7.2 Hz, 2H, –OC*H*$_2$CH$_3$); 5.28 (s, 4H, –C*H*$_2$-sulfonyl– and –C*H*$_2$N<); 6.95 (s, 1H, 2-1*H* of imidazolyl) 7.05–7.2 (m, 2H, 4,5-2*H* of imidazolyl); 7.4–7.75 (m, 7H, –Φ*H* and –Ph*H*); 7.9 (s, 1H, –Φ*H*); MS: m/z 438.1 [MH$^+$].

4.1.13 General procedure for the synthesis of compounds 9b$_{1–2}$

Compound **8b** (0.04 g, 0.1 mmol), dimethylamine or pyrrolidine (0.12 mmol), acetic acid (0.095 mL, 1.02 mmol) and NaB(OAc)$_3$H (0.074 g, 0.21 mmol) were, in that order, added to dry THF (4 mL). The mixture was irradiated with microwaves for 10 min at 130 °C. Additional amine (0.12 mmol) and NaB(OAc)$_3$H (0.074 g, 0.21 mmol) were added, and the mixture was irradiated at 130 °C for 5 min. This gave 100% conversion to product. The reaction mixture was filtered and concentrated. The residue was dissolved in methanol (1.5 mL) and conc. HCl (0.5 mL) and irradiated using microwaves at 100 °C for 5 min. The mixture was filtered and purified by flash chromatography over silica gel (benzene/methanol, 95:5) to give the desired compounds **9b$_{1–2}$**.

4.1.13.1 Ethyl 5-((dimethylamino)methyl)-1,2-(dimethyl)-1H-indole-3-carboxylate (9b$_1$). Bone powder (0.033 g, 75%); mp: 67–69 °C; ^{1}H NMR (CDCl$_3$): δ 1.45 (t, J = 7.2 Hz, 3H, –OCH$_2$C*H*$_3$); 2.65 (s, 6H, –N(C*H*$_3$)$_2$); 2.83 (s, 3H, –C*H*$_3$); 3.77 (s, 3H, –NC*H*$_3$); 4.30 (s, 2H, –C*H*$_2$–N<); 4.45 (q, J = 7.2 Hz, 2H, –OC*H*$_2$CH$_3$); 7.45 (d, 1H, –Φ*H*); 7.60 (dd, J = 8.55, 1.75 Hz, 1H, –Φ*H*); 8.15 (s, 1H, –Φ*H*); MS: m/z 275.0 [MH$^+$].

4.1.13.2 Ethyl 1,2-(dimethyl)-5-((pyrrolidin-1yl)methyl)-1H-indole-3-carboxylate (9b$_2$). Nut-brown powder (0.04 g, 83%); mp: 125–127 °C; ^{1}H NMR (CDCl$_3$): δ 1.45 (t, J = 7.2 Hz, 3H, –OCH$_2$C*H*$_3$); 1.59 (m, 4H, –pyrrolidinyl *H*); 2.25 (m, 4H, –pyrrolidinyl *H*); 2.83 (s, 3H, –C*H*$_3$); 3.77 (s, 3H, –NC*H*$_3$); 4.30 (s, 2H, –C*H*$_2$– N<); 4.45 (q, J = 7.2 Hz, 2H, –OC*H*$_2$CH$_3$);

7.45 (d, 1H, –Φ*H*); 7.78 (dd, J = 8.55, 1.75 Hz, 1H, –Φ*H*); 8.15 (s, 1H, –Φ*H*); MS: m/z 301.0 [MH^+].

4.1.14 General procedure for the synthesis of compounds $9c_{1–2}$

Compound **8c** (0.04 g, 0.12 mmol), dimethylamine or pyrrolidine (0.14 mmol), acetic acid (0.074 mL, 1.2 mmol) and $NaB(OAc)_3H$ (0.055 g, 0.25 mmol) were, in that order, added to dry THF (4 mL). The mixture was irradiated with microwaves for 10 min at 130 °C. Additional amine (0.12 mmol) and $NaB(OAc)_3H$ (0.055 g, 0.25 mmol) were added, and the mixture was irradiated at 130 °C for 5 min. This gave 100% conversion to product. The reaction mixture was filtered and concentrated. The residue was dissolved in methanol (1.5 mL) and conc. HCl (0.5 mL) and irradiated using microwaves at 100 °C for 5 min. The mixture was filtered and purified by flash chromatography over silica gel (dichloromethane/methanol, 9:1) to give the desired compounds **$9c_{1–2}$**.

4.1.14.1 Ethyl 5-((dimethylamino)methyl)-1-methyl-2-((phenyltio) methyl)-1H-indole-3-carboxylate ($9c_1$). White powder (0.032 g, 82%); mp: ^{1}H NMR ($CDCl_3$): δ 1.39 (t, J = 7.2 Hz, 3H, $–OCH_2CH_3$); 2.76 (s, 6H, $–N(CH_3)_2$); 3.71 (s, 2H, $–CH_2N<$); 3.72 (s, 3H, $–NCH_3$); 4.31 (q, J = 7.2 Hz, 2H, $–OCH_2CH_3$); 4.74 (s, 2H, $–CH_2$-sulfur–); 7.3–7.67 (m, 6H, –Φ*H* and –Ph*H*); 7.75 (d, 1H, –Φ*H*); 8.12 (s, 1H, –Φ*H*); MS: m/z 383.0 [MH+].

4.1.14.2 Ethyl 1-methyl-2-((phenyltio)methyl)-5-((pyrrolidin-1yl)methyl)-1H-indole-3-carboxylate ($9c_2$). Brown powder (0.035 g, 84%); mp: ^{1}H NMR ($CDCl_3$): δ 1.39 (t, J = 7.2 Hz, 3H, $–OCH_2CH_3$); 1.9 (s, 4H, –pyrrolidinyl *H*); 2.2 (s, 4H, –pyrrolidinyl *H*); 3.70 (s, 3H, $–NCH_3$); 3.81 (s, 2H, $–CH_2N<$); 4.31 (q, J = 7.2 Hz, 2H, $–OCH_2CH_3$); 4.74 (s, 2H, $–CH_2$-sulfur–); 7.3–7.69 (m, 7H, –Φ*H* and –Ph*H*); 8.08 (s, 1H, –Φ*H*); MS: m/z 409.0 [MH^+].

4.1.15 General procedure for the synthesis of compounds $9d_{1–2}$

Compound **8d** (0.042 g, 0.1 mmol), dimethylamine or pyrrolidine (0.15 mmol), acetic acid (0.060 mL, 1 mmol) and $NaB(OAc)_3H$ (0.055 g, 0.24 mmol) were, in that order, added to dry THF (4 mL). The mixture was irradiated with microwaves for 10 min at 130 °C. Additional amine (0.15 mmol) and $NaB(OAc)_3H$ (0.055 g, 0.24 mmol) were added, and the mixture was irradiated at 130 °C for 5 min. This gave 100% conversion to product. The reaction mixture was filtered and concentrated. The residue was dissolved in methanol (1.5 mL) and conc. HCl (0.5 mL) and irradiated using microwaves at 100 °C for 5 min. The mixture was filtered and purified by flash chromatography over silica gel (toluene/methanol, 9:1) to give the desired compounds **$9d_{1–2}$**.

4.1.15.1 Ethyl 5-((dimethylamino)methyl)-1-methyl-2-((phenyl phenyl) ethyl) -1H-indole-3-carboxylate ($9d_1$). Yellow oil (0.035 g, 78%); mp: ^{1}H NMR ($CDCl_3$): δ 1.45 (t, J = 7.1 Hz, 3H, -OCH_2CH_3); 2.35 (s, 6H, -$N(CH_3)_2$); 3.0 (s, 5H, -N-CH_3 and -CH_2-$N(CH_3)_2$); 3.24 (t, 2H, -CH_2CH_2-Ph-Ph); 3.6 (t, 2H, -CH_2CH_2-Ph-Ph); 4.45 (q, J = 7.2 Hz, 2H, -OCH_2CH_3); 7.1-7.6 (m, 11H, -Ph*H*–Ph*H* e –Φ*H*); 8.05 (s, 1H, -Φ*H*); MS: *m/z* 441.1 [MH^+].

4.1.15.2 Ethyl 1-methyl-2-((phenylphenyl)ethyl)-5-((pyrrolidin-1yl) methyl)-1H-indole-3-carboxylate ($9d_2$). Yellow powder (0.036 g, 75%); mp: ^{1}H NMR ($CDCl_3$): δ 1.45 (t, J = 7.1 Hz, 3H, -OCH_2CH_3); 1.85 (m, 4H, - pyrrolidinyl *H*); 2.15 (m, 4H, - pyrrolidinyl *H*); 2.85 (t, 2H, -CH_2CH_2-Ph-Ph); 3.08 (s, 3H, -N-CH_3); 3.2 (t, 2H, CH_2CH_2-Ph-Ph); 4.25 (s, 2H, -CH_2-N<); 4.45 (q, J = 7.2 Hz, 2H, -OCH_2CH_3); 7.2-7.4 (m, 11H, -Ph*H*–Ph*H* e –Φ*H*); 8.08 (s, 1H, -Φ*H*); MS: *m/z* 467.2 [MH^+].

4.1.16 Synthesis of 4-amino-3-iodobenzoic acid (14)

Ethyl-4-aminobenzoate (47 mmol) was dissolved in 100 ml mixture of AcOH:H_2O (9:1). $NaIO_4$ (47 mmol), NaCl (93 mmol) and KI (47 mmol) were added sequentially. The reaction mixture was stirred at room temperature over night, then diluted with EtOAc and washed with brine, then with a saturated solution of $Na_2O_3S_2$ and finally, with a saturated solution of $NaHCO_3$. The organic layer was dried over Na_2SO_4, the solvent removed under reduced pressure, and the crude product purified by column chromatography on silica gel (EtOAc:Hex 1:9) to give compound **14** (70%) as a yellow powder. ^{1}H NMR ($CDCl_3$): δ 4.61 (s, 2H, N*H*$_2$); 6.75 (d, J=8.4Hz, 1H, -Φ*H*); 7.87 (dd, J_3=8.4Hz, 1H, Φ*H*); 8.38 (s, 1H, -Φ*H*).

4.1.17 Synthesis of 4-amino-3-iodophenyl)methanol (15)

A solution of compound **14** (25 mmol) in 10 mL of diethyl ether was added dropwise to a suspension of dry diethyl ether (60ml) and lithium aluminum hydride (30 mmol) under nitrogen and cooled to 0°C. The mixture is stirred for 16 hr at room temperature and cooled again to 0°C. The mixture is carefully worked up by the *dropwise* and sequential addition of 1.1 mL of water, 1.1 mL of a 15% aqueous sodium hydroxide solution and an additional 3.4 mL of water. The reaction mixture is filtered through a coarse filtration frit to remove aluminum salts, and the latter are washed four times with 8-mL portions of diethyl ether . The combined filtrates and washings are dried over sodium sulphate and concentrated under reduced pressure to give compound **15** (81%) as a yellow powder. ^{1}H NMR ($CDCl_3$): δ 3.22 (s, 2H, -N*H*$_2$); 4.55 (s, 2H, C*H*$_2$OH); 6.75 (d, J=8.6Hz, 1H, -Φ*H*); 7.18 (dd, J_3=8.4Hz, 1H, -Φ*H*); 7.67 (s, 1H, -Φ*H*).

4.1.18 Synthesis of 4-amino-3-iodobenzaldehyde (16)

PDC (56.66 mmol) and 360 ml of anhydrous dichloromethane were added to a flask. The resulting suspension was stirred at room temperature and under nitrogen atmosphere for 40 minutes. Then, alcohol **15** was added, and the reaction mixture was stirred for 2 h. Upon completion of the oxidation as indicated by TLC, the reaction mixture was filtered and evaporated under vacuum. The crude product was purified by column chromatography on silica gel (EtOAc:Hex 3:7) to give compound **16** (80%) as a yellow powder. ^{1}H NMR ($CDCl_3$): δ 4.7 (s, 1H, -N*H*$_2$); 6.81 (d, J=8.6Hz, 1H, -Φ*H*); 7.68 (dd, J_3=8.4Hz, 1H, -Φ*H*); 8.12 (s, 1H, -Φ*H*); 9.7 (s, 1H, -C*H*O).

4.1.19 Synthesis of N-(4-formyl-2-iodophenyl)acetamide (17)

Freshly distilled acetic anhydride (60.0 mmol) was added to a solution of compound **16 (**2.0 mmol) in methylene chloride (28 ml). After the mixture was stirred for 30 h at rt, than it was concentred and purified by flash column chromatography on silica gel (EtOAc:Hex 2:8) to give compound **17** (87%) as a yellow powder. ^{1}H NMR ($CDCl_3$): δ 2.38 (s, 3H, -COC*H*$_3$); 7.78 (s, 1H, -N*H*-); 7.93 (dd, J_3=8.4Hz, 1H, -Φ*H*); 8.38 (s, 1H, -Φ*H*); 8.57 (d, J=8.6Hz, 1H, -Φ*H*); 9.91 (s, 1H, -C*H*O).

4.1.20 Synthesis of N-(4-formyl-2-iodophenyl)-N-methylacetamide (18)

A solution of compound **17** (2.08 mmol) in freshly distilled THF (7 ml) was added dropwise to a suspension of 60% NaH in mineral oil (2.28 mmol) in THF (3 ml) under nitrogen and cooled to 0°C. The reaction was agitated and maintained at 0°C until it became clear (about 30 min) and a solution of CH_3I (2.7 mmol) in THF (3 ml) was dripped. The reaction was brought to rt and kept under nitrogen and stirring for 3h. To the reaction was diluted with H_2O and extracted with EtOAc. The organic phases were anidrificate with sodium sulfate and the solvent removed. The compound **18** (yield 75%) was obtained

by crystallization in hexane. ^{1}H NMR ($CDCl_3$): δ 1.85 (s, 3H, -COC*H*$_3$); 3.2 (s, 3H, -NC*H*$_3$); 7.45 (d, J=8.6Hz, 1H, -Φ*H*); 7.95 (dd, J_3=8.4Hz, 1H, -Φ*H*); 8.42 (s, 1H, -Φ*H*); 10.0 (s, 1H, -C*H*O).

4.1.21 Synthesis of N-(2-iodo-4-((pyrrolidin-1-yl)methyl)phenyl)-N-methylacetamide (19)

Compound **18** (1.541 mmol), dimethylamine or pyrrolidine (1.849 mmol), acetic acid (0.9 mL, 15.76 mmol) and $NaB(OAc)_3H$ (3.2 mmol) were, in that order, added to dry THF (7 mL). The mixture was irradiated with microwaves for 10 min at 130 °C. The mixture was filtered and purified by flash chromatography over silica gel (dichloromethane/methanol, 95:5) to give the desired compounds **19** (85%). ^{1}H NMR ($CDCl_3$): δ 1.85 (m, 4H, - pyrrolidinyl *H*); 2.2 (s, 3H, -COC*H*$_3$); 2.7 (m, 4H, - pyrrolidinyl *H*); 3.2 (s, 3H, -NC*H*$_3$); 3.75 (s, 2H, -C*H*$_2$-N<); 7.3 (d, J=8.4Hz, 1H, -Φ*H*); (dd, J_3=8.4Hz, 1H, -Φ*H*); 7.82 (s, 1H, -Φ*H*); MS: *m/z* 359.1, 360.2 [MH^+].

4.1.22 Synthesis of 2-iodo-N-methyl-4-((pyrrolidin-1-yl)methyl) benzenamine (20)

A mixture of 19 (3.12 mmol) and NaOH (156 mmol) in ethanol (125 ml) and water (30 ml) was heated to reflux with stirring for 20 h. The mixture was cooled and the solvent was removed under vacuum. The residue was partitioned between chloroform and water. The organic phase was washed with water, dried (Na_2SO_4), and evaporated under vacuum to give compound **20** (91%), as a brown oil. ^{1}H NMR ($CDCl_3$): δ 1.85 (m, 4H, - pyrrolidinyl *H*); 2.2 (s, 3H, -COC*H*$_3$); 2.7 (m, 4H, - pyrrolidinyl *H*); 3.2 (s, 3H, -NHC*H*$_3$); 3.75 (s, 2H, -C*H*$_2$-N<); 4.0 (s, 1H, -N*H*-); 6.31 (d, J=8.6Hz, 1H, -Φ*H*); 7.08 (dd, J_3=8.4Hz, 1H, -Φ*H*); 7.22 (s, 1H, -Φ*H*); MS: *m/z* 316.9, 317.2 [MH^+].

4.1.23 Synthesis of Ethyl 1-methyl-2-(-4,8,12-trimethyltrideca-3,7,11-trienyl)-5-((pyrrolidin-1yl)methyl)-1H-indole-3-carboxylate ($9e_1$).

A mixture of compound **20** (0.068 g, 0.215 mmol), compound **3e** (0.145 g, 0.430 mmol), CuI (0.008 g, 0.043 mmol), BINOL (0.025 g, 0.086 mmol) and Cs_2CO_3 (0.142, 0.43 mmol) in DMSO (1 mL) was stirred at 50 °C for 7 h under an atmosphere of nitrogen. After this time, the mixture was partitioned between ethyl acetate and saturated NH_4Cl. The organic layer was washed with brine, dried over sodium sulfate and concentrated in vacuo. The residue was purified by flash chromatography (THF/Acetone 9:1) over silica gel to give **$9e_1$** (0.049g, 45%). ^{1}H NMR ($CDCl_3$): 1.29 (t, J = 7.1 Hz, 3H, -OCH_2CH_3); 1.59 (m, 4H, -pyrrolidinyl *H*); 1.61 (m, 9H, -C*H*$_3$ farnesyl) 1.71 (s, 3H, -C*H*$_3$ farnesyl); 2 (m, 8H, C*H*$_2$ farnesyl); 2.32 (q, 2H, -C*H*$_2$-CH_2-Φ); 2.62 (t, 2H, -CH_2-C*H*$_2$-Φ); 3.62 (s, 5H, -C*H*$_2$-N< and -NC*H*$_3$); 4.3 (q, J=7.2 Hz, 2H, -OC*H*$_2$$CH_3$); 5.1 (m, 3H, =C*H*-); 6.7 (d, J=8.6Hz, 1H, -Φ*H*); 7.3 (dd, J_3=8.4Hz, 1H, -Φ*H*); 7.6 (s, 1H, -Φ*H*); MS: *m/z* 505.1 [MH^+].

4.1.24 Synthesis of host-guest peptide (P20H10)

The synthesis of peptide was performed manually in a stepwise fashion by the solid-phase Fmoc/tBu method. First amino acid N^{α}Fmoc-Lys-(BOC)-OH (4eq), was coupled to 0.149 g of Rink-amide resin (with a degree of substitution of 0.5 mmol / g), The following protected amino acids (4 eq) were then added stepwise according to established sequence. Each coupling reaction was accomplished through the use of a four-fold amino acid molar excess with activation with an equimolar excess of HBTU (or DCC) and HOBt in the presence of DIPEA (8 eq) for 2h. The peptide resin was washed with DMF (2x), and DCM (2x), and the completeness of the coupling reaction was checked by the Kaiser test. The N^{α}-Fmoc protecting groups were removed after each coupling cycle by treatment of the protected peptide resin with piperidine in DMF (30%) for 15 min. The N-terminal Fmoc group was

removed as described above, and the peptide was released from the resin with TFA/H_2O/TIPS (90:5:5, v/v/v) for 3 h. The resin was removed by filtration, and the crude peptide was recovered by precipitation with cold ethyl ether to give a white powder. Finally the crude peptide was purified by RP-HPLC on a C18-bonded silica column (Phenomenex-Jupiter, 0.46 cm x25 cm) using a gradient of 0.1% TFA in CH_3CN at a flow rate of 2.0 mL/ min. The final product was obtained by lyophilization of the appropriate fractions after removal of the CH_3CN by rotary evaporation. Preparative RP-HPLC was carried out on Shimadzu system. Analytical RP-HPLC indicated a purity >98%. Molecular masses were determined on a Finnigan LCQ-Deca ion trap instrument fitted with an electrospray source (San Jose, CA) and molecular weights were confirmed by ESI mass spectrometry (ESI-MS: 2681.06).

4.1.25 Synthesis of 1-(Tri-O-benzoyl-α-D-arabinofuranosyl)-2-nitro imidazole (Tribenzoyl-AZA; 4)

The bromosugar **3** (0.71 mmol), described above, was dissolved in anhydrous acetonitrile (40 mL) and added to the flask containing 1-*N*-trimethylsilyl-2-nitroimidazole **2** (0.868 mmol). This was followed by the addition of mercuric cyanide (1.562 mmol), after which the reaction flask was filled with nitrogen. The reaction mixture was heated at 50°C for 16 h. TLC examination at this time showed complete conversion of the bromosugar **3** to the azomycin nucleoside **4**. The solvent was evaporated on a rotary evaporator, the residue was dissolved in CH_2Cl_2, and then washed sequentially with 30% w:v aqueous potassium iodide and then cold water. The dichloromethane phase was dried over anhydrous sodium sulfate, filtered, evaporated and purified on a silica gel column (Hexane/EtOAc 7:3) to yield **4** (40%) as a yellowish solid. The melting points, ^{1}H and ^{13}C NMR spectra for **4** was identical to those reported previously.[121-122]

4.1.26 Synthesis of 1-(α-D-arabinofuranosyl)-2-nitroimidazole (α-AZA; 5)

To **4** (0.054 mmol) was added a solution of NH_3 in CH_3OH (6 mL of 2M solution) at 0°C under nitrogen and the resulting solution was stirred 10 h at 0°C and 50 h at room temperature. The solvent was then removed under vacuum (rotovap). Purification of the residue via flash column chromatography on silica gel (CH_2Cl_2/CH_3OH 9:1) gave **5** (90%) as white solid. The melting points, ^1H and ^{13}C NMR spectra for **5** and 1-(2-benzoyl-α-D-arabinofuranosyl)-2-nitroimidazole (Monobenzoyl-AZA) were identical to those reported previously.[121-122]

4.1.27 Synthesis of 1-α-D-(5'-O-Toluensulfonyl-arabinofuranosyl)-2-nitroimidazole (Ts-AZA; 6)

Compound **5** (AZA, 0.571 mmol) was dissolved in anhydrous pyridine (2 mL, dried over KOH), the solution was cooled at 5°C, and tosyl chloride (0.856 mmol) was added to it under stirring. The reaction mixture was stirred at that temperature for 42 h, then quenched by adding few pieces of ice. The solvent was removed and the residual viscous material was purified on a silica gel column using MeOH/CH_2Cl_2 (3:97, v/v) as eluent to afford **6** (60%). The melting points, Mass spectrum, ^1H and ^{13}C NMR spectra for **6** was identical to those reported previously.[116]

4.1.28 Synthesis of 1-α-D-(5'-O-Toluensulfonyl-2',3'-Di-O-acetylarabino furanosyl)-2-nitroimidazole (DAcTs-AZA; 7)

Acetic anhydride (0.75 ml) was added to a solution of **6** (400 mg, 1 mmol) and the mixture was stirred overnight at room temperature. The reaction was quenched by addition of water (1 ml) to the reaction mixture. The solvent was removed by evaporation on a rotavapor and the impure mixture was purified on a silica gel column using CH_2Cl_2:MeOH (97:3, v/v) as eluent to afford

450 mg (88%) of **7**. The melting points, Mass spectrum, ^{1}H and ^{13}C NMR spectra for **7** was identical to those reported previously.[116]

4.2 Biological assays

4.2.1. Anti-HCV assay

4.2.1.1 Cell lines and culture conditions

The human hepatoma-derived cell line Huh-7.5 was grown in high-glucose Dulbecco's modified Eagles' medium (DMEM; Life Technologies) supplemented with 2 mM $_{L}$-glutamine, 100 U/mL of penicillin, 100 µg/mL of streptomycin, and 10% fetal bovine serum.[123] Cells were sub-cultivated twice per week, with a 1:4 split ratio.

4.2.1.2 In vitro anti-HCV assay

The antiviral activities of compounds **9a$_{1–5}$**, **9b$_{1–2}$** against HCV were measured in Huh-7.5 hepatoma cells using replication and entry assays as previously described by Pacini et al.[124] For the replication assay, an RNA transcript of a replicon containing a firefly luciferase reporter was transfected in Huh-7.5 cells; these were subsequently plated on 96-well plates in the presence of test compounds and Arbidol. For the infection assay, viral particles containing a subgenomic HCV RNA carrying a firefly luciferase reporter gene were used to infect naive Huh-7.5 cells; these were plated in a 96-well format in the presence of test compounds and Arbidol. After three days of incubation luciferase activity was measured with a Bright-Glo luciferase assay system (Promega) following the manufacturer's instructions. The EC_{50} and SI of the evaluated compounds and Arbidol were calculated.

4.2.1.3. Cytotoxicity assay

Cytotoxicity induced by the test compounds in cultures of cells was also determined. The toxicity of compounds **9a$_{1–5}$** and **9b$_{1–2}$** in Huh-7.5 cells was

evaluated by CellTiter-Blue Viability Assay (Promega) that is used to estimate the number of viable cells present in multiwall plates; the reagent is a buffered solution containing highly purified resazuin. Resazuin is dark blue in color and has little intrinsic fluorescence. Metabolically active cells can reduce resazuin to resorufin, which is pink and highly fluorescent, with an excitation maximum of 579 nm and an emission maximum of 584 nm. Nonviable cells rapidly lose metabolic capacity, do not reduce the indicator dye, and thus do not generate a fluorescent signal.

4.2.1.3 In vitro selective anti-HCV activity

The selective antiviral activity of compounds **$9a_{1–5}$**, **$9(b\text{-}d)_{1–2}$** against HCV replication was measured in the Huh 5-2 HCV replicon system (type 1b, Con1 strain), as described previously.[125]

4.2.2. Anti-HSV assay

4.2.2.1 Virus preparation

HSV-1 strain HF obtained from ATCC (American Type Culture Collection) was grown and titred in VERO cells. To produce the virus amount necessary for the experiments, the cells were incubated in RPMI medium supplemented with 2mM glutamine, 100 U/ml penicillin, 0.1mg/ml streptomycin and 2% heat inactivated FCS in a 75 cm^2 flask, and then rinsed with serum-free medium and infected with HSV 1 at a low multiplicity of infection (MOI) of 0.001 plaque-forming units (PFU)/cell. One hour post-infection (p.i.) at 37 °C, 15–20ml of RPMI with 2% FCS was added and the cells were cultured for about 3 days. Seventy two hours after virus challenge culture supernatants were harvested after three cycles of cells freezing (-80 °C)/defrosting, they were clarified by centrifugation at 800 g for 10min, titred and stored in small volumes at -80 °C. A virus stock solution containing approximately 10^9 PFU/ml was used in all the experiments.

4.2.2.2 Plaque assay

To choose the best concentration of Arbidol and its analogues to test for the antiviral activity, a preliminary plaque assay was performed. Briefly confluent monolayers of HaCat cells were treated with Arbidol, $9b_2$, $9b_1$ and $9a_2$ at different concentration (12, 6, 3 and 1 μM) for 3 h. As positive control we use a treatment with acyclovir 10 μM. The cells were then washed with PBS and infected with HSV-1 at MOI of 0.001 PFU/ cell. After 1 h of incubation at 37 °C (adsorption period), the unadsorbed virus was removed and the monolayers were incubated for an additional 72 h in DMEM medium (supplemented with 2% FCS) with carboxymethyl cellulose (CMC) (ratio 1:1). After incubation period the cells were fixed and stained with 1% crystal violet dissolved in a 10% formalin solution, the plaques were scored and the plaque number calculated based on the mean count of three replicate wells. The toxic effect of the concentrations of Arbidol and its analogues used, 12μM, 6μM, 3μM and 1μM were tested on keratinocytes in preliminary dose–response experiments, all the concentration tested did not alter cell viability.

4.2.2.3 Assays for antiviral activity

In order to identify which phase of HSV-1 replication (preadsorption/adsorption or post-adsorption period) was affected by Arbidol and its analogues, three sets of experiments were performed.

1. The confluent monolayers of HaCat cells were pretreated with Arbidol, $9b_2$, $9b_1$ and $9a_2$ 3 μM for 3 h. After the incubation, the medium was removed and the cells were infected at MOI of 5 PFU/cell in presence or not of the stimuli. After the adsorption period, the virus was removed and fresh medium at 2% FCS was added. The supernatants were collected after 24 and 48 h.
2. The confluent monolayers of HaCat were infected at MOI of 5 PFU/cell at the same time Arbidol, $9b_2$, $9b_1$ and $9a_2$ 3 μM were added.

After the adsorption period, the virus was removed and fresh medium at 2% FCS was added. The supernatants were collected after 24, 48h.

3. The confluent monolayers of HaCat were infected at MOI of 5 PFU/cell. After the adsorption period, the virus was removed and fresh medium at 2% FCS with stimuli was added. The supernatants were collected after 24 and 48 h.

The supernatant were harvested and tested for their ability to form plaques in the HaCat cells using a standard titration method. Briefly, serial-fold dilutions of the supernatants (from 10^1 to 10^7) were made and 100 µl of each dilution was added to the cell monolayers seeded in 12-well multiwells. After 1 h of adsorption, the medium was removed and fresh DMEM containing 2% FCS with carboxymethyl cellulose (CMC) (ratio 1:1) was added. After 72 h of incubation, the cells were fixed and stained with 1% crystal violet dissolved in a 10% formalin solution. The plaques were counted and the plaque number was calculated based on the mean count of three replicate wells.

4.3 Circular dichroism studies

Circular dichroism (CD) experiments were performed at 25°C on a 810-Jasco spectropolarimeter using a quartz cuvette with a path length of 1 mm, a bandwidth of 0.1 nm, a time constant of 2.0 s and a wavelength range of 190-260 nm in 0.2-nm steps. The far-UV CD spectra were performed on peptide in H_2O at 200 µM concentration, at pH 5 and 7, in lysophosphatidylcholine micelles (LPC), with or without Arbidol. The spectrum of the buffer was subtracted from all the other spectra; the results of 4 scans were then averaged. In addition, the estimation of the secondary structure composition was carried out using the algorithm K2D by DichroWeb.

REFERENCES

[1] Clarendon Press; *The Oxford English Dictionary*, **1989**; 2nd ed.

[2] Koonin EV, Senkevich TG, Dolja VV; *Biol. Direct*. **2006**; 1:29.

[3] Lawrence CM, Menon S, Eilers BJ, et al.; *J. Biol. Chem.* **2009**; 284(19):12599–603.

[4] Edwards RA, Rohwer F. Viral metagenomics; *Nat. Rev. Microbiol.* **2005**; 3(6):504–10.

[5] Paul Ahlquist; *Nat. Rev. Microbiol.* **2006**; 4:371-382.

[6] Bordenave G; *Microbes and Infection* **2003**; **5** (6): 553–60.

[7] Hurlbert R. E., *The fundamentals of microbiology 102* **1999**; chapter XI.

[8] Dimmock, N.J, Easton, Andrew J, Leppard, Keith, *Introduction to Modern Virology* **2007** sixth edition, p.4.

[9] Shors, Teri; *Understanding Viruses* **2008**; p.76-77.

[10] Collier, Leslie; Balows, Albert; Sussman, Max Topley and Wilson's; *Microbiology and Microbial Infections* **1999** ninth edition, 1:3.

[11] Dimmock, N.J, Easton, Andrew J, Leppard, Keith, *Introduction to Modern Virology* **2007** sixth edition, p.49.

[12] Breitbart M, Rohwer F; *Trends Microbiol*. **2005**; 13(6):278–84.

[13] Frederick A. Murphy; *ICTV list of virus discoveries and discoverers*.

[14] Collier, Leslie; Balows, Albert; Sussman, Max Topley and Wilson's; *Microbiology and Microbial Infections* **1999** ninth edition, 1:745.

[15] Temin HM, Baltimore D.; *Adv. Virus Res.***1972**; 17:129–86.

[16] Liu Y, Nickle DC, Shriner D, et al.; *Virology* **2004**; 10;329(1):101–8.

[17] Shors, Teri; *Understanding Viruses* **2008**; p.14-16.

[18] Collier, Leslie; Balows, Albert; Sussman, Max Topley and Wilson's; *Microbiology and Microbial Infections* **1999** ninth edition, 1:11-21.

[19] Shors, Teri; *Understanding Viruses* **2008**; p.574.

[20] Dimmock, N.J, Easton, Andrew J, Leppard, Keith, *Introduction to Modern Virology* **2007** sixth edition, p.15-16.

[21] Dimmock, N.J, Easton, Andrew J, Leppard, Keith, *Introduction to Modern Virology* **2007** sixth edition, p.55.

[22] Shors, Teri; *Understanding Viruses* **2008**; p.551-3.

[23] Tsagris EM, de Alba AE, Gozmanova M, Kalantidis K.; *Cell. Microbiol.* **2008**; 10(11):2168.

[24] Shors, Teri; *Understanding Viruses* **2008**; p.492-3.

[25] La Scola B, Desnues C, Pagnier I, Robert C, Barrassi L, Fournous G, Merchat M, Suzan-Monti M, Forterre P, Koonin E, Raoult D.; *Nature* **2008**; 455(7209):100–4.

[26] Ammerman NC, Beier-Sexton M, Azad AF.; *Current Protocols in Microbiology* **2008**; Chapter 3:Unit 3A.5.

[27] Collier, Leslie; Balows, Albert; Sussman, Max Topley and Wilson's; *Microbiology and Microbial Infections* **1999** ninth edition, 1:33-55.

[28] Caspar DL, Klug A.; *Cold Spring Harb. Symp. Quant. Biol*. **1962**; 27:1–24.

[29] Crick FH, Watson JD.; *Nature* **1956**; 177(4506):473–5.

[30] M.R. Falvo**,** S. Washburn**,** R. Superfine**,** M. Finch **,** F.P. Brooks**,** V. Chi and R.M. Taylor**;** *Biophysical Journal* **1997**; 72(3):1396–1403.

[31] Yu. G. Kuznetsov, A. J. Malkin, R. W. Lucas, M. Plomp and A. McPherson; *J Gen Virol*. **2001**; 82(9):2025–2034.

[32] Alan J. Cann; *Principles of Molecular Virology* **2005**, Fourth Edition;
Chapter 2 p.25-28.

[33] Nelson & Cox, *Lehninger Principles of Biochemistry, 3rd ed.,* **2000**; Fig. 6-24.

[34] Gunilla B. Karlsson Hedestam, Ron A.M. Fouchier, Sanjay Phogat,

Dennis R. Burton, Joseph Sodroski & Richard T . Wyatt; *Nature Reviews Microbiology **2008;*** **6**, 143-155.

[35] Rossmann MG, Mesyanzhinov VV, Arisaka F, Leiman PG.; *Curr. Opin. Struct. Biol.*. **2004**; 14(2):171–80.

[36] Suzan - Monti M, La Scola B, Raoult D; *Virus Research* **2006**;117(1):145–155.

[37] Collier, Leslie; Balows, Albert; Sussman, Max Topley and Wilson's; *Microbiology and Microbial Infections* **1999** ninth edition, 1:96-99.

[38] Pressing J, Reanney DC; *J Mol Evol*. **1984**; 20(2):135–46.

[39] Hampson AW, Mackenzie JS; *Med. J. Aust.* **2006**; 185(10):S39–43.

[40] Vladimir Trifonov, Hossein Khiabanian, and Raul Rabadan; *N. Engl. J. Med.* **2009**; 361;2.

[41] Worobey M, Holmes EC; *J. Gen. Virol.* **1999**; 80 (10):2535–43.

[42] Boevink P, Oparka KJ; *Plant Physiol.* **2005**; 138(4):1815–21.

[43] Bruce Alberts, Alexander Johnson, Julian Lewis, Martin Raff , Keith Roberts, and Peter Walter*; Molecular Biology of the Cell, 4th edition* **2002**; part V; Chapter 25.

[44] Dimmock, N.J, Easton, Andrew J, Leppard, Keith , *Introduction to Modern Virology* **2007** sixth edition, p.185-187, p.243-259.

[45] Shors, Teri; *Understanding Viruses* **2008**; p.54,60,597.

[46] Collier, Leslie; Balows, Albert; Sussman, Max Topley and Wilson's; *Microbiology and Microbial Infections* **1999** ninth edition, 1:78-89,88-89.

[47] Lwoff A, Horne RW, Tournier P. A virus system. *C. R. Hebd. Seances Acad. Sci.*. **1962**; 254:4225–7.

[48] Lwoff A, Horne R, Tournier P. A system of viruses. *Cold Spring Harb. Symp. Quant. Biol.*. **1962**; 27:51–5.

[49] Delwart EL; *Rev. Med. Virol.* **2007**; 17(2):115–31.

[50] *ICTV Virus Taxonomy* **2009.**

[51] Baltimore D; *Harvey Lect.* **1974**;70 Series:57–74.

[52] Patrick R. Murray, Ken S. Rosenthal, George S. Kobayashi, Michael A. Pfaller; Microbiology **2004** (3rd edition) p.599-607.

[53] Simplified taxonomy of main viruses infecting humans; *Antiviral InteliStrat.*

[54] Margolis TP, Elfman FL, Leib D, et al. ; *J. Virol* . **2007**; 81(20): 11069– 74.

[55] Whitley RJ; *Baron's Medical Microbiology* (4th ed.) **1996**; section 2, chapter 68.

[56] Whitley RJ, Roizman B; *Lancet*. **2001**; 357(9267):1513–8.

[57] Barton ES, White DW, Cathelyn JS, et al .; *Nature*. **2007**; 447(7142):326–9.

[58] Fisher, Bruce; Harvey, Richard P.; Champe, Pamela C.; *Lippincott's Illustrated Reviews: Microbiology (Lippincott's Illustrated Reviews Series)* **2007**; Chapter 33, pages 367–392.

[59] Bertoletti A, Gehring A; *Hepatol. Res.* **2007**; 37(3):S331–8.

[60] Rodrigues C, Deshmukh M, Jacob T, Nukala R, Menon S, Mehta A; *Indian journal of medical microbiology* **2001**; 19(3):141–4.

[61] Nguyen VT, McLaws ML, Dore GJ; *Journal of Gastroenterology and Hepatology* **2007**; 22(12):2093–100.

[62] Erik De Clercq; *Nat. Rev. drug discovery* **2002**; 1:13-25.

[63] Antonio Mastrolorenzo, Alfonso Maresca, Stefano Rusconi, Claudiu T Supuran; *Future HIV Therapy* **2008**; Vol. 2, No. 5, Pages 479-507.

[64] Anne Goffard, Nathalie Callens, Birke Bartosch, Czeslaw Wychowski, François-Loïc Cosset, Claire Montpellier, and Jean Dubuisson; *Journal of virology* **2005**, Vol. 79, No. 13, p. 8400–8409.

[65] D Durantel, C Alotte, F Zoulim; *Current Opinion in Investigational Drugs* **2007**; 8:125-129.

[66] François Helle, Czeslaw Wychowski, Ngoc Vu-Dac, Kirk R.

Gustafson, Cécile Voisset, and Jean Dubuisson; *The journal of Biological Chemistry* **2006**; Vol.281, No. 35, pp. 25177–25183.

[67] Jan Balzarini; *Antiviral Chemistry & Chemotherapy* **2007**; 18:1-11.

[68] Palese P, Shaw ML; *Fields Virology (5th edition)* **2007**; Lippincott Williams & Wilkins; pp1647-1689.

[69] Pevear D, Tull T, Seipel M, Groarke J; *Antimicrob Agents Chemother* **1999**; 43 (9): 2109–15.

[70] Florea N, Maglio D, Nicolau D; *Pharmacotherapy* **2003**; 23 (3):339–48.

[71] J. Neyts; *Antiviral Research* **2006**; 71:363–371.

[72] Bressanelli, S., Tomei, L., Roussel, A., Incitti, I., Vitale, R.L., Mathieu, M., De Francesco, R., Rey, F.A.; *Proc. Natl. Acad. Sci*. **1999**; 96, 13034–13039.

[73] Erik De Clercq; *Nature Reviews Drug Discovery* **2007**; 6:1001-1018.

[74] Teresa H. Evering, Martin Markowitz; *The PRN Notebook* **2008**; Volume 13, Pages 1–9.

[75] Maga G, Gemma S, Fattorusso C, Locatelli GA, Butini S, Persico M, Kukreja G, Romano MP, Chiasserini L, Savini L, Novellino E, Nacci V, Spadari S, Campiani G.; *Biochemisty* **2005**; 44 (28) : 9637-44.

[76] P Borowski, J Deinert, S Schalinski, M Bretner, K Ginalski, T Kulikowski, D Shugar; *Eur J Biochem* **2003**; 270:1645-53.

[77] López-Labrador FX; *Recent Pat on Anti-Infective Drug Discovery* **2008**; 3(3):157-167.

[78] Sodeik B, Griffiths G, Ericsson M, Moss B, Doms RW; *J Virol*. **1994**; 68(2):1103-14.

[79] Y.S. Boriskin, I. A. Leneva, E.-I. Pécheur and S. J. Polyak; *Current Medicinal Chemistry*, **2008**, 15(5):1-9.

[80] R. G. Glushkov and T. A. Gus'kova; *Pharmaceutical Chemistr Journal* **1999**; Volume 33, Number 3, 115-122.

[81] Surinova B. N., Karpova N. A., Kumin Yu. C., Khim. Farm. Zh.; *Chem.-Pharm. J.* **1995**, 3, 14-15.

[82] Eve-Isabelle Pe´cheur, Dimitri Lavillette, Fanny Alcaras, Jennifer Molle, Yury S. Boriskin, Michael Roberts, Francüois-Loı¨c Cosset, and Stephen J. Polyak; *Biochemistry* **2007,** *46*, 6050-6059.

[83] Yury S Boriskin1, Eve-Isabelle Pécheur and Stephen J Polyak; *Virology Journal* **2006**, 3:56:1-9.

[84] Irina A. Leneva, Rupert J. Russell, Yury S. Boriskin, Alan J. Hay; *Antiviral Research* **2009**; 81:132–140.

[85] G. Sellitto et al. / *Bioorg. Med. Chem.* **2010**, 18, 6143–6148.

[86] Le Wang, Keith W. Woods, Qun Li, Kenneth J. Barr, Richard W. McCroskey, Steven M. Hannick, Laura Gherke, R. Bruce Credo, Yu-Hua Hui, Kennan Marsh, Robert Warner, Jang Y. Lee, Nicolette Zielinski-Mozng, David Frost, Saul H. Rosenberg, and Hing L. Sham; *J. Med. Chem.* **2002**, *45*, 1697-1711.

[87] PCT/EP2007/056690.

[88] Gary A. Molander and Adam R. Brown; *J. Org. Chem.* **2006**, *71*, 9681-9686.

[89] Hartmuth C. Kolb, Michael S. VanNieuwenhze, and K. Barry Sharpless; *Chem. Rev.* **1994,** *94*, 2483-2547.

[90] Tarek Sammakia, T. Brian Hurley, Douglas M. Sammond, and Randall S. Smith; *Tetrahedron Letters*, **1996**, Vol. 37, No. 26, 4427-4430.

[91] Amit Sagi, Roy Weinstain, Naama Karton, and Doron Shabat; *J. AM. CHEM. SOC.* **2008**, *130*, 5434–5435.

[92] Yihui Chen, Masayuki Shibata , Manju Rajeswaran, Thamarapu Srikrishnan, Sundeep Dugar and Ravindra K. Pandey; *Tetrahedron Letters* **2007**, 48, 2353–2356.

[93] PCT/EP1512687A1.

[94] Maria Joselice e Silva, Antonio José Alves, Silene C. Do Nascimento; *I1 Farmaco;* **1998**, 53, 241-243.

[95] Craig **A.** Merlic, Soheil Motamed, and Bruce Quinn; *J. Org. Chem*.; **1995**, 60, 3365-3369.

[96] Shejin Zhu, Alexander L. Ruchelman, Nai Zhou, Angela Liu, Leroy F. Liub, and Edmond J. LaVoiea; *Bioorganic & Medicinal Chemistry*; **2006**, 14, 3131–3143.

[97] Lodish H, Berk A, Zipursky SL, et al.; *Molecular Cell Biology*. 4th edition **2000**; chapter 17, section 17.10 Molecula r Mechanisms of Vesicular Traffic.

[98] Irina A. Leneva, Rupert J. Russell, Yury S. Boriskin, Alan J. Hay; *Antiviral Research* **2009**, 81, 132–140.

[99] Xing Han, John H. Bushweller, David S. Cafiso and Lukas K. Tamm; *Nature Structural Biology*; **2001**, Volume 8 N.8.

[100] Albericio, F. *Solid-Phase Synthesis: A Practical Guide* **2000** (1 ed.). CRC Press. pp. 848.

[101] Hermkens, P. H. H.; Ottenheijm, H. C. J.; Rees, D. C.; *Tetrahedron* **1997**, 53 (16): 5643–5678.

[102] Alison Rodger and Bengt Nordén, *Circular Dichroism and Linear Dichroism* **1997**, Oxford University Press, UK.

[103] Gilles Mees, Rudi Dierckx, Christel Vangestel, Christophe Van de Wiele; *Eur J Nucl Med Mol Imaging* **2009**, 36:1674–1686.

[104] Piyush Kumar, Ebrahim Naimi, Alexander J . McEwan, Leonard I. Wiebe, *Bioorganic & Medicinal Chemistry* **2010**, 18, 2255–2264.

[105] Carroll VA, Ashcroft M. *Expert Rev Mol Med*. **2005** Apr 15;7(6):1-16.

[106] Dietlind Sorger, Marianne Patt, Piyush Kumar, Leonard I. Wiebe, Henryk Barthel, Anita Seese, Claudia Dannenberg, Andrea Tannapfel, Regine Kluge and Osama Sabri; *Nuclear Medicine and Biology* **2003**, 30, 317–326.

[107] Didier Le Bars; *Journal of Fluorine Chemistry* **2006**, 127, 1488–1493.

[108] Rafael Torres Martin de Rosales, Erik Årstad, Philip J. Blower; *Targ Oncol* **2009**, 4:183–197.

[109] Hodgkiss RJ. *Anticancer Drug Des* **1998**;13(6):687–702.

[110] *Molecular Imaging and Contrast Agent Database (MICAD)*: 2-(2- Nitroimidazol-1*H*-yl)-(3-[^{18}F]fluoropropyl)acetamide.

[111] J. Donald Chapman, Edward L. Engelhard, Corinne C. Stobbe, Richard F. Schneider, Gerald E. Hanks; *Radiotherapy and Oncology* **1998**, 46, 229–237.

[112] Ernst J. Postema, Alexander J. B. McEwan, Terence A. Riauka, Piyush Kumar, Dacia A. Richmond, Douglas N. Abrams, Leonard I. Wiebe; *Eur J Nucl Med Mol Imaging* **2009**, 36:1565–1573.

[113] P. Kumar, S. Emami, A.J.B . McEwana and L.I. Wiebea, *Letters in Drug Design & Discovery*, **2009**, 6, 82-85.

[114] Piyush Kumar, Leonard I. Wiebe, Elena Atrazheva and Manju Tandon; *Tetrahedron Letters* **2001**, 42, 2077–2078.

[115] Ebrahim Naimi and Piyush Kumar, Alexander J. B. McEwan, Leonard I. Wiebe; *Nucleosides, Nucleotides, and Nucleic Acids* **2005**, 24 (3):173– 178.

[116] P. Kumara, L.I. Wiebea, M. Asikoglua, M. Tandona, A.J.B. McEwanb; *Applied Radiation and Isotopes* **2002**, 57, 697–703.

[117] Piyush Kumar, Kazue Ohkura, Davood BEIKI, Leonard Irving Wiebe, and Koh-ichi Seki; *Chem. Pharm. Bull.* **2003**, 51(4) 399—403.

[118] G. Reischl, W. Ehrlichmann, C. Bieg, C. Solbacha, P. Kumar, L.I. Wiebe, H.-J. Machulla; *Applied Radiation and Isotopes* **2005**, 62, 897–901.

[119] Zhao, C. S.; Zhao, Y. F.; Chai, H. F.; Gong, P. *Bioorg. Med. Chem.* **2006**, 14, 2552.

[120] Liu, Y.; Zhao, Y.; Zhai, X.; Feng, X.; Wang, J.; Gong, P. *Bioorg. Med. Chem.* **2008**, 16, 6522.

[121] Kumar, P.; Ohkura, K.; Beiki, D.; Wiebe, L.I.; Seki, K. *Chem. Pharm. Bull.* (Tokyo) **2003**, 51, 399 –403.

[122] Kumar, P.; Wiebe, L.I.; Atrazheva, E.; Tandon, M. *Tetrahedron Lett.* **2001**, 42, 2077 – 2078.

[123] Blight, K. J.; McKeating, J. A.; Rice, C. M. *J. Virol*. **2002**, 76, 13001.

[124] Pacini, L.; Graziani, L. B.; Bartholomew, L.; De Francesco, R.; Paonessa, G. *J. Virol.* **2009**, 83, 9079.

[125] Vrolijk, J. M.; Kaul, A.; Hansen, B. E.; Lohmann, V.; Haagmans, B. L.; Schalm, S. W.; Bartenschlager, R. *J. Virol. Methods* **2003**, 110, 201.

LIST OF ABBREVIATIONS

ARB	Arbidol
BINOL	1,1'-Bi-2-naphthol
BOC	Tert-butoxycarbonyl
CC_{50}	50% cytotoxic concentration
CD	Circular dichroism
CD_3OD	Deuterated methanol
$CDCl_3$	Deuterated chloroform
CH_2Cl_2	Dichloromethane
CH_3CN	Acetonitrile
CH_3COOH	Acetic acid
CH3I	Methyl iodide
CH_3OH	Methanol
CMV	Cytomegalovirus
Cs_2CO_3	Cesium carbonate
CuI	Copper iodide
DCC	*N,N'*-Dicylohexylurea
DCM	Dichloromethane
DIPEA	*N*,*N*-Diisopropylethylamine
DMAP	4-Dimethylaminopyridine
DMF	Dimethylformamide
DMSO	Dimethyl Sulfoxide
EBV	Epstein-Barr virus
EC_{50}	50% Effective concentration
EC_{90}	90% Effective concentration
ESI/MS	Electrospray ionization mass spectrometry
EtOAc	Ethyl acetate
EtOH	Ethanol
FMOC	9-fluorenylmethyloxycarbonyl
h	Hour

H_2O	Water
HA	Haemagglutinin
HaCat	Human Keratinocyte cells
HBTU	O-Benzotriazole-N,N,N',N'-tetramethyl-uronium-hexafluoro-phosphate
HCV	Hepatitis C virus
HHV6	Human herpes virus 6
HIV	Human immunodeficiency virus
HMDS	Hexamethyldisilazane
HOBT	*N*- Hydroxybenzotriazole
HPV	Human papilloma virus
HSV	Herpes simplex virus
ICT	International Committee Taxonomy of viruses
K/2.2.2.	Kryptofix
$K_3Fe(CN)_6$	Potassium ferricyanide
KH	Potassium hydride
KI	Potassium iodide
KOH	Potassium hydroxide
$LiAlH_4$	Lithium aluminium hydride
LPC	Lisophosphatidylcholine
MOI	Low multiplicity of infection
MW	Microwave
NA	Neuraminidase
$NaB(OAc)_3H$	Sodium triacetoxyborohydride
$NaBH_4$	Sodium borohydride
NaH	Sodium hydride
$NaIO_4$	Sodium periodate
NaOH	Sodium hydroxide
nBuLi	n-Butyllithium

NH_3	Ammonia
NMR	Nuclear Magnetic Resonance
OsO_4	Osmiun Tetroxide
P.E.T	Positron Emission Tomography
P20H6	Host-guest peptide
$Pb(OAc)_4$	Lead (IV) acetate
$Pd(PPh_3)_2OAc$	Acetate bis(triphenylphosphine) palladium (II)
$PdCl_2$	Palladium chloride
PFU	Plaque-forming units
PPh_3	Triphenylphosphine
RP-HPLC	Reversed phase- High-performance liquid
RSV	Respiratory syncitial virus
rt	Room temperature
S.P.E.C.T.	Single photon emission computed tomography
SI	Selectivity index
SPPS	Solid phase peptide synthesis
SS	Selectivity Surface
TFA	Trifluoroacetic acid
THF	Tetrahydrofuran
TIPS	Triisopropylsilane
VZV	Varicellazoster virus
YFV	Yellow fever virus

Ringraziamenti

I miei più sinceri ringraziamenti vanno al mio tutor Paolo de Caprariis, già mio relatore di tesi di laurea, e soprattutto mio mentore. I miei ringraziamenti vanno ad un uomo che si è mostrato sempre presente e disponibile con i suoi suggerimenti e acuti consigli rivelatisi sempre per me veritieri e preziosi. Un grazie ad un uomo e un professionista per le opportunità che mi ha offerto.

Desidero ringraziare la prof.ssa Anna Maria D'Ursi che mi ha accompagnato in fasi significative del presente lavoro. Lei è per me una guida di competenza scientifica e di profonda umanità, nonché mia costante interlocutrice e maestra.

Un grazie colmo di sincero affetto e stima al Prof. Giuseppe Bifulco che ha sostenuto e accompagnato con preziose osservazioni e puntuali consigli il mio percorso. A lui devo la concretizzazione della mia esperienza all'estero che si è rivelata una importante esperienza lavorativa ma anche di vita.

Un grande grazie alla prof.ssa Nunziatina De Tommasi. Il suo contributo ed i suoi suggerimenti sono stati decisivi per lo svolgimento del mio progetto di Dottorato.

Ringrazio per l'ottima ospitalità il prof. Matteo Zanda ed il suo team, del Dip. di Chimica dell'Università di Aberdeen (Scotland) dove ho trascorso il secondo semestre dell' ultimo anno di Dottorato. Qui ho realizzato che la competenza e la rigorosità scientifica sono due virtù essenziali nel lavoro di ricerca sperimentale. Ringrazio, in particolare, il PostDoc Sergio Dall'Angelo, instancabile ed esperto chimico del gruppo, con cui ho condiviso piacevolmente diverse ore di lavoro.

Ringrazio tutti i miei compagni di percorso, compresi tesisti, laureati e dottorandi per aver condiviso le mie difficoltà e le mie soddisfazioni, colorando di tinte vivaci le mie giornate di studio. Ringrazio, in particolare, la Dott. Aurora Faruolo e la Dott. Manuela Grimaldi che hanno contribuito in modo attivo alla realizzazione del mio lavoro.

Ringrazio, infine, la mia famiglia e Rocco, certezze intramontabili nel mio percorso di vita, per avermi sostenuto in tutti questi anni e per avermi dato la forza di lottare e non mollare mai neanche nei momenti più difficili. Ad essi vanno tutta la mia stima, il mio rispetto e la mia riconoscenza.